AGE-DEPENDENT EFFECTS OF SHORT-TERM INTERMITTENT FASTING AND RAPAMYCIN TREATMENT IN ZEBRAFISH (*DANIO RERIO*) BRAIN

A DISSERTATION SUBMITTED TO
THE GRADUATE SCHOOL OF ENGINEERING AND SCIENCE
OF BILKENT UNIVERSITY
IN PARTIAL FULFILLMENT OF THE REQUIREMENTS FOR
THE DEGREE OF
DOCTOR OF PHILOSOPHY
IN
NEUROSCIENCE

By
Ergül Dilan Çelebi Birand

May 2020

AGE-DEPENDENT EFFECTS OF SHORT-TERM INTERMITTENT FASTING AND RAPAMYCIN TREATMENT IN ZEBRAFISH (*DANIO RERIO*) BRAIN

By Ergül Dilan Çelebi Birand

May, 2020

We certify that we have read this thesis and that in our opinion it is fully adequate, in scope and in quality, as a thesis for the degree of Doctor of Philosophy.

_____

Michelle Marie Adams

(Advisor)

_____

Ali Osmay Güre

_____

Çağdaş Devrim Son

_____

Özlen Konu Karakayalı

_____

Erkan Kiriş

Approved for the Graduate School of Engineering and Science

_____

Prof. Dr. Ezhan Karaşan

Director of the Graduate School of Engineering and Science

ABSTRACT

AGE-DEPENDENT EFFECTS OF SHORT-TERM INTERMITTENT FASTING AND RAPAMYCIN TREATMENT IN ZEBRAFISH (*DANIO RERIO*) BRAIN

Ergül Dilan Çelebi Birand

Ph.D. in Neuroscience

Advisor: Michelle M. Adams

May, 2020

World populations are rapidly aging, and there is an urgent need to develop interventions that prevent or reverse age-related deterioration of health. To date, several approaches have been developed to extend health span. Among these, non-genetic interventions have a higher potential to be utilized in translational studies. Caloric restriction (CR) and its pharmacological mimetic rapamycin, are two applications that have been shown to reliably extend life and health span across species. Despite a growing body of knowledge on how CR and rapamycin show their beneficial effects, their molecular mechanisms in the brain are not completely understood. Furthermore, most studies applied life-long CR, which is not suitable for translational research. To fill this gap, we investigated whether short-term durations of a CR approach intermittent fasting (IF) or rapamycin altered cellular and molecular markers of critical processes in the brain as well as metabolic parameters in the body. To assess how the age of the subjects affect the outcome of the

treatments, we included young (6-10 months old) and old (26-31 months) zebrafish, which has recently emerged as a suitable model for gerontological research. Our results demonstrated that IF decreased whole-body glucose and cortisol levels, and increased neural progenitor marker DCAMKL1 in young and old animals. While this proliferation-promoting effect was preceded by suppression of mTOR activity in young, the upregulation of *foxm1* and reduced autophagic flux as measured by LC3-II/LC3-I ratio were observed in old animals. Rapamycin, on the other hand, did not alter the metabolic parameters and induced entirely different molecular profiles at young and old ages. The most notable changes in young animals were reduced mTOR activity, LC3-II/LC3-I ratio and expression levels of a global proliferation marker PCNA. In old animals, the marker of activated astrocytes (i.e. GFAP) was decreased, indicating lower neuroinflammation, whereas excitatory-inhibitory balance as measured by PSD-95/Gephyrin ratio was shifted towards a more excitatory state. These results suggested that IF and rapamycin induced distinct metabolic profiles in young and old animals. Furthermore, there was an age-dependent reciprocal relationship between proliferation and autophagy, which might be partly due to differential regulation of mTOR activity. Interestingly, rapamycin treatment was more effective in suppressing mTOR activity in young animals, and compared to IF. Nevertheless, these results suggested that rapamycin crosses the blood-brain barrier in zebrafish, and that short-term durations of IF or rapamycin were sufficient to alter the expression levels of key proteins involved in critical mechanisms in the brain.

Keywords: Aging, brain, mTOR, intermittent fasting, rapamycin, zebrafish, metabolism, neurogenesis, glia, synaptic transmission, autophagy

ÖZET

KISA SÜRELİ ARALI ORUÇ VE RAPAMİSİN UYGULAMALARININ ZEBRA BALIĞI (*DANIO RERIO*) BEYNİNDEKİ YAŞA BAĞLI ETKİLERİ

Ergül Dilan Çelebi Birand

Nörobilim Lisansüstü Programı, Doktora

Tez Danışmanı: Michelle M. Adams

Mayıs, 2020

Dünya nüfusu hızla yaşlanmaktadır ve sağlık durumunda yaşa bağlı gerilemenin engellenmesini veya geriye çevrilmesini sağlayacak müdahalelerin geliştirilmesine ivedi ihtiyaç duyulmaktadır. Şimdiye kadar sağlıklı yaşam süresini uzatmaya yönelik çeşitli yaklaşımlar geliştirilmiştir. Bu yaklaşımlar arasında genetik tabanlı olmayan müdahaleler, insanlarda uygulanabilirlik açısından daha yüksek bir potansiyele sahiptir. Kalori kısıtlaması (KK) ve KK'nın farmakolojik mimetiği rapamisin, farklı canlı türlerinde yaşam ve sağlıklı yaşam süresini güvenilir bir şekilde uzattığı gösterilen uygulamalardır. KK ve rapamisinin yararlı etkilerini nasıl gösterdiğine dair artmakta olan bilgiye rağmen bunların beyindeki moleküler mekanizmaları henüz tam olarak anlaşılabilmiş değildir. Dahası birçok çalışma, insanlarda yapılacak çalışmalar için elverişli olmayan bir yaklaşım olan yaşam boyu KK uygulamasını incelemiştir. Bu boşluğu doldurmak için bir KK yaklaşımı olan aralı oruç (AO) ve rapamisinin kısa süreli uygulamalarının beyindeki kritik işlemlerin hücresel ve moleküler belirteçleri ile vücuttaki metabolik parametreleri değiştirme durumunu inceledik. Deneklerin yaşının tedavi sonucunu nasıl etkilediğini değerlendirmek için

yakın zamanda gerontoloji çalışmalarında uygun bir model olarak ortaya çıkan zebra balıklarının genç (6-10 aylık) ve yaşlı (26-31 aylık) bireylerini çalışmamıza dahil ettik. Bulgularımız, AO uygulamasının genç ve yaşlı hayvanlarda tüm vücut glikoz ve kortizol seviyelerini düşürdüğünü, nöral progenitör hücre belirteci DCAMKL1'i ise artırdığını göstermiştir. Genç hayvanlarda bu çoğalma destekleyici etkinin önünde mTOR aktivitesinin baskılanması yer alırken yaşlı hayvanlarda *foxm1* ifadesinin arttığı ve LC3-II/LC3-I oranı ile ölçülen otofajik akının azaldığı gözlemlenmiştir. Diğer tarafta rapamisin, metabolik parametreleri değiştirmemiş, genç ve yaşlı hayvanlarda tamamen farklı moleküler profillere sebep olmuştur. Genç hayvanlarda en kayda değer değişimler mTOR aktivitesi, LC3-II/LC3-I oranı ve geniş çaplı hücre çoğalması belirteci olan PCNA ifadesindeki azalmalar olmuştur. Yaşlı hayvanlarda ise etkinleştirilmiş astrosit belirteci (GFAP) seviyeleri düşmüş, bu durum nöroinflamasyonun azaldığını işaret etmiştir. Ayrıca PSD-95/Gephyrin oranı ile ölçülen eksitatör-inhibitör iletim dengesi eksitatör duruma kaymıştır. Bu bulgular, AO ve rapamisinin genç ve yaşlı hayvanlarda farklı metabolik profillere sebep olduğunu göstermiştir. Dahası hücre çoğalması ve otofaji arasında yaşa bağlı bir karşılıklı ilişki görülmüştür. Bu ilişkinin mTOR aktivitesinin ayrışık düzenlenmesine kısmen bağlı olması muhtemeldir. İlginç bir şekilde rapamisin muamelesi, mTOR aktivitesini baskılama konusunda genç hayvanlarda ve AO uygulamasına göre daha etkili olmuştur. Bununla birlikte elde edilen bulgular, rapamisinin zebra balığında kan-beyin bariyerini geçtiğini ve kısa süreli AO ve rapamisin uygulamalarının beyindeki kritik mekanizmalarda görevli anahtar proteinlerin ifade seviyelerini değiştirmeye yeterli olduğunu göstermiştir.

Anahtar Kelimeler: Yaşlanma, beyin, mTOR, aralıklı oruç, rapamisin, zebra balığı, metabolizma, nörogenez, glia, sinaptik iletim, otofaji

To my beloved family…

Acknowledgements

First and foremost, I would like to express my heart-felt gratitude to my advisor Professor Michelle Adams for providing a very productive environment along with her continuous support and guidance. It was a real privilege to be her PhD student. Her encouraging attitude helped me gain invaluable experience as a young scientist and I will always be grateful for everything I have learned from her.

I would like to thank my thesis committee members Associate Professor Ali Osmay Güre and Associate Professor Çağdaş Devrim Son for agreeing to be on my thesis progress committee and guiding me throughout the years. I am sincerely grateful for Associate Professor Özlen Konu and Assistant Professor Erkan Kiriş for kindly accepting to be on my thesis defense committee.

I thank the past and present members of the Adams Lab for their support, help and fruitful discussions that enriched our work environment. I thank Narin Ilgım Ardıç for patiently quantifying hundreds of Western blot images and helping with dissections, Elif Tuğçe Karoğlu Eravşar for helping me with the statistical analysis, Göksemin Fatma Şengül for her help during the feeding and drug treatment experiments, Melek Umay Tüz Şaşik for her guidance during the experimental procedures. I also thank Begün Erbaba, Hande Özge Aydoğan, Naz Mengi, Bilge Aşkın, Duygu Mutlu, Duygu Macaroğlu, Füsun Doldur Ballı and Ayşegül Dede. I would like to thank Bilkent University Molecular Biology and Genetics Department Zebrafish Facility manager Tülay Arayıcı and veterinarian Gamze Aykut for their excellent assistance with the animal care and experiments.

This work was supported by The Scientific and Technological Research Council of Turkey (TUBITAK) 1001 Research Program (Grant number: 214S236) that was awarded to Professor Michelle Adams (2015-2016), and later led by Assistant Professor Hulusi Kafalıgönül (2016-2018). I would like to thank Dr. Hulusi Kafalıgönül for his continuous support and valuable feedback. His positive attitude gave me strength that I will never forget. I am sincerely grateful for having an opportunity to work with him.

I would like to share my greatest gratitude with my MBG family: Verda Bitirim, Begüm Han Horuluoğlu, Gözde Güçlüler, Deniz Cansen Kahraman, Tamer Kahraman, Merve Mutlu, Gülşah Dal Kılınç, Büşra Yağabasan, Şeyma Demirsoy. I also thank my then mentors, now friends Sinem Yılmaz Özcan, Gurbet Karahan and Nilüfer Sayar Atasoy, and my then intern, now friend Beril Simay Üner. We had an incredible journey together and these memories will remain for the rest of my life. I feel very blessed to have met them.

Last but not least, I would like to express my endless gratitude to my amazing family for their love, support and encouragement. My parents Zuhal Çelebi and Yaşar Çelebi bought me my first microscope when I was only nine years old, and provided everything to help me pursue my dream of becoming a scientist. I am thankful for my brother Çağatay Çelebi for teaching me responsibility and unconditional love. I thank Güher Birand, Ayşegül Birand Özsoy, Nar Özsoy and Kerem Özsoy for being a great family to me. Finally, I am profoundly thankful to my dear spouse Can Birand, for his never-ending patience, incredible support and love. This would not have been possible without you.

Contents

Chapter 1 Introduction 1

1.1. Aging 1

1.2. Age-related functional and structural changes in the brain 3

1.2.1. Cognitive changes during normal aging 4

1.2.2. Age-related structural changes in the brain 5

1.3. Age-related cellular and molecular changes in the brain 9

1.3.1. Changes in synaptic integrity and composition 10

1.3.2. A primary hallmark of aging: Loss of homeostasis 18

1.3.3. Deregulated nutrient sensing in aging 19

1.3.4. Impaired neurogenesis and cell senescence 22

1.4. Anti-aging interventions 23

1.4.1. Dietary interventions 24

1.4.2. Pharmacological interventions 25

1.5. Zebrafish as a gerontological model 26

1.6. Aims of this thesis 27

Chapter 2 Materials and Methods 30

2.1. Materials 30

2.1.1. Reagents for drug treatment and dietary restriction experiments 30

2.1.2. Reagents for protein isolation 30

2.1.3. Western Blot reagents and antibodies 31

2.1.4. Quantitative Reverse Transcription Polymerase Chain Reaction (RT-qPCR) primers 34

2.1.5. Reagents for cortisol isolation and measurement of whole-body glucose 35

2.2. Methods 35

2.2.1 Animal Experiments 35

2.2.2. Protein Expression Experiments 42

2.2.4. Gene Expression Experiments 46

2.2.5. Body Cortisol Measurements 49

2.2.6. Whole-body Glucose Measurements 52

2.2.7. Statistical Analysis 52

Chapter 3 Results 55

3.1. Changes in the body weight and body mass index in response to different durations of treatment 55

3.1.1. Intermittent fasting decreases the body weight in old animals 55

3.1.2. Intermittent fasting decreases the body mass index in old animals 57

3.2. Changes in whole-body glucose and cortisol levels 58

3.2.1. Whole-body glucose levels decrease in animals subjected to intermittent fasting..... 58

3.2.2. Whole-body cortisol levels decrease in animals subjected to intermittent fasting..... 63

3.3. The suppression of mTOR activity through intermittent fasting and rapamycin treatment is age-dependent 65

3.3.1. Changes in the expression levels of total p-mTOR^{Ser2481}, 4E-BP1, p-4E-BP1, and p-4E-BP1/4E-BP1 in response to IF and RAPA..... 65

3.3.2. Changes in the expression levels of total S6, p-S6, and their ratio in response to IF and RAPA 68

3.4. The effects of intermittent fasting and rapamycin on the expression levels of key synaptic proteins, and markers of autophagy or proliferation 72

3.4.1. Changes in the expression levels of postsynaptic and presynaptic proteins involved in neurotransmission 72

3.4.2. Changes in the expression levels of autophagic flux markers 77

3.4.3. Changes in the markers of global proliferation, neurogenesis, and activated astrocytes..... 79

3.5. The expression levels of genes involved in the mTOR pathway, proliferation and autophagy 83

3.5.1. Changes in the expression levels of genes in the nutrient signaling pathway . 84

3.5.2. Changes in the expression levels of rapamycin-responsive genes..... 87

3.5.3. Changes in the expression levels of autophagy-related genes 89

3.6. Principal component analysis for the proteins and genes of interest 91

3.6.1. PCA for the protein expression data 91

3.6.2. PCA for the gene expression data 97

Chapter 4 Discussion 101

Chapter 5 Conclusion and Future Directions..... 113

Bibliography 118

Curriculum Vitae and Publications 145

Appendix..... 150

List of Figures

Figure 1.1. The World Health Organization's 2050 projections of the percentage of population over 60 years by country 1

Figure 1.2. Hallmarks of brain aging 10

Figure 2.1. Preparation of cortisol standard solutions through serial dilution 50

Figure 2.2. Workflow diagram for the statistical analysis. 53

Figure 3.1. Changes in the mean body weight and BMI in response to IF and RAPA treatment throughout 8 weeks. 56

Figure 3.2. Changes in the whole-body glucose levels in response to IF and RAPA treatment. 60

Figure 3.3. Changes in the whole-body glucose levels in response to different durations of IF and RAPA treatment 61

Figure 3.4. The levels of whole-body glucose normalized to trunk weight in response to IF and RAPA treatment 62

Figure 3.5. Changes in the whole-body cortisol levels in response to IF and RAPA treatment 64

Figure 3.6. Changes in the expression levels of p-mTOR^{Ser2481}, 4E-BP1, p-4E-BP1 and p-4E-BP1/4E-BP1 in response to IF and RAPA treatment in young and old animals. 66

Figure 3.7. Representative western blots for p-mTOR^{Ser2481}, 4E-BP1, p-4E-BP1 and β-tubulin in old experiment groups at 4, 6 and 8 weeks.. 68

Figure 3.8. Changes in the expression levels of S6, p-S6 and p-S6/S6 in response to IF and RAPA treatment 70

Figure 3.9. Changes in the p-S6/S6 ratio in response to different durations of IF and RAPA treatment. 71

Figure 3.10. Representative western blots for S6, p-S6 and β-tubulin in old experiment groups at 4, 6 and 8 weeks 71

Figure 3.11. Changes in the expression levels of PSD-95, GEP and PSD-95/GEP, and SYP in response to IF and RAPA treatment 74

Figure 3.12. Changes in the expression levels of GEP in response to different durations of IF and RAPA treatment 75

Figure 3.13. Representative western blots for PSD-95, GEP, β-tubulin and SYP in old experiment groups at 4, 6 and 8 weeks 76

Figure 3.14. Changes in the expression levels of LC3-I, LC3-II and LC3-II/LC3-I in response to IF and RAPA treatment 78

Figure 3.15. Representative western blots for LC3-I and LC3-II in old experiment groups at 4, 6 and 8 weeks 79

Figure 3.16. Changes in the expression levels of PCNA, DCAMKL1 and GFAP in response to IF and RAPA treatment 82

Figure 3.17. Representative western blots for DCAMKL1, GFAP, PCNA and β-tubulin in old experiment groups at 4, 6 and 8 weeks. 83

Figure 3.18. Log_2 fold change values in the expression levels of *ztor*, *akt1* and *igf1* transcripts encoding proteins in the nutrient signaling pathway. 85

Figure 3.19. Log_2 fold change values in the expression levels of *ztor* in response to

different durations of IF and RAPA 86

Figure 3.20. Log_2 fold change values of rapamycin-responsive genes *ddc* and *foxm1*. 88

Figure 3.21. Log_2 fold change values of autophagy-related genes *atg5* and *lc3b* 90

Figure 3.22. Log_2 fold change values of *lc3b* in response to different durations of IF and RAPA 90

Figure 3.23. Visualization of the samples on scatterplot matrices for the principal components of the significantly affected proteins obtained from PCA 96

Figure 3.24. Visualization of the samples on scatterplots for the principal components of the significantly affected genes obtained from PCA 99

Figure 3.25. Heatmaps for the gene expression data 100

Figure 4.1. Schematic representation of progenitor types identified by the proliferative marker expression in the adult brain. 107

Figure A.1. Copyright permission for Figure 1.1. 151

Figure A.2. Copyright permission for reuse of figures published in Rejuvenation Research 152

List of Tables

Table 2.1. Western blot antibodies and their working conditions 32

Table 2.2. Sequences and melting temperatures (T_m) of forward and reverse primers for RT-qPCR experiments 34

Table 2.3. Distribution of animals across experiment groups 37

Table 2.4. Feeding schedule for the experiment groups on odd weeks of the experiment..... 38

Table 2.5. Feeding schedule for the experiment groups on even weeks of the experiment..... 39

Table 2.6. BSA samples that were used as standards to measure protein concentrations. 43

Table 2.7. Reaction protocol for cDNA synthesis 48

Table 3.1. Eigenvalues, explained variance and component loading scores for each principal component of protein expression data……92

Table 3.2. Correlation coefficients and significance levels of the correlations for the protein expression data 93

Table 3.3. Letter coding for the proteins in Table 3.2 94

Table 3.4. Eigenvalues, explained variance and component loading scores for each principal component of gene expression data..... 97

Table 3.5. Correlation coefficients and significance levels of the correlations for the gene expression data 98

Abbreviations

4E-BP1	eIF4E-binding protein 1
ABP	AMPA binding protein
AD	Alzheimer's Disease
AI	Aged cognitively impaired
AKT1	AKT serine/threonine kinase 1
AL	*ad libitum*-fed
AMP	adenosine monophosphate
AMPA	alpha-amino-3-hydroxy-5-methyl-4-isoxazole propionic acid
AMPAR	AMPA-type receptor
AMPK	AMP-activated protein kinase
ANOVA	Analysis of variance
APS	Ammonium persulfate
ATG5	Autophagy-Related 5
AU	Aged cognitively unimpaired
BMI	Body mass index
BrdU	Bromodeoxyuridine
BSA	Bovine serum albumin
B_0	Zero standard
CA	Cornu ammonis area
CaM kinase	Ca^{2+}/calmodulin-dependent protein kinase
cDNA	Complementary DNA

CI	Cognitive impairment
CNS	Central nervous system
CR	Caloric restriction
C_t	Cycle threshold
DCAMKL1	Doublecortin-like kinase 1
DDC	Aromatic-L-amino-acid-decarboxylase
ddH_2O	Double-distilled water
DG	Dentate gyrus
DMSO	Dimethyl sulfoxide
DNA	Deoxynucleic acid
DPBS	Dulbecco's phosphate-buffered saline
DR	Dietary restriction
DTT	Dithiothreitol
EC	Entorhinal cortex
E/I	Excitatory-inhibitory
eIF4E	Eukaryotic translation initiation factor 4E
FDA	The Food and Drug Administration
FKBP12	12-kDa FK506-binding protein
FOXM1	Forkhead Box M1
GABA	γ-aminobutyric acid
GEP	Gephyrin
GFAP	Glial fibrillary acidic protein
GLUT	Glucose transporter
GRIP	Glutamate receptor-interacting protein
IF	Intermittent fasting

IGF-1	Insulin-like growth factor 1
KMO	Kaiser-Meyer-Olkin Measure of Sampling Adequacy
MAP1LC3	Microtubule-associated protein 1A/1B light chain 3
mEPSC	Miniature excitatory postsynaptic current
mIPSC	Miniature inhibitory postsynaptic current
MM	Master mix
mTOR	Mammalian target of rapamycin
mTORC1	mTOR complex 1
mTORC2	mTOR complex 2
NMDA	*N*-methyl-d-aspartate
NMDAR	NMDA-type receptor
NO_3	Nitrate
NPC	Neural progenitor cell
NSB	Non-specific binding
NSC	Neural stem cell
O.D.	Optical density
PC	Principal component
PCA	Principal component analysis
PCNA	Proliferating cell nuclear antigen
PFC	Prefrontal cortex
PI3K	Phosphoinositide 3-kinase
pMM	Master mix containing primer pairs
POI	Protein of interest

PSD	Postsynaptic density
PSD-95	Postsynaptic density protein 95
PVDF	Polyvinylidene fluoride
RAPA	Rapamycin-treated group
RNA	Ribonucleic acid
RT-qPCR	Quantitative reverse transcription polymerase chain reaction
S6	Ribosomal protein S6
SDS	Sodium dodecyl sulfate
SE	Standard error
SGL	Subgranular layer
SVZ	Subventricular zone
SYP	Synaptophysin
TBS	Tris buffered saline
TBS-T	TBS-Tween20
TEMED	N,N,N',N'-tetramethylethane-1,2-diamine
T_m	Melting temperature
TOR	Target of rapamycin
WHO	World Health Organization

Chapter 1

Introduction

1.1. Aging

The populations are rapidly aging across the world. The accelerated rates of aging are due to reduction of childhood mortality in the low-income countries, and lower levels of mortality among older individuals in the high-income countries. This increase in average life expectancy is projected to lead to a doubling of the proportion of people aged 60 years or older by 2050 [1].

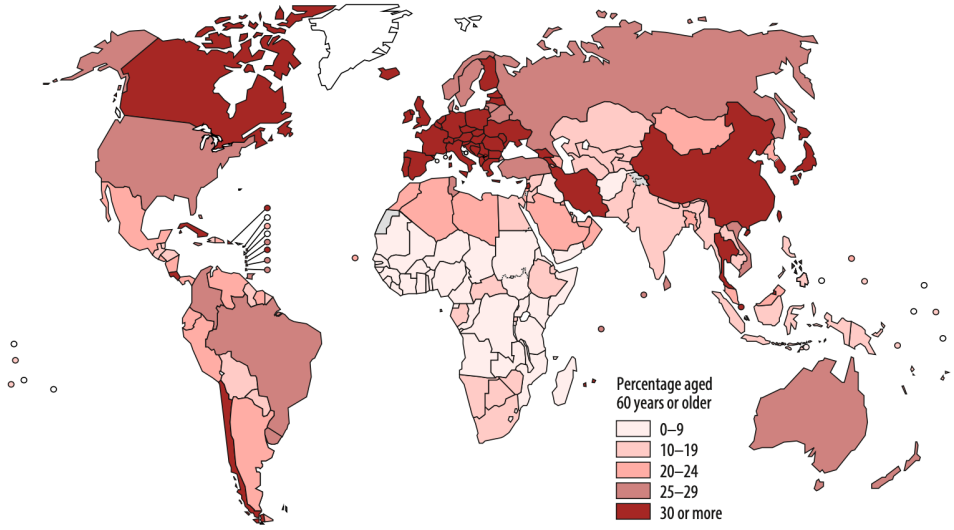

Figure 1.1. The World Health Organization's 2050 projections of the percentage of population over 60 years by country. Reprinted from the *World report on ageing and health*, ISBN: 978 92 4 156504 2, WHO, Demographic and epidemiological changes / Health in older age, Page 44, Copyright (2015), and with permission from WHO**.**

Living longer has been one of the greatest aspirations of humans for centuries, however, the life span increase is not without consequences. Aging has profound effects on health, societies, and global economy. The increased requirement for health care and inability to lead an independent lifestyle either due to age-related diseases or declines in certain abilities alter the society dynamics. Increased life expectancy without extending the healthy life span (i.e. health span) will lead to a larger proportion of people that is dependent on health care for a longer period of time. Furthermore, every individual ages differently, and the contribution of older people to the society is limited due to outdated stereotypes [2]. Therefore, there is an urgent need to develop strategies that will reduce the burden on healthcare providers and funding bodies and improve the quality of life in aging population.

The World Health Organization (WHO), launched an action plan on "*Healthy Ageing 2020-2030*" in 2015 for preserving the physical and cognitive capacity in the aged population, while providing a better and a safer environment for the elderly [2]. Good health and wellbeing through a healthier lifestyle (e.g. better nutrition, exercise) has been one of the steps that was listed in this multisectoral and international action plan. As a consequence, this necessitates a clear dissociation of healthy aging from pathological aging. Understanding the normal course of aging in

the absence of age-related diseases is therefore vital for managing the issues of older people. This approach may not only help us interpret the dysfunctional biological processes that lead to pathological aging, but also benefit from building an age-friendly environment that will facilitate the integration of older population in the society in a more effective manner.

1.2. Age-related functional and structural changes in the brain

Advancing age is associated with many major changes in the body. These include but are not limited to: Gradual decline in cognitive function [3], changes in body composition and loss of muscle mass (i.e. sarcopenia) [4], deterioration of the collagen network and bone density [5], changes in cardiovascular structure and function [6], and immunosenescence [7]. While these changes have pathological implications such as cardiovascular and metabolic diseases, they are also observed during the course of normal aging. Understanding how advancing age affects this vast variety of processes will contribute to our search for finding the fine line between normal and pathological aging and facilitate development of palliative therapies.

Among these age-related changes, understanding how cognitive function deteriorates with age is particularly important since maintenance of cognitive skills is crucial for communication and independent lifestyle. Therefore, investigating the cellular and molecular correlates of the cognitive skills that are especially prone to age-related decline is very important. Identification of the mechanisms underlying critical

functional processes, and their alterations with respect to age will provide us with therapeutic targets.

1.2.1. Cognitive changes during normal aging

Cognitive impairment (CI) is among the most common conditions that are observed during aging. The prevalence of CI was reported as 37% in people >60 years in Iran [8], 19% in people >65 in Spain [9], 12.6% in people <60 years in the People's Republic of China [10], and 25% in people aged >50 in India [11]. The level of CI ranges from mild to severe, and mild CI is often associated with normal aging. The manifestations of CI include deficits in short-term memory, difficulty in finding words, and decrease in processing speed [12]. A nascent form of dementia has been linked to CI, however, recent studies suggested that mild CI is not always proceeded by dementia [13]; and although mild CI might be regarded as a transition between normal aging and dementia, they are in fact different paradigms [12], [14].

Cognitive domains that measurably decline with age are attention, executive function, language, memory, and sensory perception [15]. Another cognitive skill that is affected by age is learning potential, also known as cognitive plasticity. Advancing age has been associated with lower performance in tasks related to verbal memory [16]. However, there are also domains and abilities that do not change with age. For example, general knowledge, vocabulary and sensory memory are stable with age [15]. Therefore, there is a need to dissociate these functional domains and understand the biological processes that stabilize them or cause their deterioration during aging.

1.2.2. Age-related structural changes in the brain

Aging is associated with numerous structural, cellular and molecular changes in the brain. While the debate over the ultimate consequences of these changes still continues, and it is not clear whether age-related deterioration in the brain is inevitable, the quest for finding remedies persists. One thing we have learned so far is that these changes are heterogeneous, and certain types of cells and brain areas are more prone to accumulation of damage than others [17]. The complexity of alterations, and their dramatically diverse effects on cognitive skills limit the potential to come up with a uniform approach. Nevertheless, targeting each contributor or a combination of them might prove useful in our fight against aging.

1.2.2.1. Neuron number

Neurons have been long considered as the primary target of age-related changes that underlie cognitive decline. Therefore, the effects of advancing age on the number of neurons, their structure (e.g. axons, dendrites, and even the cell body), and function have been extensively studied. The initial hypothesis was that aging causes significant neuron and synapse loss, which leads to the detrimental effects on cognitive abilities.

This conviction was in fact based on observations from as early as 1955, suggesting a significant amount of neuron death in aged humans [18]. These calculations relied on measuring neuron density in a given area. However, Coleman and Flood presented the limitations of this approach in a detailed review [19]. In this 1987 review, they listed a number of factors such as species, strains, as well as tissue

processing and counting methods that could potentially introduce a bias. This revelation was owing to the advances in technology and development of more sophisticated counting methods [20] involving morphometric procedures [21]. Later, stereological methods were introduced for more accurate and unbiased estimation of the neuronal changes during aging [22].

The studies using these techniques revealed species-, region- and cell-type-specific neuron loss during aging. In humans, a significant decrease in neuron number was observed in the subiculum (52%) and hilus (31%) of the dentate gyrus, respectively [23]. While the Cornu Ammonis area 1 (CA1) of the hippocampus showed a substantial neuron loss in the patients with Alzheimer's Disease (AD), it was not affected by normal aging [24]. H. Haug reported that the number of human cerebral cortex neurons does not change or experience only a small decrease during aging. The only exception was extrapyramidal human cortex (area 6), which is implicated in motor activity and showed signs of aging earlier than other areas [25].

More recent studies supported the notion that there is no strong evidence for significant decline in the neuron number in the human entorhinal cortex and subregions of rat hippocampus during aging that could translate into a biologically meaningful effect on cognitive skills [26], [27]. Entorhinal cortex (EC) is a part of the hippocampal memory system, connecting the hippocampus and neocortex, and EC has been shown to be severely affected in the brains of AD patients, but not in normal aging groups [26]. Neuron loss was also absent in other areas related to learning and memory such as neocortex, superior prefrontal cortex and temporal cortex in normally aged humans and primates [28].

1.2.2.2. Dendrites

Structural changes in the brain during aging are not limited to the neuron number. Dendrites, the extensions of neurons that are assigned with the crucial task of receiving signals from neighboring cells and propagating them to the soma, are also prone to age-related changes. Dendrites are highly dynamic, particularly during development, and retain their plastic nature into adulthood. Dendritic branches, density, and patterns contribute to the neuron function since dendrites constitute up to 95% of the receptive surface, and distinct morphologies were observed in different types of neurons [19], [29].

Several studies reported increase in dendritic proliferation during normal aging in human and macaque monkey [30], [31]. The extent of dendritic branches were larger in nondemented old humans (average age, 79) compared to younger adults (average age, 51), and people with senile dementia (average age, 76) [30]. In the prefrontal cortex neurons of macaques, the number of branches and dendritic length increased significantly from young to middle age, followed by a highly significant decrease towards old age [31]. Since the maintenance of dendritic structure is critical for the survival of neurons, the increasing pattern has been suggested as a compensatory mechanism for the age-related decrease in neuron number that protect the integrity of the functional compartments in the brain [30].

On the contrary, later studies revealed opposite patterns in different regions. For instance, dendrites of the pyramidal neurons in the human motor cortex regressed with age [32]. In Sprague-Dawley rats, loss of dendrites was observed in auditory

cortex [33], further supporting that these patterns were both species/strain- and region-specific.

1.2.2.3. Synapses

Albeit the initial view on significant neuron and dendrite loss in the whole brain has been replaced with a refined hypothesis of asynchronous region-specific changes during aging, scientists continued to observe gray and white matter loss during normal human aging [34]–[36]. These findings drove the attention to structural changes in another important component of the neurons involved in connectivity: synapses. Some studies reported a decrease in synapse density with age in the neocortex of humans with AD [37] as well as the number of presynaptic terminals in the frontal cortex of people without dementia [38]. In rat dentate gyrus (DG), a subregion in the hippocampal formation that has been linked to learning and memory, a significant decrease in synapse number and density has been shown [39]. However, adding to the controversy, later studies with unbiased counting methods using electron microscopy instead of light microscopy concluded that the synapse number per neuron was not affected by age [40].

Taken together, the lack of major changes during normal aging in humans, nonhuman primates and rodents suggests that learning and memory deficits in old individuals of these species are likely to arise from more subtle changes rather than large scale structural rearrangements. Growing evidence indicates that cellular and molecular mechanisms might contribute to functional deteriorations in the aging

brain more than initially anticipated. Some of these mechanisms will be covered with regard to aging in section 1.3.

1.3. Age-related cellular and molecular changes in the brain

Recent advances in aging research provided evidence that the course of aging is controlled, at least in part, by evolutionarily conserved cellular, genetic and molecular processes. These include the changes in synaptic elements involved in neurotransmission, which are restricted to the nervous system, as well as global mechanisms that affect peripheral and nervous tissues. In their 2013 review, López-Otín et al. defined these changes as "the hallmarks of aging" and grouped them into three categories: Primary, antagonistic, and integrative hallmarks [41].

The primary hallmarks are regarded as the main contributors to aging phenotype. These are genomic instability, telomere attrition, epigenetic alterations, and loss of homeostasis. The antagonistic hallmarks are thought to initially protect against cellular damage; however, their chronic activation eventually becomes detrimental. Deregulated nutrient sensing, mitochondrial dysfunction, and cellular senescence fall into this category. Finally, integrative hallmarks are the phenotypical consequences of the first two categories. These are stem cell exhaustion and altered intercellular communication, which are the manifestations of age-related loss of function.

Most of these hallmarks are evident in the aging brain. However, since brain has a unique energy metabolism, its dysregulation is likely to be the major factor in determining brain health status. Taking this into account, Mattson et al. defined ten

hallmarks of brain aging as nine established hallmarks interacting with dysregulated energy metabolism in their 2018 review (Figure 1.2) [42]. Some of these hallmarks that are relevant to the scope of this thesis will be reviewed here.

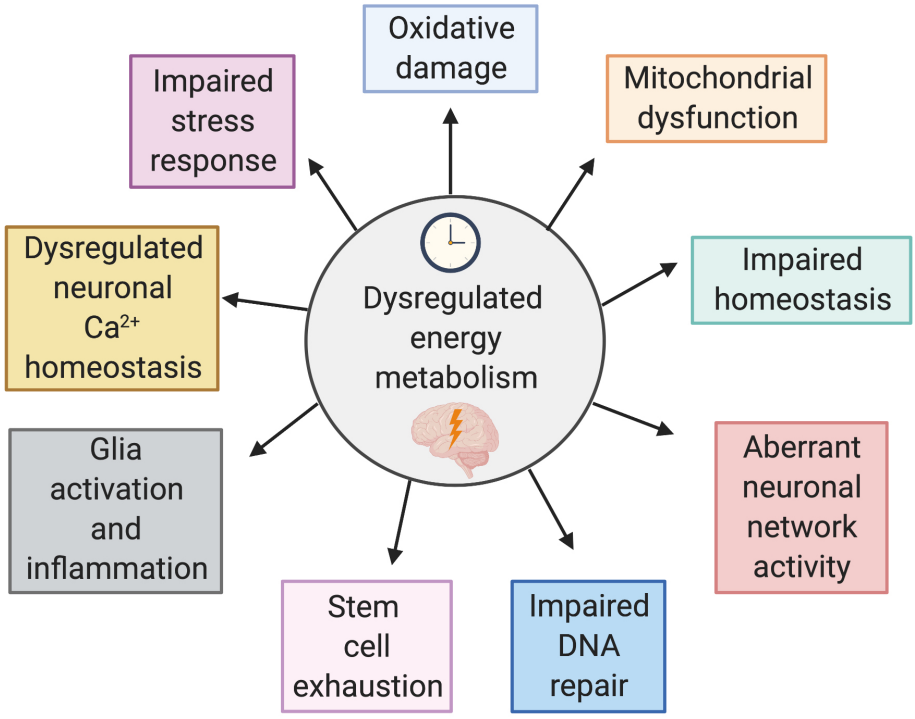

Figure 1.2. Hallmarks of brain aging. The illustration is adapted from Mattson et al.'s 2018 review [42], and created with BioRender.

1.3.1. Changes in synaptic integrity and composition

Synaptic transmission is a key factor in neuronal circuitry and function. Deficiencies in both the presynaptic and postsynaptic elements have severe consequences that impair the synaptic functioning. Therefore, understanding the molecular mechanisms that take place in both elements, and finding how these mechanisms change during

normal aging could provide us with appropriate targets to prevent or reverse age-related cognitive decline.

The intercellular communication at the synapses, by the simplest definition, are carried out by the synaptic vesicles carrying neurotransmitters at the presynaptic site, and their receptors at the postsynaptic site. Many processes occur at both sites to transmit, receive, and process the signal, and hundreds of proteins are required to work in harmony to ensure the efficiency of communication. Some of the key proteins, their functions, and how they change in response to advancing age will be reviewed in this section.

1.3.1.1. Presynaptic elements

One of the most critical components of the presynaptic site are the membranous organelles called synaptic vesicles. These vesicles have an essential role in transforming the electrical stimulus that is propagated in the cell body into chemical signals by storing the neurotransmitters that are produced in the presynaptic cell. When the action potential arrives at the nerve terminal, voltage-gated Ca^{2+} channels allow Ca^{2+} influx. The change in membrane potential triggers the fusion of vesicles with the plasma membrane, and neurotransmitters are released into the synaptic cleft through exocytosis. Empty vesicles are retrieved by endocytosis, recycled and refilled with neurotransmitters to be utilized in another round of exocytosis [43], [44].

The release of neurotransmitters from synaptic vesicles is mediated by different proteins that are either embedded in the lipid bilayer of vesicular membrane (e.g. synaptophysin, synaptotagmin and proteins with SNARE motifs such as synaptobrevin) or proteins associated with the cytoplasmic surface of vesicles (e.g. synapsins I-II and Ca^{2+}/calmodulin-dependent protein kinase (CaM kinase) II) [43]. In this complex pool of proteins with distinct functions and binding partners, it is important to differentiate the constant factors from the ones with a rather supporting role. Studies approaching this process from a "vesicocentric" point of view revealed components that are present in majority, if not all, of the vesicles [44].

The SNARE proteins, Rab5, and synaptophysin are among the obligatory components [44]. Of these, synaptophysin is a major integral protein spanning the vesicle membrane and is involved in vesicle fusion and neurotransmitter release. As a substrate for protein kinases including CaM kinase II, its phosphorylation status is implicated in vesicle docking and recycling [43]. Furthermore, when in a complex with synaptobrevin, synaptophysin has been shown to provide a pool of available vesicles during development and synapse maturation [45]. Therefore, it is often regarded as a marker of synaptic vesicles and integrity.

Growing evidence link changes in synaptophysin expression to age-related cognitive decline [46]. For instance, cognitively impaired aged (AI) rats had reduced synaptophysin immunoreactivity in the CA3 region of hippocampus, relative to young or cognitively unimpaired aged (AU) animals [47]. Synaptophysin protein levels were significantly lower in people with dementia compared to nondemented controls, although there was no correlation between age and synaptophysin

expression [48]. Furthermore, in both humans with AD [49] and rodent models of AD [50], synaptophysin levels were reduced in hippocampus. The age-related decline in synaptophysin expression was also evident during normal aging in different subregions of rat hippocampus [51].

1.3.1.2. Postsynaptic elements

Spines are extensions of the neurons that may protrude from the soma, dendrites, or the axon hillock, and are specialized structures for synaptic transmission [52]. Receptors for the neurotransmitters are mostly localized to a cytoskeleton-bound matrix of receptor-associated proteins found in spines [53]. These matrices contain proteins that facilitate clustering of receptors and anchoring them to the plasma membrane, as well as signaling molecules that process and transduce the input to downstream cascades. The contents of a matrix therefore dictate its function.

Postsynaptic density (PSD), for instance, is predominantly a marker of excitatory synapses. As one of the most complex structures found in spines, PSD is estimated to harbor hundreds of receptor, adaptor, and signaling proteins [54]. The two types of ionotropic receptors for the major excitatory neurotransmitter in the central nervous system (CNS), glutamate, are *N*-methyl-d-aspartate (NMDA) and alpha-amino-3-hydroxy-5-methyl-4-isoxazole propionic acid (AMPA). Although both the NMDA and AMPA type receptors (NMDAR and AMPAR, respectively) have been observed within PSD, NMDARs are consistently found while AMPAR content varies highly, and some excitatory synapses completely lack AMPARs [55].

Both the NMDARs and AMPARs are composed of subunits with distinct ligand sensitivity profiles, kinetic properties and interaction partners [56], [57]. Assembly patterns of these subunits define the key features and functions of NMDARs and AMPARs. Not surprisingly, the expression levels of both NMDAR and AMPAR subunits have been shown to be affected by age. Age-related declines were observed in the expression levels of NR1, NR2A and NR2B subunits of NMDAR and the GluR1 and GluR2 subunits of AMPAR in the CA3 region of rat hippocampus [58], and of NR1 and GluR2 in the neocortex of macaques [59].

On the opposite side of the glutamatergic excitatory systems is the inhibitory neurotransmission. The primary inhibitory neurotransmitter in the mammalian CNS is γ-aminobutyric acid (GABA). There are three classes of GABA receptors: $GABA_A$, $GABA_B$ and $GABA_C$. The majority of fast inhibitory transmission is mediated by $GABA_A$, whose action is in a dynamic balance with fast excitatory transmission [60].

$GABA_A$ channels form a pentameric structure that is assembled by different subunits, and contains an intrinsic Cl^- channel [60]. The types of subunits in a $GABA_A$ receptor not only determine the receptor function and drug responses in pharmacological studies, but also the cellular localization of the receptor. Although the $GABA_A$ receptors are predominantly postsynaptic, they have been also observed in presynaptic and extrasynaptic locations as a consequence of their subunit composition [61].

There are contradicting reports on the age-related changes in GABAergic neurotransmission. Both GABA and $GABA_A$ receptor levels were reported to be unchanged in the brains of aging rats [62]. Studies measuring receptor binding suggested different patterns for the binding affinity of GABA receptors: binding decreased in the brains of aging rats in one study [63], and was not affected in another [64]. In humans, GABA receptor number was increased while the GABAergic terminal density was decreased during aging [65]. These inconsistent observations compelled the researchers to try a different approach for investigating age-related changes in neurotransmitter dynamics. Since both the excitatory AMPA and NMDA, and inhibitory GABA receptors require clustering proteins for cellular localization, stability, and functional regulation, studies inclined towards measuring their levels [66]–[68].

The NMDA-type ionotropic glutamate receptors interact with the PDZ domain of postsynaptic density protein 95 (PSD-95) via the C-terminal of NR2 subunit. As mentioned earlier, PSD harbors many proteins, however PSD-95 has been shown to be the main component of these postsynaptic excitatory scaffolds, and the localization of NMDA receptors in postsynaptic site requires intact PSD-95 [69]. On the other hand, AMPA-type receptors, although colocalize with NMDA-type receptors in PSD, bind to other proteins containing PDZ domain. These include glutamate receptor-interacting protein (GRIP) and AMPA receptor-binding protein (ABP) [66].

The clustering of GABA receptors at postsynaptic sites are mainly mediated through gephyrin. Initially, gephyrin was thought to be in an interaction exclusively with the receptors for another inhibitory neurotransmitter: glycine [68]. More recent studies involving pharmacological agents or mutants lacking either gephyrin or $GABA_A$ receptor subunits suggested that gephyrin is essential for the stabilization of $GABA_A$ [70].

Advancing age has been associated with changes in postsynaptic clustering proteins. In humans, PSD-95 protein level was found to be positively correlated with age [48]. In the pathological cases of cognitive impairment in rats [71] or AD in humans [72], the expression of PSD-95 was reduced, yet other studies showed either increase or no change in PSD-95 protein levels [73], [74]. Although these opposing observations could be due to regional differences, contradictory data exists even for the same brain regions.

The reports on gephyrin are also conflicting, since there were species- and region-specific patterns during aging. For instance, gephyrin levels were stable across life span in zebrafish [75]. On the contrary, gephyrin clusters became more prominent in mature synapses as compared to young synapses during synaptogenesis in rat cerebellar cortex [76]. Furthermore, age-related increases in gephyrin protein levels and message were observed in dorsal cochlear nucleus, suggesting a mechanism for hearing loss [77], and in AI rats [71]. In addition to changes observed in normal aging, gephyrin have been shown to accumulate in the brains of humans with AD [78], although another study suggested the complete opposite pattern of a significant global decrease in postmortem brains [79].

1.3.1.3. Excitatory-inhibitory balance

Recent studies suggested that the balance between excitatory and inhibitory neurotransmission is as equally imperative as the expression levels of neurotransmitter receptors and clustering proteins in cognitive functioning. Maintenance of the excitatory-inhibitory (E/I) balance is an integral part of neuronal plasticity, learning, memory and behavior. The data obtained via electrophysiological and biochemical methods showed that E/I imbalance is associated with age-related cognitive decline [80].

In aged humans, increased prefrontal cortex (PFC) activity has been shown to correlate with memory impairments. This increase was attributed to lower E/I ratio due to higher inhibitory tone in old cohort as compared to young cohort, which had a stable E/I ratio [80]. In AI rats, electrophysiological recordings of miniature excitatory and inhibitory postsynaptic currents (mEPSCs and mIPSCs, respectively) showed a decrease in mEPSCs [81] or enhanced mIPSCs [82], suggesting an imbalance in E/I due to a shift towards inhibition. Furthermore, studies investigating the ratio of excitatory and inhibitory clustering proteins reported a significant decrease in PSD-95/gephyrin density in AI rats compared to young cohort, but not AU animals [83].

On the contrary, a declining trend in intrinsic inhibitory tone during aging has been observed in non-human primates and rats [77, 81]. This observation was also supported by the 30-60% reduction in synapse density in prefrontal layer I, whose major content is GABAergic neurons [80]. Other studies that reported a reduced

inhibition in aged animals indicate region- and species-specific changes, as well as the impact of individual differences in cognitive skills [85].

Nevertheless, E/I imbalance appears to be the common denominator regardless of the direction. Considering the part that E/I takes while responding to plastic changes driven by intrinsic and environmental factors, the imbalance pertains to cognitive decline. Therefore, the measures that are taken for slowing down or reversing the brain aging must take E/I balance into account.

1.3.2. A primary hallmark of aging: Loss of homeostasis

The hallmarks of aging as described by López-Otín et al. were principally based on the widely accepted idea that aging is accompanied, if not caused, by the accumulation of damage over time [86]. A chief mechanism that has been linked to age-related diseases through damage control is the protein homeostasis, also known as proteostasis. The proteome quality and functionality is ensured by the intrinsic control mechanisms that stabilize newly synthesized proteins, detect unfolded proteins, and target them for degradation through proteolytic pathways [87].

There are two main mechanisms for regulating the proteome quality: autophagy-lysosome and ubiquitin-proteasome pathways. Moreover, both have been shown to exhibit decreased activity in aged models [88], [89]. While mutant models with proteasome or autophagy inhibition showed phenotypes that resemble age-related pathologies, the life span extending interventions or genetic manipulations have been shown to initiate autophagic and proteolytic cascades [88].

Of these interventions, which will be covered in section 1.4., rapamycin treatment promotes longevity particularly through induction of autophagy [90]. Moreover, life span extension via rapamycin strictly requires autophagy induction in *Caenorhabditis elegans* and *Drosophila melanogaster*, yet the mechanisms in mammals are more complex and involve additional pathways such as inhibition of protein synthesis [88]. Autophagy is therefore a protective, rather than a destructive mechanism, and aberrant autophagy has been observed in accelerated aging models [91].

Removal of damaged/dysfunctional molecules is particularly important for neurons since they are post-mitotic, and generation of new neurons is limited and restricted to a few areas in the adult brain. Age-related impairments in waste management through autophagic and proteasomal mechanisms are evident in the brain. Several studies reported accumulation of autophagosomes and polyubiquitinated proteins, mitochondrial dysfunction in neurons [42]. Furthermore, aggregation of damaged molecules is established as an early step in the events that lead to neuronal death [92]. Thus, defective homeostatic mechanisms have been implicated in both normal and pathological aging.

1.3.3. Deregulated nutrient sensing in aging

Extracellular and intracellular nutrient levels are ever-fluctuating in response to environmental ques. The ability of the cells to sense these changes and initiate appropriate downstream cascades is a key step in survival. Elaborate mechanisms have thus evolved to detect levels of macronutrients such as amino acids, glucose and other sugars, and lipids. These could be summarized as anabolic reactions that

allow storage during nutrient abundance, and catabolic mechanisms that utilize internal reserves through autophagy or proteasome-mediated degradation when nutrient levels are scarce [93].

The brain has a considerably higher metabolism level and energy requirement than other organs, making it more sensitive to fluctuations in nutrient levels [94]. Different mechanisms are integrated through hormonal signals to fulfill the brain's energy needs, especially under conditions of nutrient limitation. For instance, starvation leads to degradation of amino acids to synthesize glucose and ketone bodies, which are brain's fuels [93].

Glucose sensing involves glucose transporters (GLUTs) at the plasma membrane and insulin/insulin-like growth factor 1 (IGF-1), adenosine monophosphate (AMP)-activated protein kinase (AMPK), and phosphoinositide 3-kinase (PI3K)-AKT pathways both at the membrane and intracellular domains [41], [93]. One of the significant proteins at the intersection of amino acid and glucose sensing, as well as autophagy is the target of rapamycin (TOR).

1.3.3.1. TOR signaling

TOR, as the name indicates, is the target of rapamycin: a macrolide compound. First isolated from a microorganism called *Streptomyces hygroscopicus*, which has been found in soil samples from Easter Island (Rapa Nui), rapamycin was initially identified as an antifungal compound [95]. Subsequent studies revealed that rapamycin is also an immunosuppressant and a potent inhibitor of cell growth, which

attracted attention as a valuable tool to investigate proliferation. These studies led to the identification of its molecular target (i.e. TOR) in yeast [96]. Shortly after, TOR homolog has been identified in mammals [97], and named mammalian target of rapamycin (also known as mechanistic target of rapamycin, mTOR). Interestingly, it is now known that mTOR is an evolutionarily conserved serine-threonine kinase belonging to the PI3K family [98], having homologs in *Caenorhabditis elegans*, *Drosophila melanogaster*, and in zebrafish (*Danio rerio*) [99]–[101]. In addition to its critical role in transitioning from anabolic to catabolic programs, TOR is involved in numerous cellular mechanisms including transcription, translation, proliferation, growth and survival [102].

mTOR is known to interact with many proteins in two multiprotein complexes, the mTOR complex 1 (mTORC1) and mTOR complex 2 (mTORC2) [103]. Both the amino acid and glucose sensing activities are suggested to be conveyed through mTORC1. For instance, mTORC1 promotes anabolic processes such as protein and lipid synthesis during nutrient abundance [104]. Insulin-IGF-1 pathway activation triggers the upstream effectors of mTORC1: PI3K-AKT.

Acute rapamycin treatment inhibits mTORC1 by interacting with the 12-kDa FK506-binding protein (FKBP12), a component in mTORC1, and disrupting the assembly of the protein complex. Although mTORC2 has been regarded as rapamycin-resistant, growing evidence suggest that its function is impaired by prolonged exposure to rapamycin [105]. The notion that deregulated nutrient sensing is a hallmark of aging originates from life and health span-extending effects of

mTOR inhibition through both genetic manipulations, and non-genetic interventions such as rapamycin and dietary restriction (DR).

With regards to brain aging, mTOR signaling has been implicated in regulation of synaptic protein synthesis through integrating signals relayed by neurotransmitter receptors at the postsynaptic sites [106]. Moreover, postsynaptic scaffolding proteins PSD-95 and gephyrin have been shown to be coupled with mTOR pathway, with gephyrin being an actual binding partner of mTOR [107], [108]. Noting the necessity for a balanced energy metabolism during healthy brain aging, mTOR is undeniably a key factor connecting nutrient signaling and autophagy to brain-specific programs such as synaptic protein synthesis and neurotransmission [109].

1.3.4. Impaired neurogenesis and cell senescence

While brain was once thought to not have a regenerative capacity, the evidence for neural stem cells (NSCs) in the adult brain suggest otherwise. Adult NSCs have the capacity for self-renewal and proliferation, and through the latter mechanism they give rise to neural progenitor cells (NPCs). Neuronally-committed NPCs undergo several cycles of cell division before they differentiate into neurons and glia. Although the neurogenic zones are restricted to a few areas in the adult brain such as the subventricular zone (SVZ) and subgranular layer (SGL) of DG, the potential they harbor for plasticity is promising [110].

The generation of new neurons in SVZ and SGL declines with age, however reports on cell proliferation rate suggest species-specific differences [111]. Whether the reductions in neurogenesis contribute to cognitive impairment is also not clear.

Hippocampus is one of the regions that is affected by age-related molecular changes which may lead to functional decline, yet it contains a well-defined neurogenic region. Some studies even suggested an inverse correlation between the maintenance of hippocampal neurogenesis and preservation of cognitive skills in rats [112], indicating a need for further investigations.

Still, understanding the mechanisms that cause age-related decline in the neurogenesis is necessary to assess to what extent the newly generated neurons are incorporated into functional circuits in the aging brain. Several mechanisms have been proposed as the basis for impaired neurogenesis. These are reduced mitochondrial metabolism, oxidative stress, accumulation of deoxyribonucleic acid (DNA) damage and impaired repair mechanisms, as well as inflammation [42]. In relation to these changes, increased number of senescent neural progenitor cells has been observed during aging. Interestingly, some NPCs might be destined to become senescent since isolated human NPCs have been observed to undergo senescence in vitro [113].

1.4. Anti-aging interventions

As we continue to uncover the changes that occur during aging, some mechanisms have emerged as potential therapeutic targets to reverse or slow down age-related functional deterioration. Several genetic, dietary, and pharmacological interventions have been shown to extend life and health span across species. Since the main concern with these approaches is the translational potential, and the genetic

manipulations that yielded long-lived mutants is not applicable in humans, many studies focused on dietary and pharmacological remedies.

1.4.1. Dietary interventions

The longevity-promoting effects of dietary restriction (DR), or caloric restriction (CR) have been reported as early as 1935 [114]. DR has been shown to reliably extend life span in a broad range of organisms, from yeast to primates, thus suggesting evolutionarily conserved responses [115]. These include improved glucose regulation, increased resistance to stressors, suppressed inflammation, activation of repair programs, and attenuation of cellular damage [116], [117]. At the cellular level, the master regulator of these responses is the nutrient sensing pathway which is seemingly centered around mTOR signaling.

The traditional DR approach follows a moderate reduction of daily calorie intake without causing malnutrition. When the *ad libitum* food intake of rodents was reduced by 30-60%, both the average and maximal life span increased. The onset of age-related diseases was delayed in calorically-restricted animals, and their prevalence decreased [117].

Later studies introduced intermittent fasting (IF) as an equally effective approach as reducing the daily calorie intake for extending life span. This is achieved through mTOR inhibition, and subsequent induction of autophagy which leads to removal of damaged molecules and overall cellular homeostasis. As a mechanism regulated by mTOR, IF reduces global protein synthesis [116]. One of the earliest reports of the IF-induced longevity showed 83% increase in life span of rats that have been

maintained on alternate-day feeding, an IF regimen [118]. Furthermore, IF promotes healthy aging by enhancing multiple cognitive domains such as learning and memory, and reversing effects of age-related diseases [119].

1.4.2. Pharmacological interventions

Experimental evidence from long- and short-lived mutants acknowledged the role of mTOR on life span. Lifespan extension by introducing mutations in mTOR gene was achieved in different organisms such as budding yeast (*Saccharomyces cerevisiae)*, worm (*Caenorhabditis elegans)*, fruit fly (*Drosophila melanogaster*), and mammals [109]. These data provided grounds that mTOR inhibition might slow down aging.

Rapamycin, which has been approved for use in humans by the U.S. Food and Drug Administration (FDA) [120] is a potent, well-characterized inhibitor of mTOR. It is now established that rapamycin extends life span, delay age-related impairments, and improve parameters of health [109]. As an autophagy-inducing agent, rapamycin has been suggested to prevent cognitive impairment by counteracting the accumulation of misfolded proteins in mouse models of AD. Furthermore, rapamycin seems to augment vascular function and hinder neuroinflammation in the CNS.

A major drawback of utilizing rapamycin for anti-aging therapies is its side effects. Although several rapamycin homologs (i.e. rapalogs) with milder side effects have been developed, there is still a need for finding the optimum dose and duration. This is particularly true for observing the beneficial effects in the brain since studies focusing on the brain are limited.

1.5. Zebrafish as a gerontological model

Various model organisms from different phylogenetic levels are used for aging research. Each organism, from yeast to worms, flies to rodents and nonhuman primates provide valuable information regarding the very complex process of aging. Yet until recently, a large gap between invertebrate and vertebrate models existed. This gap was filled with zebrafish (*Danio rerio*), a freshwater fish native to India [121].

Zebrafish first attracted attention as a model to study developmental biology due to its transparent embryos which develop *ex utero*. Their high fecundity and low-cost husbandry allow generation of large populations fairly quickly, easily and inexpensively. While the life span of zebrafish (3-4 years) is about 50% longer than mouse and this could be considered as a disadvantage for gerontology, it is considerably less than nonhuman primates. Moreover, the life span of zebrafish is a contributing factor to its suitability as a bridge model for aging research [121].

Zebrafish are diurnal vertebrates, and as humans, age gradually [122], [123]. Circadian clock is now recognized as an integral part of the molecular processes regulating aging. Similar to the observations from mammals, zebrafish aging involved selective alterations in circadian clock, reduced nighttime sleep, progressive decline in melatonin, and expression levels of circadian genes [122]. As part of the gradual aging, age-related changes such as accumulation of DNA damage, oxidative damage, stress-related markers, and senescence have been reported in zebrafish [121], [123], [124]. The zebrafish genome has been fully

sequenced, showing 70% homology with human genome, which granted further means to investigate molecular and genetic processes underlying age-related changes [125].

In the context of brain aging, zebrafish have recently emerged as a convenient model to study brain function. Zebrafish CNS is morphologically similar to mammalian CNS at both the macro and cellular levels. Major neurotransmitters, receptors, and proteins involved in cellular metabolism are similar in structure and function that have been observed in the mammals. Finally, zebrafish behavior spans multiple domains including anxiety, mood/depression, cognitive and social skills [125]. In spite of these advantages, zebrafish have not been employed fully in the aging research. Considering the ease of testing drugs and compounds, zebrafish offers a unique model for developing therapeutics [126].

1.6. Aims of this thesis

Despite the growing evidence for the benefits of IF, and DR in general, there are controversial reports on the magnitude of effects. The responses to dietary interventions are influenced by feeding paradigms, diet composition, duration, genetic background, gender, and age of the subjects at the onset of intervention [116]. Therefore, there is need for understanding how these factors determine the response to IF.

In terms of translation to humans, several impediments to the applicability of IF exist. Cultural norms have been dictating a diet of three meals per day as a way of

healthy living for so long that it is a challenge to change the common view. Another drawback is the initial side effects of IF such as irritability, feeling cold, hunger, and fatigue. However, these negative side effects have been reported in less than 15% of the participants, usually disappeared within a month, and followed by overall improvements in mood and physiological parameters [116], [127]. Nonetheless, researchers have been pursuing to identify compounds, either natural or synthetic, that could mimic the effects of IF to eliminate the aforementioned obstacles associated with a diet-based remedy.

As the most conventional DR mimetic, rapamycin has been used extensively in aging research. While the life and health span extending effects of rapamycin have been shown in a variety of organisms, its reported side effects limit the applications in humans. Similar to evidence from DR studies, the effects of rapamycin differ between tissues, ages, and genders [128]. Despite their inhibitory action on mTOR, to what degree rapamycin mimics DR is still not well-understood. Furthermore, most studies on longevity-promoting interventions are done with lifelong DR or drug treatment, which is not feasible in humans and there is need for understanding their short-term effects. The growing body of data on general health parameters and cognitive performance is not accompanied by brain-specific effects, which needs to be addressed separately due to unique brain metabolism and blood brain barrier. Finally, females are still underrepresented since most studies utilize male organisms only.

In this study, we aimed to apply different short-term durations of IF and rapamycin in wild type male and female zebrafish to investigate: (i) How young and old

animals respond to these interventions to understand whether the age at the onset of intervention affects the outcome (ii) the minimum short-term duration to observe significant effects, (iii) the efficacy of rapamycin as a CR mimetic, (iv) the mechanisms of action for IF and rapamycin irrespective of the gender of the subjects, which is essential for comprehension of the global aging patterns.

Chapter 2

Materials and Methods

2.1. Materials

2.1.1. Reagents for drug treatment and dietary restriction experiments

Rapamycin (Catalog #: R0395) was purchased from Sigma, USA. Dimethyl sulfoxide (DMSO) was purchased from Applichem, Germany (Catalog #: A3672). Rapamycin was dissolved in DMSO to reach 100 µM stock concentration. The stock solution was aliquoted and stored at -20ºC. Measurements of pH and nitrate (NO_3) levels in tank water were carried out by using commercially available kits purchased from Sera, Germany (Catalog #: 04310 for pH and Catalog #: 04510 for NO_3).

2.1.2. Reagents for protein isolation

For isolation of total protein from brain tissues, RIPA buffer containing 50mM Tris (Catalog #: T1503, pH 8.0), 150mM NaCl (Catalog #: S5886), 0.1% sodium dodecyl sulfate (SDS; Catalog #: 05030), and 1% NP-40 (Catalog #: NP40S) was prepared. All chemicals used in RIPA buffer were purchased from Sigma, USA. A protease inhibitor (Sigma; Catalog #: 05892970001) was added from a 2X stock right before the homogenization procedure.

2.1.3. Western Blot reagents and antibodies

Acrylamide gels were prepared to separate proteins based on their molecular weights. 10% resolving gel was prepared by mixing double-distilled water (ddH_2O), 1.5 M Tris-HCl (18.171g Tris base in 100 mL ddH_2O; pH=8.8), 10% SDS, 30% acrylamide/bis-acrylamide mix (Sigma, Catalog #: A6050), 10% ammonium persulfate (APS) and N,N,N',N'-tetramethylethane-1,2-diamine (TEMED). To prepare 5% stacking gel, ddH_2O, 30% acrylamide/bis-acrylamide mix, 0.5 M Tris-HCl (6g Tris base in 100 mL ddH_2O; pH=6.8), 10% SDS and 10% APS and TEMED (Sigma; Catalog #: T9281) were mixed.

To load protein samples in gel, 2X Laemmli buffer was prepared by mixing 4% SDS (4 mL from 10% stock), 2 mL glycerol, 0.004% bromophenol blue (100 µL from 4% stock), and 2.5 mL of 0.125M Tris-HCl (pH=6.8). Dithiothreitol (DTT) was freshly added each time with 1:10 final concentration in buffer.

10X running buffer was prepared by mixing 30.285 g Tris base, 144.134 g glycine (Sigma; Catalog #: G8898), and 10% SDS in 800 ml ddH_2O. pH was adjusted to 8.3 by adding 1:1 HCl:ddH_2O. HCl was purchased from Scharlau, Spain (Catalog #: AC07742500). The volume was filled up to 1 L after adjusting the pH and the buffer was stored at room temperature. Before running the gels, buffer was diluted to 1X and cooled down at 4ºC.

Transfer buffer was prepared by mixing 6 g Tris base, 28 g glycine, and 400 ml methanol purchased from Isolab, Germany (Catalog #: 947043). The volume was

adjusted to 2 L by adding ddH_2O and stored at 4ºC.

10X Tris buffered saline (TBS) was prepared by mixing 12g Tris base and 80g NaCl in 800ml ddH_2O. The pH of the solution was adjusted to 7.6 by adding 1:1 HCl:ddH_2O. The volume was then increased to 1L with ddH_2O, and stored at room temperature. For preparation of blocking buffers and washing the membranes, 10X TBS was diluted to 1X with ddH_2O and Tween-20 (Sigma; Catalog #: 8221841000) was added to obtain 0.003% TBS-Tween20 (TBS-T).

Blocking buffers were prepared by dissolving either 5% non-fat milk powder or bovine serum albumin (BSA) in TBS-T, depending on the requirements of the antibodies. Blocking buffers were prepared fresh each time, and stored at 4°C until the blocking step. Specificities of primary and secondary antibodies, dilution factors and amount of protein loaded on gel for detection of each protein are given in Table 2.1.

Table 2.1. Western blot antibodies and their working conditions

Primary Antibody	**Manufacturer**	**Catalog Number**	**Dilution**	**Amount of Protein (µg)**	**Antibody Dilution Buffer**
α-4E-BP1	Cell Signaling Technology, USA	9644	1:1.000	40	5% BSA in TBS-T
α-β-Tubulin	Cell Signaling Technology, USA	2146	1:5.000	10 - 40	5% milk in TBS-T
α-DCAMKL1	Abcam, UK	ab109029	1:1.000	40	5% milk in TBS-T

α-Gephyrin	Santa Cruz Biotechnology, USA	sc-6411	1:1.000	40	5% BSA in TBS-T
α-GFAP	Abcam, UK	ab53554	1:1.000	40	5% BSA in TBS-T
α-LC3A/B	Cell Signaling Technology, USA	12741	1:4.000	40	5% milk in TBS-T
α-PCNA			1:1.000	40	5% milk in TBS-T
α-Phospho-4E-BP1	Cell Signaling Technology, USA	2855	1:1.000	40	5% BSA in TBS-T
α-Phospho-mTOR	Cell Signaling Technology, USA	2974	1:2.000	40	5% BSA in TBS-T
α-Phospho-S6					5% BSA in TBS-T
α-PSD-95	Abcam, UK	ab18258	1:5.000	10	5% milk in TBS-T
α-S6					
α-Synaptophysin	Abcam, UK	ab32594	1:20.000	10	5% milk in TBS-T
Secondary Antibody	**Manufacturer**	**Catalog Number**	**Dilution**	**Antibody Dilution Buffer**	
α-goat	Abcam, UK	ab97100	1:10.000	5% BSA in TBS-T	
α-mouse	Abcam, UK	ab97023	1:5.000	5% milk in TBS-T	
α-rabbit	Cell Signaling Technology, USA	7074	1:5.000	5% milk in TBS-T	

2.1.4. Quantitative Reverse Transcription Polymerase Chain Reaction (RT-qPCR) primers

The primer pairs targeting each gene of interest being: *ztor* and *akt1* ([129], *ddc* and *foxm1* [130], *atg5* and *lc3b* [131], have been previously validated in zebrafish. The primer pair targeting *igf1* was designed and validated by our group [132]. Sequences for the forward and reverse primers are given in Table 2.2. Primers were received in lyophilized form and prior to use, each were dissolved in nuclease-free water purchased from Thermo Fisher Scientific, USA (Catalog #: AM9937). For quantitative gene expression analysis, primer mixes were prepared by diluting the primer pairs with a dilution factor of 1:20 in nuclease-free water.

Table 2.2. Sequences and melting temperatures (T_m) of forward and reverse primers for RT-qPCR experiments

Gene	Forward Primer (5'-3')	Reverse Primer (5'-3')	T_m (ºC)
foxm1	GACACATGACCCTGAAGGAGA	AGAGTGAGACAGCGGTTTGC	60
ddc	CCTGCCTGTACGGAGCTAGA	CTGGATCAGCCTGACGATTT	60-58
atg5	CAACTGTGGATGGGTCTG	GAGCGTCTGGATGAATGG	63
lc3b	CCTCCAACTCAACTCCAACC	GCCGTCTTCGTCTCTTTCC	66
igf1	GGGCATTGGTGTGATGTCTT	CCAGTGAGAGGGTGTGGGTA	65-69
ztor	AGATCATCAACCGAGTGCGG	AGGGCACCATCCAATGTAGC	60
akt1	TCGGCAGGTGTCTTCTCAAT	ACCCATTGCCATACCACGAG	60

2.1.5. Reagents for cortisol isolation and measurement of whole-body glucose

Homogenization of fish trunks were carried out in ice cold 1X (Dulbecco's phosphate-buffered saline) DPBS, which was purchased from Thermo Fisher Scientific (Catalog #: 14190144). During the cortisol isolation, diethyl ether (Merck, Germany; Catalog #: M100921) was used for phase separation. Cortisol was resuspended in RD-45 reagent supplied in Parameter Cortisol Assay Kit (R&D Systems, USA; Catalog #: KGE008B)

2.2. Methods

2.2.1 Animal Experiments

The protocol for the animal experiments in this study was approved by the Bilkent University Local Animal Ethics Committee (HADYEK) on February 24, 2014 with the decision number 2014/11. The procedures were in accordance with the international guidelines for the handling and use of laboratory animals. The stocking densities and optimum water parameters such as temperature, pH and nitrate (NO_3) levels were determined based on the recommended guidelines for the handling of zebrafish [133]–[135].

2.2.1.1 Animal Husbandry

In total, 209 fish were used in this study. All fish belonged to the AB strain and had a wild-type background. The experiments were carried out in three separate cohorts. Out of 209 animals, 107 were young (6-10 months old) and 102 were old (26-31

months old) adults. Both males and females were included in the experiments and evenly distributed across groups to observe general patterns that are independent of gender, since we observed gender-specific effects of aging in a previous study published by our group [75].

For both age groups, we crossed wild-type fertile males and females, collected embryos, and raised them under standard conditions (27.5°C on a 14L:10D light cycle) in İhsan Doğramacı Bilkent University Molecular Biology and Genetics Department Zebrafish Facility, Ankara, Turkey. All fish were fed twice a day with standard fish flakes (Sera, Germany), and once a day with artemia (Sera, Germany) in a recirculating tank system (Tecniplast, Italy).

For the dietary restriction and rapamycin treatment experiments, the fish were separated based on their age, and allowed to habituate in 8L glass tanks (Pet store, Ankara, Turkey) containing 4L system water. After the initial habituation period, fish were randomly selected and distributed into different treatment groups. The distribution of animals across groups are given in Table 2.3. Upon group assignment, fish were left for a second habituation period for up to a week. During both habituation periods, all animals were fed *ad libitum* as described earlier. Fish were weighed individually in system water prior to the initiation of the experiments. The number of fish per group was set to a maximum of 18 to minimize density-induced stress, and these fall within a range that has been shown to be an appropriate stocking density [136].

Table 2.3. Distribution of animals across experiment groups. AL: *ad libitum*-fed control group, IF: intermittent fasting group, RAPA: rapamycin-treated group.

	Female	Male	Total
Young AL	19	17	36
Young IF	19	18	37
Young RAPA	17	17	34
Old AL	13	17	30
Old IF	11	25	36
Old RAPA	15	21	36

2.2.1.2. Feeding and drug treatment procedures across life span

The intermittent fasting and rapamycin treatment experiments continued for 8 weeks in total, and were carried out in an isolated room in Zebrafish Facility to prevent contamination of the main system. Throughout the 8-week periods, fish were maintained under standard temperature and light conditions. Glass aquaria with 8 L volume were purchased from a pet store, and filled with 4 L system water. Since these aquaria were not connected to the Tecniplast system; appropriate water temperature, oxygenation and circulation were provided by 100 W aquarium heaters (Ada; Catalog #: HL-100), and filters (Venusaqua, China; Catalog #: VS-410F). Each age and treatment group were housed separately.

The feeding schedule for the dietary restriction was adapted from a previous study by our group [137], [138]. Detailed information regarding the amount and type of food provided to each experiment group is given in Table 2.4. (on odd weeks) and Table 2.5. (on even weeks). In summary, rapamycin-treated animals were under the same feeding schedule (90 mg fish flakes twice a day, 10 mg artemia three times a week) with *ad libitum*-fed (AL) counterparts. Animals in the intermittent fasting (IF) groups were fed every other day with 45 mg fish flakes twice a day, and 10 mg artemia once a week.

Table 2.4. Feeding schedule for the experiment groups on odd weeks of the experiment. AL: *ad libitum*-fed control group, IF: intermittent fasting group, RAPA: rapamycin-treated group.

	Mon	Tue	Wed	Thu	Fri	Sat	Sun
AL	180 mg dry food and 10 mg artemia	180 mg dry food	180 mg dry food 10 mg artemia	180 mg dry food	180 mg dry food and 10 mg artemia	180 mg dry food	180 mg dry food
IF	90 mg dry food		90 mg dry food and 10 mg artemia		90 mg dry food		90 mg dry food
RAPA	180 mg dry food and 10 mg artemia	180 mg dry food	180 mg dry food and 10 mg artemia	180 mg dry food	180 mg dry food and 10 mg artemia	180 mg dry food	180 mg dry food

Table 2.5. Feeding schedule for the experiment groups on even weeks of the experiment. AL: *ad libitum*-fed control group, IF: intermittent fasting group, RAPA: rapamycin-treated group.

	Mon	Tue	Wed	Thu	Fri	Sat	Sun
AL	180 mg dry food and 10 mg artemia	180 mg dry food	180 mg dry food and 10 mg artemia	180 mg dry food	180 mg dry food and 10 mg artemia	180 mg dry food	180 mg dry food
IF		90 mg dry food		90 mg dry food and 10 mg artemia		90 mg dry food	
RAPA	180 mg dry food and 10 mg artemia	180 mg dry food	180 mg dry food and 10 mg artemia	180 mg dry food	180 mg dry food and 10 mg artemia	180 mg dry food	180 mg dry food

Artemia was prepared in an oxygenated container by mixing 3X salt and 3X artemia eggs in 500 mL dH_2O. The eggs were then let to hatch with constant air supply. After 48 hours, hatched shells are discarded, live artemia was rinsed with dH_2O to remove saline water, and are fed to the animals. Dry fish flakes were manually ground using a mortar and pestle. Ground flakes were then weighed, aliquoted and stored at room temperature.

Rapamycin treatment protocol was adapted from a previously published study [139], and optimized for our experiment design. Rapamycin aliquots were prepared as described in section 2.1.1. Working solutions were added into the aquaria water in 1:1000 dilution (i.e. 4 mL in 4 L). To eradicate any potential effects of DMSO, the

same amount of DMSO was added into the aquaria housing AL and IF groups.

According to the Food and Drug Administration (FDA) of the United States, rapamycin has a half-life of 62±16 hours [120]. To keep the biological activity of rapamycin constant throughout 8 weeks, we replaced at least half and at most three-quarters of the aquarium water with fresh system water every three days and added rapamycin aliquots at the designated amounts. Since the aquaria was not connected to the main setup, which has an automatic recirculation system, there was a need to supply all experiment groups with fresh water. Therefore, we applied the same aquarium cleaning schedule to AL and IF groups and added DMSO into their water.

Prior to cleaning, water samples were collected from each aquarium to measure chemical parameters such as pH and NO_3 levels. The protocols for pH and NO_3 measurements are given in Section 2.2.1.3. Water volume in aquaria was then reduced, and glass walls were wiped clean with tissue paper. Filters were removed, cleaned under running water and rinsed in dH_2O. The water volume was then adjusted to 4 L by adding fresh system water.

2.2.1.3. pH and NO_3 measurements

The optimum pH has been reported to be between 6.8 and 7.5 [140]. A commercially available kit was purchased from Sera to measure pH levels. The manufacturer's guidelines were followed. According to this protocol, measurement vial was filled to the 5 mL mark with the water sample to be tested. Four drops of the pH reagent were added, and the vial was shaken until the reagent was evenly distributed. The vial was

then placed on the color chart, colors were compared, and the corresponding pH value was recorded.

Decomposition of the organic material such as food leftover and excretion by fish cause elevations in nitrogenous wastes. These parameters affect the water quality and general health of the fish. Conversion of ammonia and nitrite into nitrate (NO_3) decreases toxicity, however elevated NO_3 levels have also been implicated in growth defects. Earlier reports suggest that maximum NO_3 concentration should not exceed 100 mg/L [141].

The levels of NO_3 in water samples were measured by using another commercially available kit (Sera, Germany). According to the manufacturer's protocol, measurement vial was filled to the 10 mL mark. Six drops of reagents 1 and 2 were added, and the vial was shaken after adding each reagent. Then, one measurement spoon of reagent 3 was added and the vial was shaken vigorously for 15 seconds. Finally, six drops of reagent 4 were added and evenly distributed. After 5 minutes of incubation at room temperature, the color was compared to the color chart and the NO_3 concentration was recorded.

2.2.1.4. Euthanasia and tissue harvesting

At the end of 4, 6 and 8 weeks, approximately one third of the animals in each aquarium was taken. Animals were first weighed in system water while they were still alive, and then euthanized in iced (system) water. Bodies were dried, dry body weight and length were measured. Fish were then decapitated using a sterile surgical blade. Trunks were visualized under a dissection microscope for gender

confirmation. Gills and eyes were removed from the head, then brains were dissected. All tissues were weighed, and immediately snap frozen in liquid nitrogen. Samples were stored at -80°C until further experiments. To be able to observe individual patterns of biological differences, all samples were processed separately.

2.2.2. Protein Expression Experiments

2.2.2.2. Protein isolation from brain tissues

To isolate total protein, each brain tissue was homogenized in fresh RIPA buffer. The contents of this buffer are given in section 2.1.2. To prepare 1 mL RIPA buffer, 75 µL of 2M NaCl (1.1688 g of NaCl dissolved in 10 mL sterile ddH_2O), 50 µL of 1M Tris-HCl (pH=8), 10 µL of NP-40, and 10 µL of SDS (10%) were mixed in 355 µL sterile ddH_2O. Then, 500 µL of 2X protease inhibitor was added. For homogenization, 60 µL of RIPA buffer per 1 mg of tissue was added. Homogenization was performed by passing the solution through a 25-gauge 2mL syringe several times, until the tissue was completely disintegrated (Beybi, Turkey). To allow lysis to occur, homogenates were incubated on ice for 30 minutes, and gently mixed twice during incubation. Samples were centrifuged at 13.000 rpm for 20 minutes at +4°C. Supernatants were aliquoted and stored at -80°C.

2.2.2.3. Bradford assay

To measure protein concentrations, a Bradford Assay was performed. Bradford reagent (Sigma, USA; Catalog #: B6916) and an aliquot of 1 mg/mL bovine serum albumin (BSA), which was used as a standard and purchased from Sigma (Catalog #:

A2153), were brought to room temperature. A 96-well plate was prepared with BSA standards and protein samples. BSA standards were prepared as described in Table 2.6. Amounts are given in µL, "S" stands for the standard, and "S: 0" was designated as blank solution.

Table 2.6. BSA samples that were used as standards to measure protein concentrations.

	S: 0	S: 0.5	S: 1	S: 2	S: 3	S: 4	S: 5
BSA	0	0.5	1	2	3	4	5
ddH_2O	5	4.5	4	3	2	1	0

Protein samples were prepared as 0.5 µL of sample and 4.5 µL of ddH_2O. Both the samples and BSA standards were added onto the wells in duplicates. Then, 250 µL of Bradford reagent was added into each well. The plate was placed on a shaker that was set to 250 rpm, and incubated for 45 seconds. Next, the plate was removed from the shaker. Samples were incubated at room temperature for 10 minutes. The values of light absorbance were read from a spectrophotometer. The wavelength (λ) was set to 595 nm. A standard curve was drawn from the absorbance readings of BSA standards. The sample concentrations were calculated based on the standard curve.

2.2.2.4. Western blot experiments

Total protein samples were mixed with 2X Laemmli buffer and boiled at 95°C for 10 minutes. Samples were cooled down and loaded into gel. PageRuler Prestained Protein Ladder (Thermo Fisher Scientific, USA; Catalog #: 26616) was used as

marker. Gels were attached to Mini-PROTEAN Tetra Cell Electrophoresis System (BioRad, USA), tank was filled with ice cold 1X running buffer, and proteins were run at 90 V for 30 minutes. After 30 minutes, the loading dye reached resolving gel, and the running condition was changed to 120 V. The gels were run at 120 V for 80-120 minutes depending on the protein of interest. Each sample was run at least three times per protein of interest. Replicate samples were subjected to a systematic rotation on gel.

Following gel separation, stacking gels were removed. Resolving gels were placed between a fiber pad followed by two Whatmann papers (GE Healthcare Life Sciences, USA; Catalog #: 3030-917), and polyvinylidene fluoride (PVDF) membrane (Thermo Fisher, USA; Catalog #: LSG-88518) followed by two Whatmann papers and another fiber pad. The sandwiches were stabilized in cassettes, and cassettes were attached to the blotting module for wet transfer. The tank was filled with transfer buffer and proteins were transferred to the PVDF membrane by running at 90V for 90 minutes at 4°C.

Membranes were blocked in either 5% non-fat milk powder in TBS-T for primary antibodies prepared in 5% milk—TBS-T, or 5% bovine serum albumin (BSA) in TBS-T for those done in 5% BSA—TBS-T. Blocking was performed at room temperature for 1 hour on a shaker. Blocking buffers were prepared fresh for each experiment.

Primary antibody incubation was performed overnight at +4°C on a shaker. Next day, antibodies were collected for reuse, and membranes were washed in TBS-T.

Washing step was performed at room temperature on a shaker, and continued for 30 minutes with 5-5-10-5-5 minutes intervals. Used TBS-T was discarded and replaced with fresh TBS-T at the end of each interval.

Secondary antibody incubation was performed at room temperature on a shaker. After an hour of incubation, membranes were washed as described in the previous paragraph. Detailed information about the primary and secondary antibodies are given in Table 2.1.

After the washing step, membranes were prepared for signal detection. SuperSignal™ West Femto Maximum Sensitivity Substrate (Thermo Fisher Scientific, USA; Catalog #: 34095) was used as the chemiluminescence detection reagent. Working solution was prepared by mixing equal volumes of luminol/enhancer and stable peroxide buffer. Membranes were incubated in the working solution for 5 minutes at room temperature in a dark place. Excess reagent was removed, and membranes were left in ChemiDoc™ XRS+ (BioRad, USA) for image acquisition.

2.2.2.5. Quantification of band intensities

Band intensities were quantified using ImageJ software (NIH, USA) by a person who was blind to the information about the samples. This was done to achieve an unbiased quantification and analysis. To compare protein expression levels between experiment groups, the band intensities were double-normalized using the formulae given below. Each value was first normalized to the band intensity of the protein of interest (POI) in the 4-week AL sample within the gel (i.e. within-gel

normalization). This has been previously described as a method to ensure reliable results [58]. Following the first normalization step, within-gel normalized value of POI was divided by the within-gel normalized value of β-tubulin (i.e. β-tubulin normalization).

$$\text{Within-gel normalization} = \left(\frac{\text{Band intensity of POI}}{\text{Average band intensity of POI}}\right)$$

$$\beta\text{-Tubulin normalization} = \left(\frac{\text{Within-gel normalized value of POI}}{\text{Within-gel normalized value of } \beta\text{-Tubulin}}\right)$$

2.2.4. Gene Expression Experiments

2.2.4.1. Total RNA isolation

Total ribonucleic acid (RNA) was isolation from the snap-frozen fish brains were performed with the TRIzol reagent (Thermo Fisher Scientific; Catalog #: 15596018) according to the manufacturer's instructions. Brains were homogenized in 400 µL of TRIzol reagent using 26-gauge, 1 mL insulin syringes (Beybi, Turkey). After homogenization, samples were incubated at room temperature for 5 minutes. Then, 40 µL of chloroform was added and the tubes were shaken vigorously for 15 seconds. Samples were incubated at room temperature for 3 minutes, and centrifuged for 15 minutes at 12.000 x g at 4°C. This allows phase separation. The upper aqueous phases were transferred to a new Eppendorf tube, and lower phenol-chloroform phases were saved for protein isolation.

For RNA precipitation, 200 µL of isopropanol was added. Samples were incubated for 10 minutes at room temperature, and then centrifuged for 10 minutes at 12.000 x g at 4°C. Since RNA precipitates and forms a pellet after this step, the supernatants were discarded.

The pellets containing RNA were washed with 400 µL of 75% ethanol. After adding 75% ethanol and vortexing the tubes briefly, the samples were centrifuged for 5 minutes at 7.500 x g at 4°C. The supernatants were discarded. The samples were air dried for 10 minutes and resuspended in 40 µL of nuclease-free water. The RNA concentrations were measured using NanoDrop™ 2000 (Thermo Fisher Scientific, USA) and the samples were stored at -80°C.

2.2.4.2. DNase treatment

To avoid DNA contamination in RNA, samples were treated with TURBO DNA-*free*™ Kit (Thermo Fisher Scientific, USA; Catalog #: AM1907) according to the manufacturer's instructions. For 10 µL of RNA sample, 7 µL of nuclease-free water, 2 µL of TURBO DNase-Buffer and 1 µL of TURBO DNase were added into the reaction. Samples were incubated for 30 minutes at 37°C. Then, 2 µL (10% of the reaction volume) of DNase Inactivation Reagent was added. Samples were incubated for 5 minutes at room temperature, and centrifuged at 10.000 x g for 1.5 minutes. The supernatants were collected, and DNase-treated RNA concentrations were measured using the NanoDrop™ 2000.

2.2.4.3. cDNA synthesis

Complementary DNA (cDNA) was synthesized from DNase-treated RNA sample using the iScript™ cDNA Synthesis Kit (Bio-Rad, USA; Catalog #: 1708891). The starting material for cDNA synthesis was 500 ng/µL DNase-treated RNA. Reactions were prepared by mixing varying volumes of RNA and nuclease-free water, 5x iScript Buffer, and 1 µL of iScript reverse transcriptase. Incubations were carried out in Bio-Rad C1000 Thermal Cycler following the protocol given in Table 2.7. The resulting cDNA products were stored at -20°C.

Table 2.7. Reaction protocol for cDNA synthesis

Protocol Step	Temperature (ºC)	Duration
Priming	25	5 minutes
Reverse transcription	46	20 minutes
Inactivation	95	1 minute
Hold (optional)	4	Variable

2.2.4.4. Quantitative reverse transcription polymerase chain reaction (RT-qPCR)

To measure gene expression levels, RT-qPCR experiments were performed. Reactions were prepared in LightCycler® 480 SYBR Green I Master (Roche, Switzerland; Catalog #: 04707516001) to detect fluorescence intensity. First, master mix (MM) containing SYBR Green I and nuclease-free water was prepared. Then, master mixes containing primer pairs (pMM) were prepared by mixing MM and

primer mix, which contained forward and reverse primers diluted in nuclease-free water (dilution factor= 1:20). Reaction volume was 20 µL containing 2 µL of undiluted cDNA and 18 µL of pMM. Final concentration of each primer in the reaction was 5 µM.

Reactions were added onto LightCycler® 480 Multiwell Plate 96 (Roche, Switzerland; Catalog #: 04729692001) without direct exposure to light. The plates were sealed, centrifuged at 1500 rpm for 2 minutes and loaded to LightCycler® 480 instrument (Roche). The cycle threshold (C_t) values were obtained from the LightCycler® 480 software (Roche, Switzerland).

The gene expression levels relative to housekeeping gene β-actin were calculated using the $2^{-\Delta C_t}$ formula. The fold changes were calculated based on the average relative expression values of a gene of interest in all samples using the $2^{-\Delta\Delta C_t}$ formula. To normalize data, the fold change values were subjected to $\log_2$ transformation.

2.2.5. Body Cortisol Measurements

2.2.5.1. Cortisol isolation from fish trunks

Frozen fish trunks were weighed and homogenized in 5 mL ice cold 1X DPBS for 30 seconds (Thermo Fisher Scientific, USA; Catalog #: 14190144) using a tissue homogenizer (VWR, USA; Model #: VDI25). The homogenizer was cleaned with 10% SDS, 70% ethanol and ddH_2O prior to use, and with 70% ethanol followed by ddH_2O between samples. Diethyl ether (Merck, Germany; Catalog #: M100921) was

added until the volume reached 30 mL. Samples were centrifuged at full speed for 20 minutes. The upper aqueous phase containing cortisol was collected from each sample and transferred to a new 50 mL falcon. The falcons were left under a running fume hood and air dried overnight. Next morning, the cortisol residues were resuspended in 400 µL of RD5-43 reagent, which was provided in the Parameter Cortisol Assay Kit (R&D Systems, USA; Catalog #: KGE008B). Resuspensions were stored at 4°C until cortisol measurement.

2.2.5.2. Measurement of cortisol concentration

Cortisol concentration in samples obtained from fish trunks were measured by using the Parameter Cortisol Assay Kit following the manufacturer's instructions. All reagents that were provided in the kit were brought to room temperature before use. Wash buffer was prepared by mixing 20 mL of Wash Buffer Concentrate and 480 mL of ddH_2O. Cortisol stock solution was prepared by reconstituting the Cortisol Standard with ddH_2O, which produces a 100 ng/mL stock solution. The standard was mixed and left on a shaker for 15 minutes with gentle agitation. Cortisol standards were prepared by serial dilution of stock solution. Preparation of the standards are depicted in Figure 2.1.

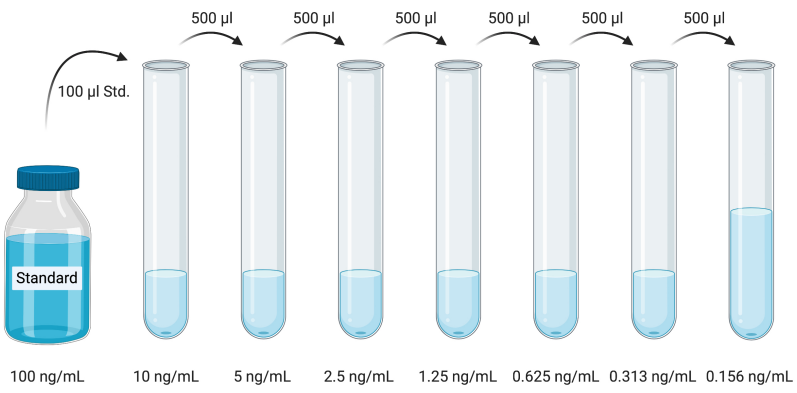

Figure 2.1. Preparation of cortisol standard solutions through serial dilution. The dilution buffer was RD5-43 reagent. The illustration is adapted from the Parameter Cortisol Assay Kit product manual and created with BioRender.

For the high standard (10 ng/mL), 900 µL of RD5-43 was added and for the rest of the standards, 500 µL of RD5-43 was pipetted into the tubes. From the stock solution, 100 µL was added into the high standard. Then, 500 µL of 10 ng/mL standard was transferred to the tube designated for 5 ng/mL standard. The same dilution strategy was applied for the other standards. The pipette tips were replaced in between standards. The calibrator diluent RD5-43 was used as the zero standard (B_0). The standards were used within 60 minutes of preparation. Finally, color reagents A and B were mixed in equal volumes to prepare Substrate Solution. The mixture was protected from light and used within 15 minutes.

Calibrator Diluent RD5-43 was added into the non-specific binding (NSB) and B_0 wells of the 96-well plate provided in the kit. For NSB, 150 µL of RD5-43 and for B_0, 100 µL of RD5-43 was used. 100 µL of standard solutions or samples (diluted 1:2 and 1:4 in RD5-43) were added into the allocated wells. Please note that all the standards, blanks, and samples were added to the well in duplicates. Next, 50 µL of Cortisol Conjugate and 50 µL of Primary Antibody Solution were added to all wells. The plate was covered and incubated for 2 hours at room temperature on an orbital shaker which was set to 500 rpm.

After the primary antibody incubation, wells were aspirated and washed with the Wash Buffer four times. Wells were inverted after the last wash and blotted against

clean paper towels for complete removal of the Wash Buffer. Next, 200 µL of Substrate Solution was added to each well. The plate was covered and incubated for 30 minutes in dark at room temperature. Finally, 50 µL of Stop Solution was added to each well. The reactions in the wells were mixed thoroughly.

The optical density (O.D.) was measured in a spectrophotometer that was set to 450 nm. Wavelength correction was set to 540 nm. To calculate the results, O.D.s of the duplicates were averaged and a standard curve was generated with O.D.s of the standards. Finally, the cortisol concentration/trunk weight ratio was calculated for each sample.

2.2.6. Whole-body Glucose Measurements

Frozen fish trunks were homogenized in 2 mL ice cold 1X DPBS for 1 minute using a tissue homogenizer (VWR, USA; Model #: VDI25). The homogenizer was cleaned with 70% ethanol and ddH_2O prior to use, and with 70% ethanol followed by ddH_2O between samples. Homogenates were centrifuged at 5000 rpm for 5 minutes. A 10 µL of the supernatant was tested by using a Contour Plus Glucometer (Bayer, Germany). Whole-body glucose concentrations were recorded and glucose-to-trunk weight ratios were calculated for each sample.

2.2.7. Statistical Analysis

The statistical analyses were performed using the IBM SPSS software (IBM, New York, USA) as described in Figure 2.2. Levene's Test for Equality of Variances and tests for normality (Kolmogorov-Smirnov or Shapiro-Wilk tests) were run in order

to determine whether the data was suitable for parametric tests. A one-way analysis of variance (ANOVA) was performed for each factor (i.e. age, treatment, and duration) when the assumptions were met. Post-hoc analysis with Bonferroni correction was performed to conduct pairwise comparisons. Two- and three-way ANOVAs were run for the instances that a significant overall effect by an independent variable was obtained from a one-way ANOVA. These variables were: Age with two levels (young and old), treatment group with three levels (AL, IF, RAPA), and duration with three levels (4, 6, and 8 weeks). The significance levels were set at $p \leq 0.05$ in all cases.

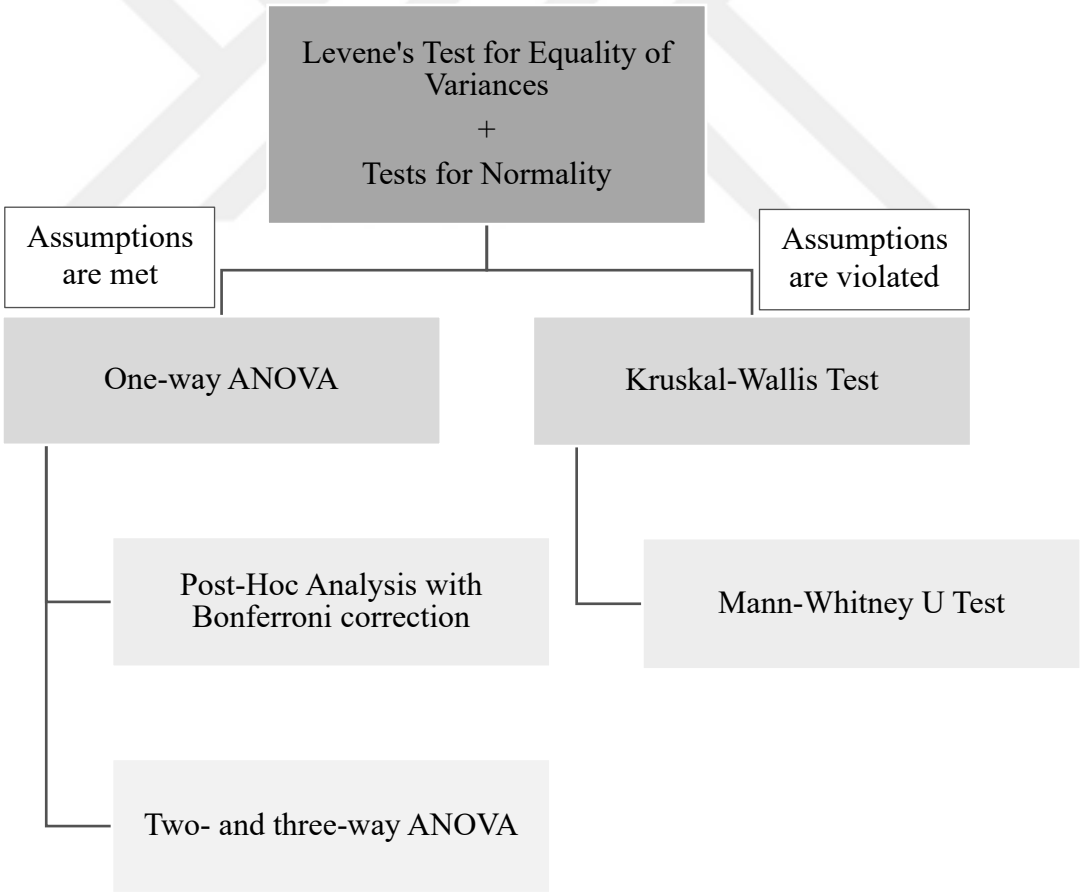

Figure 2.2. Workflow diagram for the statistical analysis.

A nonparametric test, Kruskal-Wallis, was performed when the data violated the assumptions for ANOVA. Mann-Whitney U test was performed as a nonparametric alternative to the post-hoc analysis. For all the instances that a nonparametric test was used, the significance levels were set based on the pre-hoc analysis for reporting only the real significant changes with a more stringent cutoff .

Principal component analysis (PCA) was performed by using the IBM SPSS software. This was done to further investigate how the expression levels of genes and proteins of interest change relative to each other in response to intermittent fasting and rapamycin treatment in young and old animals. Furthermore, the PCA approach allows us to understand how these factors cluster into the components and whether they are correlated with each other. The principal components were extracted based on the eigenvalues set above the 0.5 level. To confirm that the data was suitable for dimension reduction and component extraction, Kaiser-Meyer-Olkin Measure of Sampling Adequacy (KMO) and Bartlett's Test of Sphericity were performed. Component rotation method was Varimax with Kaiser normalization.

Data was visualized by using GraphPad Prism (San Diego, California, USA) and IBM SPSS software. Since we did not observe a duration effect on most of the test variables that were analyzed, data from three durations (i.e. 4, 6 and 8 weeks) were combined to increase the statistical power for each analysis, and represented as a combined mean for all experiment groups. The data from different durations was only separately visualized when the effect of duration was significant.

Chapter 3

Results

3.1. Changes in the body weight and body mass index in response to different durations of treatment

3.1.1. Intermittent fasting decreases the body weight in old animals

To assess whether different short-term durations of intermittent fasting (IF) and rapamycin treatment (RAPA) changed the body weight, we compared the mean dry weight values at the end of 4, 6, and 8 weeks. Our results demonstrated significant overall effects of age ($F_{(1,\ 208)}$=89.299; p≤0.001) and treatment ($F_{(2,\ 208)}$=18.969; p≤0.001) on body weight, but no effect of duration ($F_{(2,\ 208)}$=0.923; p=0.399). There was a significant interaction between treatment and duration ($F_{(4,\ 208)}$=3.512; p≤0.01).

Young and old IF animals showed different patterns in body weight changes. The body weight measurements of young IF (Y-IF) group were stable across 8 weeks (Figure 3.1.A). Old IF (O-IF) group experienced a gradual decrease in body weight, and the difference in body weight between 4 and 8 weeks was significant (Figure 3.1.B; p≤0.001). Although Y-IF group did not show a decrease in body weight throughout the experiment, both Y-IF and O-IF groups had significantly lower mean

weights as compared to *ad libitum* (AL)-fed counterparts (Y-AL and O-AL, respectively) at the end of 6 and 8 weeks (Figures 3.1.A and 3.1.B; $p \leq 0.05$). Interestingly, the mean body weight of Y-AL group increased significantly between 4 and 8 weeks (Figures 3.1.A; $p \leq 0.01$). In contrast, no changes were observed in O-AL group.

The body weight changes were also compared for the rapamycin-treated (RAPA) groups, in order to rule out possible adverse effects of the drug on eating habits. Both the RAPA and AL groups were fed *ad libitum*, and there were no significant differences in body weight between these groups. Furthermore, body weight of the young and old RAPA groups (Y-RAPA and O-RAPA, respectively) were higher than that of Y-IF and O-IF groups after 6 and 8 weeks (Figures 3.1.A and 3.1.B; $p \leq 0.05$). These results suggested that RAPA did not cause loss of appetite, and the body weight of RAPA and AL animals followed a similar pattern.

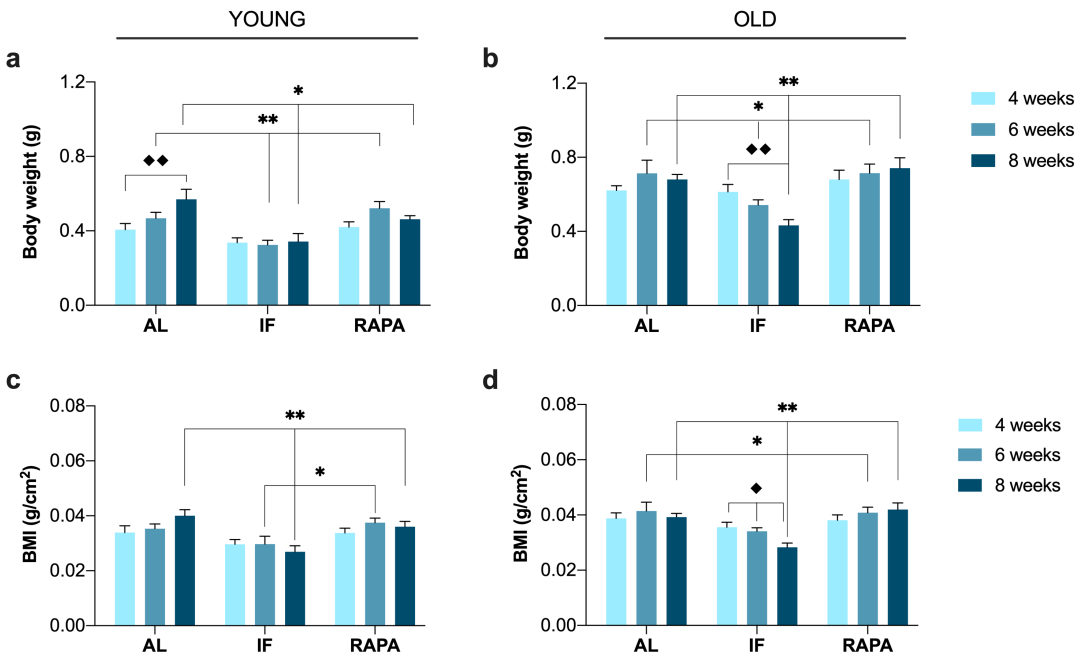

Figure 3.1. Changes in the mean body weight and BMI in response to IF and RAPA treatment throughout 8 weeks. Significant changes in body weight (a, b) and BMI (c, d) were observed within and across treatment groups in young (a, c) and old (b, d) animals. BMI is calculated from the body weight and length measurements at the end of each dietary period. Mean body weight values after 4, 6 and 8 weeks of treatment are shown as grams (g), and the mean BMI values as grams/centimeters^2 (g/cm^2) on the graphs. The error bars represent one standard error (SE). Diamonds represent within-group differences (◆◆: $p \leq 0.01$, ◆: $p \leq 0.05$), whereas asterisks represent across-group differences (**: $p \leq 0.01$, *:$p \leq 0.05$). AL: *ad libitum*-fed control group, IF: intermittent fasting group, RAPA: rapamycin-treated group. N=10-14 per group at a given duration. Reproduced from the figures that first appeared in Rejuvenation Research [142], and reprinted with permission from Mary Ann Liebert, Inc.

3.1.2. Intermittent fasting decreases the body mass index in old animals

To further analyze whether IF and rapamycin treatment caused changes in growth patterns, we compared the mean body mass index (BMI) of animals. BMI was calculated from dry body weight and length measurements of each animal at the end of the experiment (please see the formula below). We observed patterns of change that were similar to those observed in body weight (Figures 3.1). There were significant overall effects of age ($F_{(1,\ 206)}=12.917$; $p \leq 0.001$) and treatment ($F_{(2,\ 206)}=25.329$; $p \leq 0.001$) on BMI (Figures 3.1.C and 3.1.D). As was the case for body weight, duration itself did not have an effect on BMI ($F_{(2,\ 206)}=0.956$; $p=0.386$), while

the interaction between duration and treatment was significant ($F_{(4,\ 206)}$=2.845; $p \leq 0.05$).

$$BMI = \left(\frac{\text{Dry body weight (g)}}{\text{Body length (cm)}^2}\right)$$

In Y-IF group, BMI followed a similar pattern with body weight since there were no significant changes across 8 weeks (Figure 3.1.C). The mean BMI of O-IF animals decreased significantly between 4-8 and 6-8 weeks (Figure 3.1.D; $p \leq 0.05$). The differences in BMI between treatment groups validated the results from body weight measurements. In both Y-IF and O-IF groups, we observed significantly lower BMI than AL-fed counterparts starting from the 6th week of intervention. Significant differences were observed between Y-IF and Y-RAPA at 6 weeks ($p \leq 0.05$), Y-IF and both Y-AL and Y-RAPA at 8 weeks ($p \leq 0.01$). Similarly, O-IF group had a significantly lower BMI than both O-AL and O-RAPA after 6 and 8 weeks ($p \leq 0.05$ and $p \leq 0.01$, respectively).

3.2. Changes in whole-body glucose and cortisol levels

3.2.1. Whole-body glucose levels decrease in animals subjected to intermittent fasting

There is a well-established link between diet and metabolism [143]–[145]. Since brain has a very high energy requirement and accounts for about 25% of the glucose consumption [146], metabolic changes have consequences on its functioning [147].

In order to identify possible links between metabolism and cellular and molecular changes in the brain, we investigated whether a metabolic parameter such as glucose levels were altered by IF or its mimetic, rapamycin. Since glucose is the primary energy source for the brain [147], its regulation via diet or drug treatment might have implications on the modulation of cellular and molecular markers that we have investigated.

Our results demonstrated overall effects of age ($\chi^2_{(1)}$ =9.859; p=0.002) and treatment ($\chi^2_{(2)}$=13.851; p=0.001) on whole-body glucose levels (Figure 3.2). Blood or plasma glucose levels have been previously shown to be decreased by IF [148]. In conjunction with the literature, we observed lower whole-body glucose levels in IF animals of both ages than their AL-fed counterparts (Figures 3.2; $p \leq 0.01$).

The effect of age was predominantly observed on IF and RAPA groups. In O-IF and O-RAPA groups, the whole-body glucose concentration was higher compared to their young counterparts (Figure 3.2; *U*=44.500, p=0.013 and *U*=66.000, p=0.019, respectively). Again, this is consistent with the existing literature reporting an increase in glucose levels with the advancing age [149].

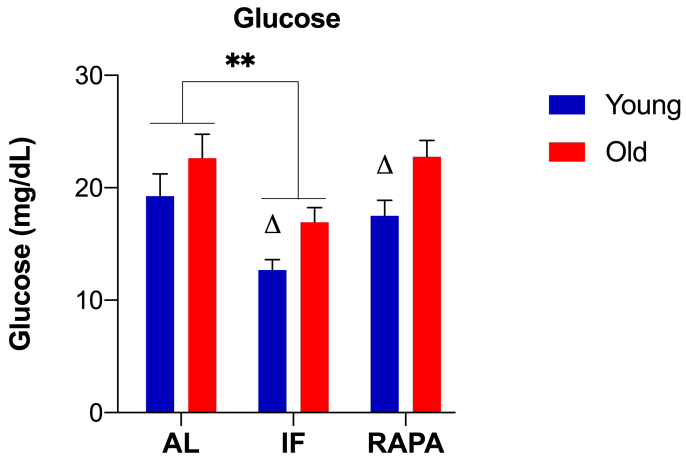

Figure 3.2. Changes in the whole-body glucose levels in response to IF and RAPA treatment. Significant effects of age and treatment were observed on whole-body glucose levels. The combined mean of glucose values at different durations are shown as mg/dL on the graphs. Asterisks and triangles represent across-group and age differences (**: p≤0.01, Δ: p≤ 0.05), respectively. AL: *ad libitum*-fed control group, IF: intermittent fasting group, RAPA: rapamycin-treated group. N=13-16.

Finally, duration also affected the whole-body glucose levels (Figure 3.3; $\chi^2_{(2)}$=5.946; p=0.051). However, this effect was only observed in AL groups, and between 4 and 6 weeks. The glucose levels increased from 4 to 6 weeks in both Y-AL (Figure 3.3.A; *U*=3.000, p=0.046) and O-AL (Figure 3.3.B; *U*=1.500, p=0.037). Interestingly, we did not observe such an increase in RAPA animals of both ages. Nevertheless, Y-RAPA and O-RAPA groups had higher glucose levels, suggesting a mild glucose intolerance, which has been previously reported as a consequence of rapamycin treatment [150].

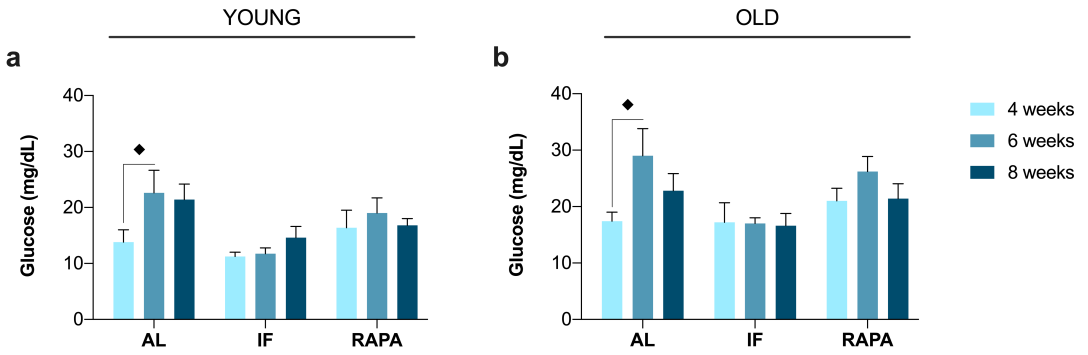

Figure 3.3. Changes in the whole-body glucose levels in response to different durations of IF and RAPA treatment. Significant changes in glucose levels were observed within treatment groups in young (a) and old (b) animals. Mean glucose values after 4, 6 and 8 weeks of treatment are shown as mg/dL on the graphs. The error bars represent one standard error (SE). Diamonds represent within-group differences (◆: $p \leq 0.05$). AL: *ad libitum*-fed control group, IF: intermittent fasting group, RAPA: rapamycin-treated group. N=4-6 per group at a given duration. Reproduced from the figures that first appeared in Rejuvenation Research [142], and reprinted with permission from Mary Ann Liebert, Inc.

We then normalized the whole-body glucose levels to trunk weight (i.e. glucose/trunk) and analyzed whether there were effects of age, treatment or duration on this parameter. This calculation has been done since we aimed to understand how changes in glucose levels were reflected in the whole-body. Our results demonstrated that only age had a significant effect on glucose/trunk levels ($\chi^2_{(1)}=11.710$; $p=0.001$), but not treatment or duration (Figure 3.4).

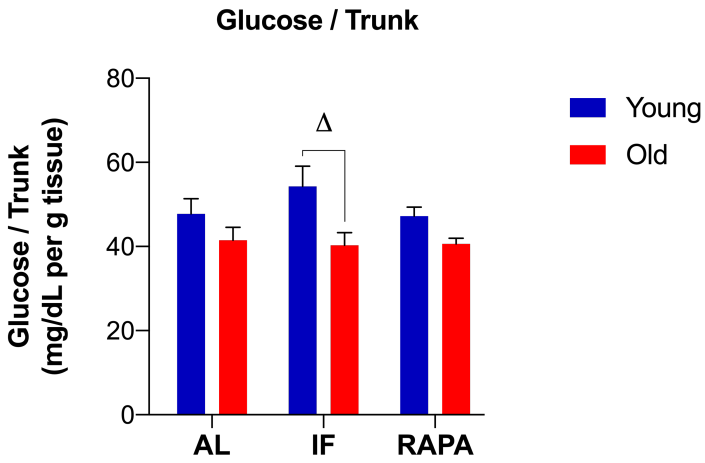

Figure 3.4. The levels of whole-body glucose normalized to trunk weight in response to IF and RAPA treatment. A significant difference in glucose/trunk levels was observed between Y-IF and O-IF. The combined mean of glucose/trunk values at different durations are shown as mg/dL per gram tissue on the graphs. The error bars represent one standard error (SE). Triangle represents age difference (Δ: $p \leq 0.05$). AL: *ad libitum*-fed control group, IF: intermittent fasting group, RAPA: rapamycin-treated group. N=13-16 per group.

Furthermore, the effect of age was limited to IF groups, with Y-IF having a higher mean glucose/trunk ratio than O-IF ($\chi^2_{(1)}=6.025$; $p=0.014$). Finally, the glucose/trunk ratio was higher in Y-RAPA than in O-RAPA, which was marginally significant ($\chi^2_{(1)}=5.460$; $p=0.019$) since the significance threshold was set at $p \leq 0.017$ for this comparison after applying a pre-hoc analysis. Nevertheless, these results suggested that the trunk weight overrides any treatment or duration effects due to young animals having lower body weight and ergo, trunk weight, than old animals.

3.2.2. Whole-body cortisol levels decrease in animals subjected to intermittent fasting

We further investigated metabolic parameters by measuring whole-body cortisol levels. Cortisol is a steroid hormone, often used as a biomarker of stress [151]. Cortisol is also known to regulate glucose levels by promoting gluconeogenesis and glucose release in response to stressors [152], [153]. Furthermore, IF and rapamycin have been shown to induce a mild stress, promoting a state of hormesis by activating molecular stress response mechanisms [154], [155]. Therefore, we were able to assess both the stress levels and confirm results from the glucose experiments by measuring whole-body cortisol levels.

To obtain comparable results with the glucose measurements, we analyzed both the cortisol levels (Figure 3.5.A) and cortisol concentration that is normalized to trunk weight (i.e. cortisol/trunk, Figure 3.5.B). Our results showed an effect of treatment on cortisol levels (Figure 3.5.A; $\chi^2_{(2)}$=10.216; p=0.006) but not on cortisol/trunk (Figure 3.5.B; $\chi^2_{(2)}$=2.972; p=0.226). Interestingly, the difference between IF and RAPA was significant (*U*=348.500, p=0.001), while the IF-AL difference was not. The treatment effect was more prominent in young animals since Y-IF had a significantly lower cortisol concentration than Y-RAPA (Figure 3.5.A; *U*=73.500, p=0.008), whereas O-IF–O-RAPA difference was marginally significant (Figure 3.5.A; *U*=102.000, p=0.059).

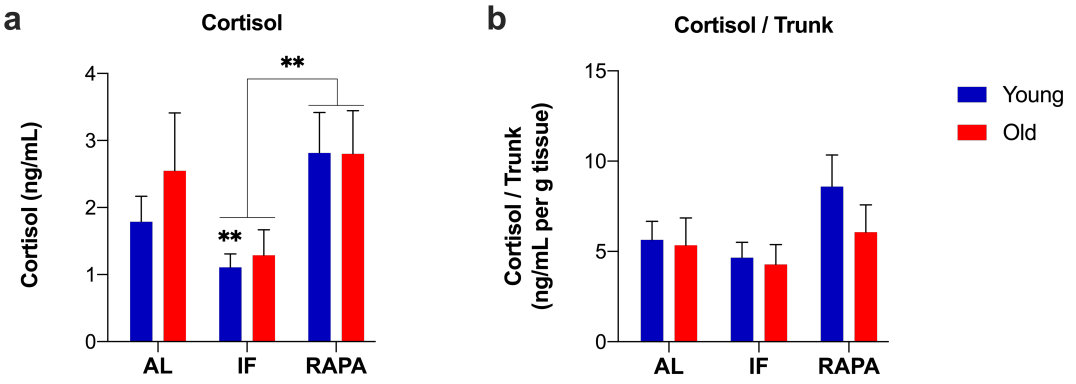

Figure 3.5. Changes in the whole-body cortisol levels in response to IF and RAPA treatment. Significant differences were observed in whole-body cortisol concentration across treatment groups (a), but not in cortisol/trunk ratio (b). The IF regimen significantly decreased cortisol concentration, and the difference between Y-IF and Y-RAPA was significant (a). The combined mean of cortisol or cortisol/trunk values at different durations are shown as ng/mL or ng/mL per gram tissue, respectively, on the graphs. The error bars represent one standard error (SE). Asterisks represent across-group differences (**: $p \leq 0.01$). AL: *ad libitum*-fed control group, IF: intermittent fasting group, RAPA: rapamycin-treated group. N=14-19.

These results suggested a decrease in cortisol levels in response to IF, and a slight increase in response to RAPA. Furthermore, this pattern was observed in both ages although the effect was stronger in young animals, indicating that stress response to both interventions is similar across lifespan. There were no significant effects of age and duration on both of these measurements.

3.3. The suppression of mTOR activity through intermittent fasting and rapamycin treatment is age-dependent

To investigate the molecular mechanisms of IF and rapamycin treatment in the brain, we initially analyzed the activity of mTOR since its inhibition has been shown to be a common response to both interventions [156]. Since mTOR is phosphorylated by the kinases acting upstream on the PI3K/AKT/mTOR pathway, as well as by itself (i.e. autophosphorylation) [157], [158], we first quantified mTOR autophosphorylation on Serine at 2481st residue (i.e. p-mTOR^{Ser2481}) to understand how IF and RAPA effects the signaling cascade upstream of mTOR. Next, we quantified the expression levels of two well-characterized downstream targets of mTOR: The eukaryotic translation initiation factor 4E (eIF4E)-binding protein 1 (4E-BP1) and ribosomal protein S6 (S6) [159]. Since mTOR is a kinase and propagates the signal by phosphorylating its downstream targets, we quantified both the total and phosphorylated versions of 4E-BP1 (i.e. p-4E-BP1) and S6 (i.e. p-S6). Finally, the ratio of phospho-protein to the total protein (p-4E-BP1/4E-BP1 and p-S6/S6) were calculated and analyzed as a measure of mTOR activity.

3.3.1. Changes in the expression levels of total p-mTOR^{Ser2481}, 4E-BP1, p-4E-BP1, and p-4E-BP1/4E-BP1 in response to IF and RAPA

Our results suggested a significant treatment effect on p-mTOR^{Ser2481} in young animals, but not in old (Figure 3.6.A; $\chi^2_{(2)} = 11.808$, $p=0.003$). Both the IF and RAPA suppressed mTOR autophosphorylation as evidenced by the reduced p-mTOR^{Ser2481} levels in Y-IF and Y-RAPA as compared to Y-AL ($p \leq 0.004$). There

were no overall effects of age ($\chi^2_{(1)}$ = 0.793, p=0.373) or duration ($\chi^2_{(2)}$ = 0.836, p=0.658).

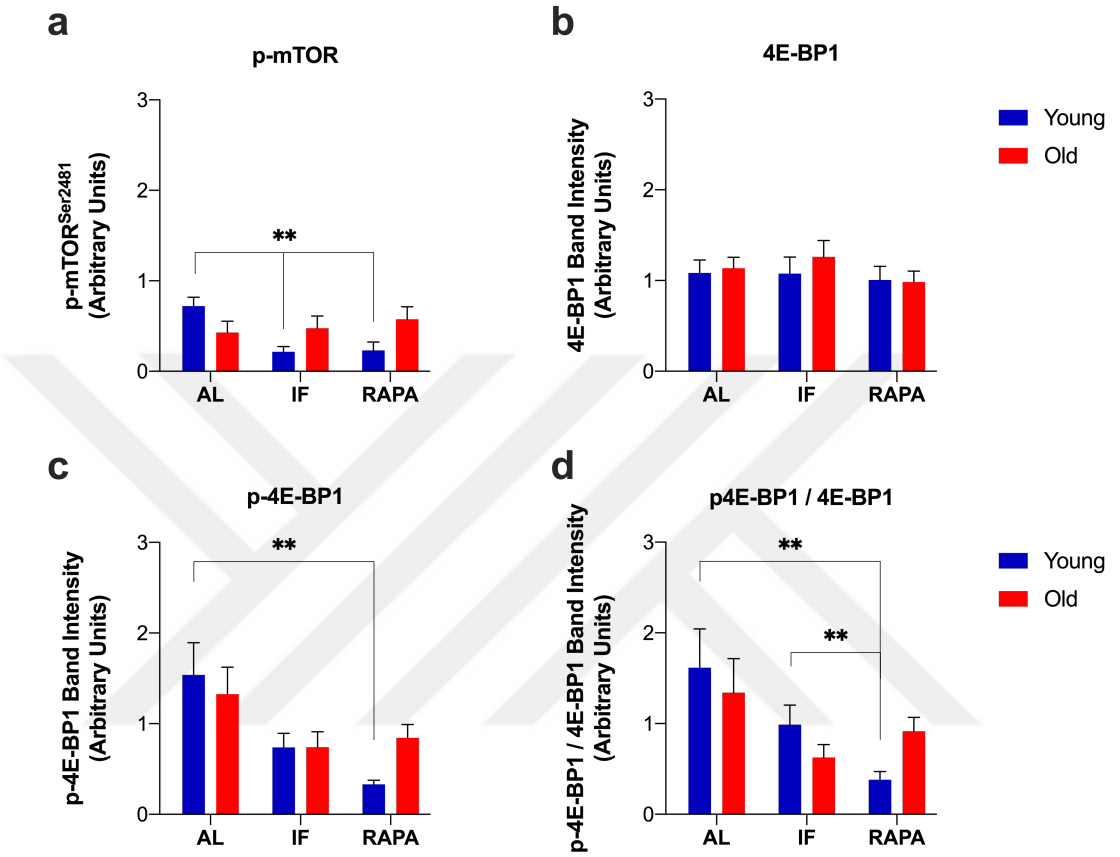

Figure 3.6. Changes in the expression levels of p-mTOR^{Ser2481}, 4E-BP1, p-4E-BP1 and p-4E-BP1/4E-BP1 in response to IF and RAPA treatment in young and old animals. Significant differences in the p-mTOR^{Ser2481} (a), p-4E-BP1 (c), and p-4E-BP1/4E-BP1 (d) levels were observed between treatment groups, but not in 4E-BP1 (b). Both the IF and RAPA decreased p-mTOR^{Ser2481} levels in young animals (a), but not in old. The expression levels of p-4E-BP1 (c) and p-4E-BP1/4E-BP1 (d) were downregulated in Y-RAPA animals, suggesting an age- and treatment-dependent inhibition of mTOR activity. The data from different durations are represented as a combined mean for each group. The double-normalized mean band

intensity values are given in arbitrary units. Error bars represent one standard error (SE). Asterisks represent across-group differences (**: p≤0.01). AL: *ad libitum*-fed control group, IF: intermittent fasting group, RAPA: rapamycin-treated group. N=9-14 per group. Reproduced from the figures that first appeared in Rejuvenation Research [142], and reprinted with permission from Mary Ann Liebert, Inc.

The total 4E-BP1 levels (Figure 3.6.B) were not significantly altered by age ($F_{(1, 77)}$= 0.415, p=0.522), treatment ($F_{(2, 77)}$=0.659, p=0.521) or duration ($F_{(2, 77)}$=0.939, p=0.397). While the total protein levels remained stable across treatment and age groups, treatment significantly affected p-4E-BP1 levels (Figure 3.6.C; $\chi^2_{(2)}$ = 14.664, p=0.001). This treatment effect was stronger in young animals, and the difference between Y-RAPA and Y-AL was significant (*U*= 2.000, p≤0.001). The suppression of 4E-BP1 phosphorylation through IF was not as effective as RAPA in young animals since the difference between Y-IF and Y-AL was marginally significant (*U*= 48.000, p=0.036). Interestingly, IF had a more suppressive effect in old animals than RAPA. Although the O-IF–O-AL difference was only of a marginal significance (*U*= 34.000, p=0.035), it was still a larger difference than that was observed in O-RAPA–O-AL (*U*= 45.000, p=0.214).

Finally, there was a significant treatment effect on p-4E-BP1/4E-BP1 levels (Figure 3.6.D; $\chi^2_{(2)}$ = 7.674, p=0.022). Again, this was only reflected as significant differences between treatment groups in young animals, but not in old. The p-4E-BP1/4E-BP1 ratio was significantly lower in Y-RAPA animals as compared to Y-IF (*U*= 19.000, p=0.006) and Y-AL (*U*= 10.000, p=0.001). The most notable difference in old animals, although only marginally significant, was between O-IF and O-AL

(Figure 3.6.D; *U*= 30.000, p=0.048). Taken altogether, these results indicate that IF and rapamycin inhibit the mTOR activity in the brain in an age-specific manner, and that the degree of mTOR inhibition depends on the age of the subjects and treatment type. All bands were observed at the expected molecular weights (Figure 3.7).

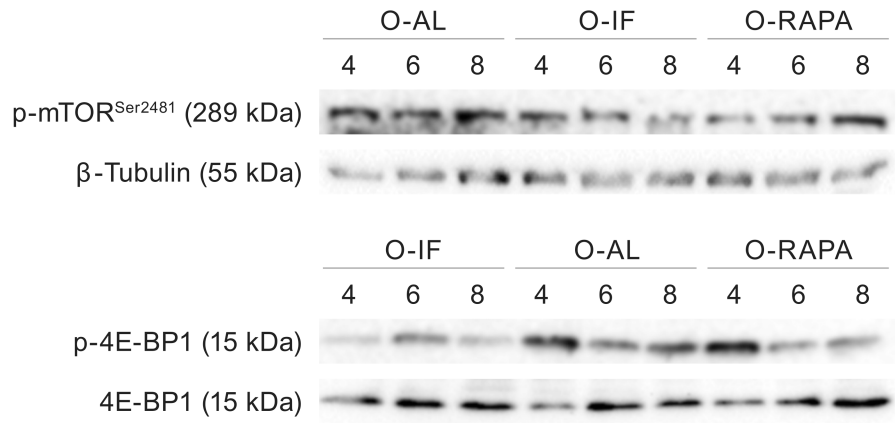

Figure 3.7. Representative western blots for p-mTOR^{Ser2481}, 4E-BP1, p-4E-BP1 and β-tubulin in old experiment groups at 4, 6 and 8 weeks. The bands at approximately at 289 kDa correspond to p-mTOR^{Ser2481}, at 15 kDa correspond to 4E-BP1 and p-4E-BP1, and the bands at 55 kDa correspond to β-tubulin. O-AL: old *ad libitum*-fed group, O-IF: old intermittent fasting group, O-RAPA: old rapamycin-treated group. Reproduced from the figures that first appeared in Rejuvenation Research [142], and reprinted with permission from Mary Ann Liebert, Inc.

3.3.2. Changes in the expression levels of total S6, p-S6, and their ratio in response to IF and RAPA

To understand if another target of mTOR is affected by IF and RAPA treatment, we quantified the expression levels of S6, p-S6 and their ratio (p-S6/S6). There were no

treatment effects on any of these measures. Age, on the other hand, significantly affected S6 ($\chi^2_{(1)}$ = 8.673, p=0.003) and p-S6 ($\chi^2_{(1)}$ = 6.304, p=0.012) expression levels.

Interestingly, old animals had higher S6 and p-S6 levels (Figures 3.8.A and 3.8.B, respectively). However, treatment-specific pairwise comparisons led to only marginally significant differences. For instance, O-IF group had higher p-S6 levels than Y-IF (Figure 3.8.B; *U*=58.000, p=0.078). The expression levels of S6 was numerically higher in O-RAPA and O-AL groups as compared to Y-RAPA (*U*=51.000, p=0.068) and Y-AL (*U*=31.500, p=0.097) groups (Figure 3.8.A).

The p-S6/S6 ratio was not affected by age (Figure 3.8.C; $\chi^2_{(1)}$ = 0.548, p=0.459), but was under a significant duration effect (Figure 3.9; $\chi^2_{(2)}$ = 6.626, p=0.036). The difference in the p-S6/S6 ratio between 6 and 8 weeks was significant (*U*=181.000, p=0.018), while it was marginally significant between 4 and 6 weeks (*U*=158.000, p=0.050). However, these overall duration effects were not observed within groups in young (Figure 3.9.A) or old animals (Figure 3.9.B). All bands were observed at the expected molecular weights (Figure 3.10).

Taken together, these results suggest that IF and RAPA did not significantly alter the expression levels of S6 and p-S6, as well as their ratio. The effect of age as reflected by higher S6 and p-S6 levels in old animals indicate that the age-dependent regulation of S6 and its phosphorylation override any treatment effect. Furthermore, the suppression of mTOR activity through diet or drug treatment might have distinct

consequences on different downstream elements of the mTOR pathway since mTOR inhibition had a stronger effect on 4E-BP1 phosphorylation than on S6.

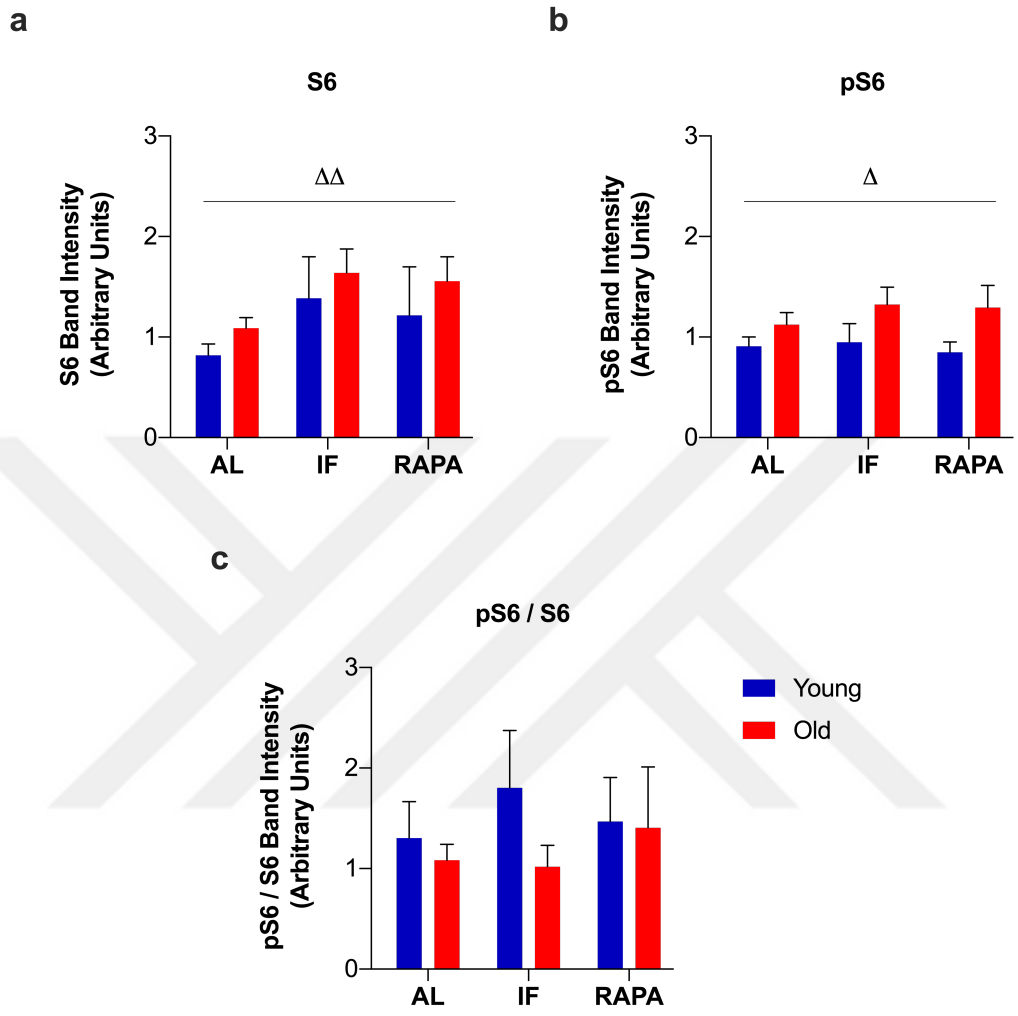

Figure 3.8. Changes in the expression levels of S6, p-S6 and p-S6/S6 in response to IF and RAPA treatment. Significant overall age effect was observed in S6 (a) and p-S6 (b), but not in p-S6/S6 ratio (c). There were no significant across-group differences. The data from different durations are represented as a combined mean for each group. The double-normalized mean band intensity values are given in arbitrary units. Error bars represent one standard error (SE). Empty triangles represent significant age effect (ΔΔ: $p \leq 0.01$, Δ: $p \leq 0.05$). AL: *ad libitum*-fed control group, IF: intermittent fasting group, RAPA: rapamycin-treated group. N=10-16.

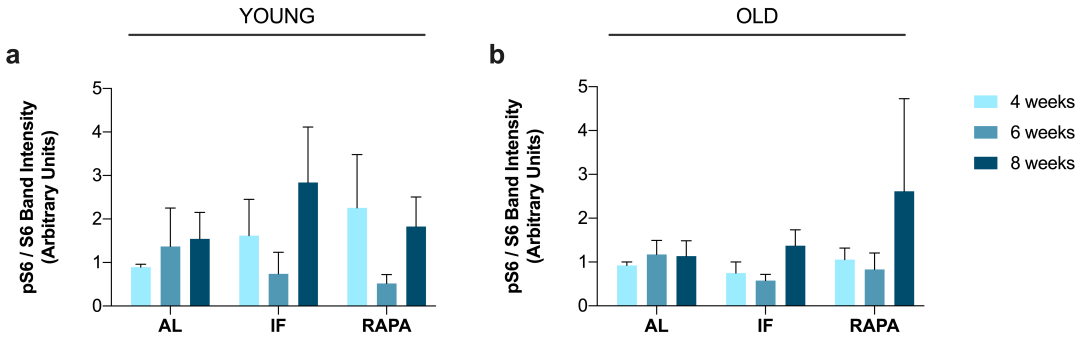

Figure 3.9. Changes in the p-S6/S6 ratio in response to different durations of IF and RAPA treatment. Significant overall duration effect was observed in p-S6/S6 ratio, and the difference between 6 and 8 weeks was significant. There were no significant within or across-group differences. The double-normalized mean band intensity values are given in arbitrary units. Error bars represent one standard error (SE). AL: *ad libitum*-fed control group, IF: intermittent fasting group, RAPA: rapamycin-treated group. N=3-6 per group at a given duration.

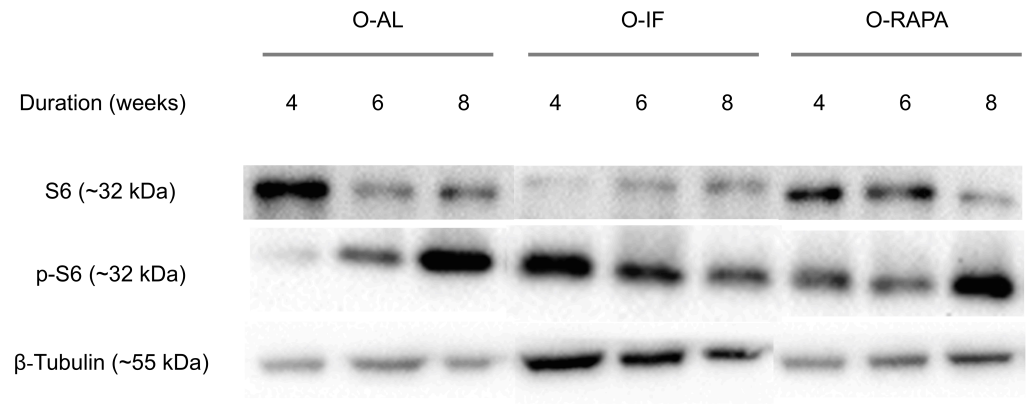

Figure 3.10. Representative western blots for S6, p-S6 and β-tubulin in old experiment groups at 4, 6 and 8 weeks. The bands at approximately 32 kDa correspond to S6 and its phosphorylated version, p-S6, and the bands at 55 kDa correspond to β-tubulin. O-AL: old *ad libitum*-fed group, O-IF: old intermittent fasting group, O-RAPA: old rapamycin-treated group.

3.4. The effects of intermittent fasting and rapamycin on the expression levels of key synaptic proteins, and markers of autophagy or proliferation

The IF regimen, and its mimetic, rapamycin, have been shown to promote longevity and improve cognitive functions across species [156], [160]. There is growing evidence regarding their molecular mechanisms of action that is obtained through both *in vitro* and *in vivo* studies, yet their implications in the brain remain insufficiently explored. To fill this gap, we quantified the expression levels of some proteins involved in several different aspects of brain homeostasis. These were: 1. Proteins localized in postsynaptic and presynaptic compartments with fundamental roles in neurotransmission 2. Markers of autophagic flux, a mechanism that has been shown to be required for synaptic maintenance and reorganization, as well as overall homeostasis [161] 3. Markers of overall proliferation, neurogenesis, and astrogliogenesis. With these analyses, we aimed to provide evidence for the molecular and cellular alterations that may underlie the beneficial effects of IF and RAPA on the cognitive skills that are subjected to age-related deterioration.

3.4.1. Changes in the expression levels of postsynaptic and presynaptic proteins involved in neurotransmission

We first investigated how postsynaptic markers changed in response to IF and RAPA by quantifying the postsynaptic density-95 (PSD-95) and gephyrin (GEP) as markers of excitatory and inhibitory synapses, respectively (Figures 3.11.A and 3.11.B). Our results showed an effect of age on the expression levels of PSD-95

(Figure 3.11.A; $\chi^2_{(1)}$ = 9.181, p=0.002). Interestingly, the levels of PSD-95 were higher in old animals of all treatment groups, with the higher expression in O-RAPA group compared to Y-RAPA being statistically significant (p=0.012).

The anchor protein in the inhibitory synapses, GEP, was affected by duration (Figure 3.12; $\chi^2_{(2)}$ = 7.485, p=0.024) and treatment, although the latter was limited to old animals (Figure 3.11.B; $\chi^2_{(2)}$ = 6.870, p=0.032). While the GEP expression was similar in O-AL and O-RAPA groups, it was significantly higher in O-IF (O-IF – O-RAPA: p=0.011). Interestingly, duration effect was also significant for old age ($\chi^2_{(2)}$ = 10.371, p=0.006) and longer durations of both IF and RAPA downregulated GEP expression in old animals. However, the differences between 4 weeks and later durations were significant for O-RAPA, while they failed to reach a statistical significance in O-IF (Figure 3.12). Furthermore, since the GEP expression levels were higher in O-IF compared to O-RAPA throughout the experiment, the average GEP expression was also higher in O-IF than in O-RAPA. These results suggested that in our setup, inhibitory postsynaptic transmission is affected in an age- and treatment-dependent manner.

In addition to individual markers of excitatory and inhibitory postsynaptic compartments, we compared the ratio of PSD-95/GEP as an indicator of excitatory/inhibitory (E/I) balance. The maintenance of E/I balance is an essential aspect of healthy brain aging due to its involvement in neuronal plasticity [84]. Furthermore, E/I has been shown to be altered by the advancing age [162] and dietary manipulations [163].

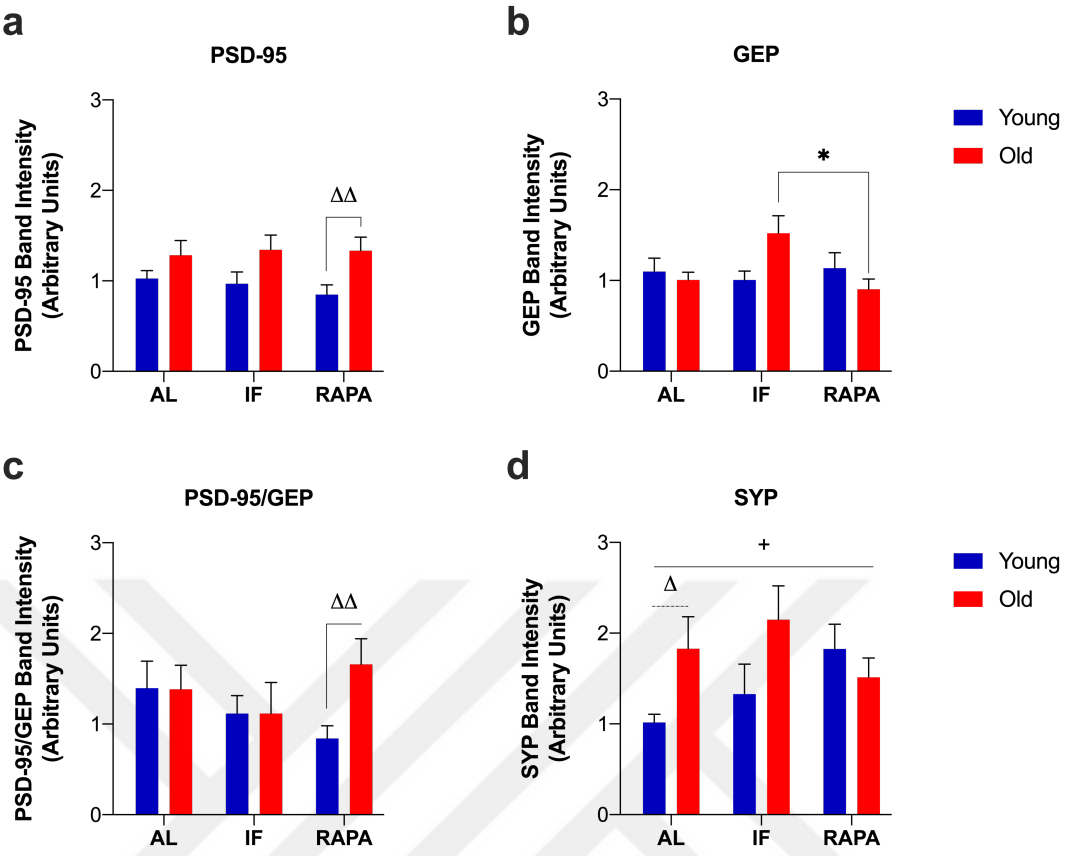

Figure 3.11. Changes in the expression levels of PSD-95, GEP and PSD-95/GEP, and SYP in response to IF and RAPA treatment. Significant age effects were observed in PSD-95 (a), PSD-95/GEP (c) and SYP (d). The GEP expression was significantly higher in O-IF (b). The data from different durations are represented as a combined mean for each group. The double-normalized mean band intensity values are given in arbitrary units. Error bars represent one standard error (SE). Empty triangles represent significant age differences (ΔΔ: $p \leq 0.01$, Δ: $p \leq 0.05$). Plus sign represents significant overall age effect (+: $p \leq 0.05$). N=11-16 per group. Reproduced from the figures that first appeared in Rejuvenation Research [142], and reprinted with permission from Mary Ann Liebert, Inc.

We observed a significant effect of treatment on PSD-95/GEP levels only in old animals (Figure 3.11.C; $\chi^2_{(2)} = 7.694$, $p=0.021$). Moreover, there was an age effect

which was limited to RAPA group ($\chi^2_{(1)} = 6.193$, p=0.013). The significantly higher PSD-95/GEP ratio in O-RAPA as compared to Y-RAPA, along with the lack of alterations in IF and AL groups suggested that RAPA treatment shifted the brain towards a more excitatory state.

The signal transmission between neurons is achieved by the harmonious events occurring at both the postsynaptic and presynaptic sites. Therefore, to understand whether IF and RAPA alter the presynaptic activity, we quantified synaptophysin (SYP) expression levels. SYP is a Ca^{2+}-binding presynaptic vesicle protein [164], [165], and its expression has been shown to be changed with the advancing age [166], [167]. Our results demonstrated a significant age effect on the SYP expression levels (Figure 3.11.D; $\chi^2_{(1)} = 5.108$, p=0.024). Consistent with the previous reports, old animals had higher basal levels of SYP [168]. This was particularly evident in the AL groups, since SYP expression was higher in O-AL than in Y-AL (Figure 3.11.D; p=0.055). Interestingly, RAPA treatment dissociated the age effect and led to similar SYP expression levels in young and old animals.

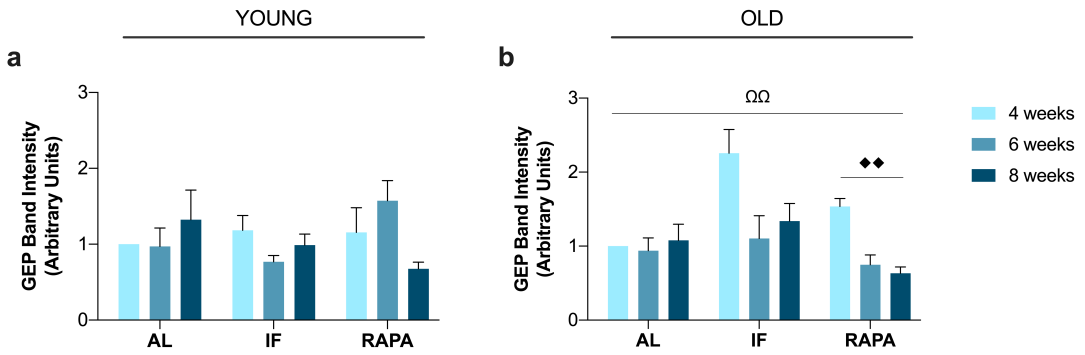

Figure 3.12. Changes in the expression levels of GEP in response to different durations of IF and RAPA treatment. Significant overall duration effect was

observed in GEP. Duration did not significantly affect GEP in young animals (a) as it did in old animals (b). The double-normalized mean band intensity values are given in arbitrary units. Error bars represent one standard error (SE). Omega represents significant overall duration effect (ΩΩ: $p \leq 0.01$), and diamond represents significant within-group differences (◆◆: $p \leq 0.01$). AL: *ad libitum*-fed control group, IF: intermittent fasting group, RAPA: rapamycin-treated group. N=4-7 per group at a given duration. Reproduced from the figures that first appeared in Rejuvenation Research [142], and reprinted with permission from Mary Ann Liebert, Inc.

Overall, the observed patterns suggested that the primary determinant for regulating the expression levels of these presynaptic and postsynaptic markers is the age of the subjects. Treatment effect was observed in GEP and PSD-95/GEP, which did not cause any changes in the E/I balance in IF groups, but a shift towards excitotoxicity in O-RAPA animals. Finally, the age effect on the SYP expression levels was strong enough to override any short-term treatment effects. All bands were observed at the expected molecular weights (Figure 3.13).

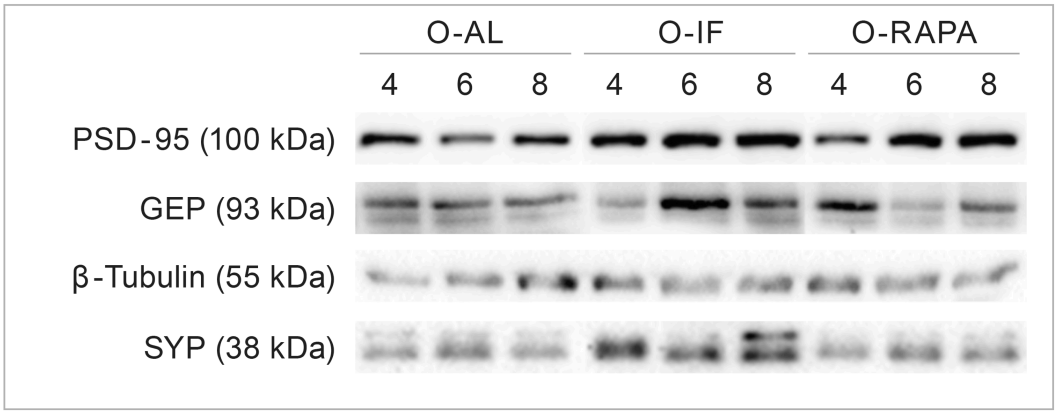

Figure 3.13. Representative western blots for PSD-95, GEP, β-tubulin and SYP in old experiment groups at 4, 6 and 8 weeks. The bands at approximately 100 kDa correspond to PSD-95, at 93 kDa to GEP, at 38 kDa to SYP, and the bands at 55 kDa to β-tubulin. O-AL: old *ad libitum*-fed group, O-IF: old intermittent fasting group, O-RAPA: old rapamycin-treated group. Reproduced from the figures that first appeared in Rejuvenation Research [142], and reprinted with permission from Mary Ann Liebert, Inc.

3.4.2. Changes in the expression levels of autophagic flux markers

To extend our understanding of the molecular changes related to IF and RAPA in the brain, we investigated whether autophagy, a mechanism required for synaptic homeostasis [161] was induced. Autophagy has been shown to be repressed by mTOR activation [169], and life span extension through diet or pharmacological mTOR inhibitors is mediated through induction of autophagy [170], [171]. For this purpose, we analyzed Microtubule-associated protein 1A/1B light chain 3 (MAP1LC3, hereafter referred to as LC3), a widely used marker of autophagosomes and an indirect indicator of autophagic flux [172]. There are two isoforms of LC3: LC3-I and LC3-II. The cytosolic form of LC3 (i.e. LC3-I) undergoes lipidation through the conjugation of phosphatidylethanolamine to form LC3-II. Only after lipidation, LC3-II is recruited to the autophagosomal membranes [173].

We quantified both forms of LC3, as well as their ratio (i.e. LC3-II/LC3-I). There were no effects of age, treatment or duration on LC3-I (Figure 3.14.A) and LC3-II (Figure 3.14.B). On the other hand, there were both significant treatment ($\chi^2_{(2)}$

=8.518, p=0.014) and age effects ($\chi^2_{(1)}$ =7.376, p=0.007) on the LC3-II/LC3-I ratio (Figure 3.14.C). The treatment effect was age-dependent, since RAPA decreased the LC3-II/LC3-I ratio in young animals (*U*= 30.000, p=0.005) whereas IF decreased it in the old animals (*U*= 22.000, p=0.023) as compared to AL-fed age-matched counterparts. Interestingly, LC3-II/LC3-I ratio was higher in O-AL and O-RAPA than their young counterparts (p≤0.02). All bands were observed at the expected molecular weights (Figure 3.15).

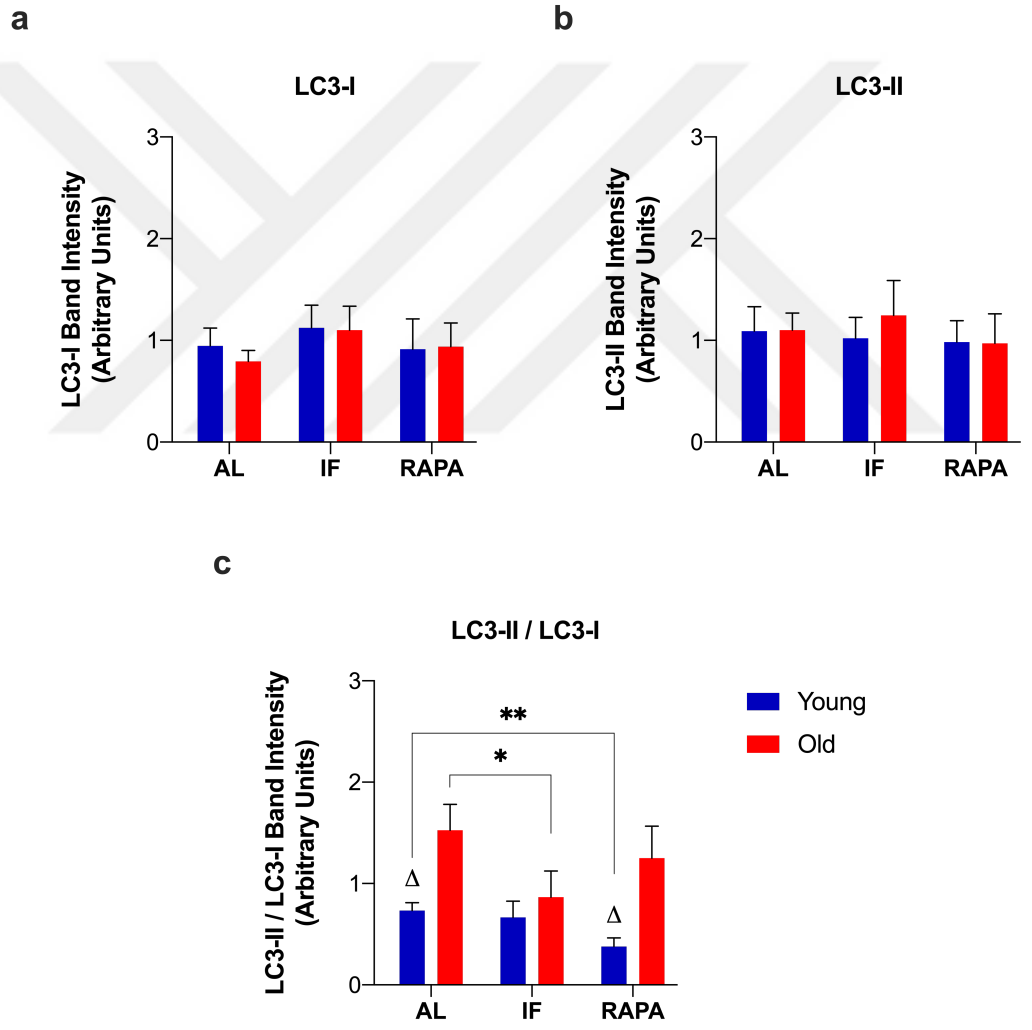

Figure 3.14. Changes in the expression levels of LC3-I, LC3-II and LC3-II/LC3-I in response to IF and RAPA treatment. There were no significant effects of age and duration on LC3-I (a) and LC3-II (b). Significant differences in LC3-II/LC3-I

were observed between groups (c). The data from different durations are represented as a combined mean for each group. The double-normalized mean band intensity values are given in arbitrary units. Error bars represent one standard error (SE). Empty triangles represent significant age differences (Δ: $p \leq 0.05$). Asterisks represent significant across-group differences (**: $p \leq 0.01$, *: $p \leq 0.05$). N=9-14. Reproduced from the figures that first appeared in Rejuvenation Research [142], and reprinted with permission from Mary Ann Liebert, Inc.

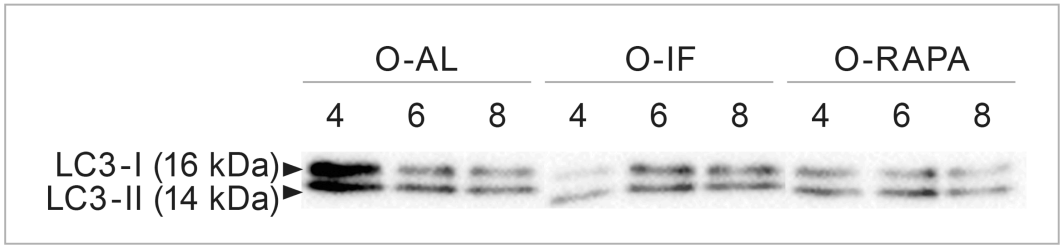

Figure 3.15. Representative western blots for LC3-I and LC3-II in old experiment groups at 4, 6 and 8 weeks. The bands at approximately 16 kDa correspond to LC3-I and bands at 14 kDa to LC3-II. O-AL: old *ad libitum*-fed group, O-IF: old intermittent fasting group, O-RAPA: old rapamycin-treated group. Reproduced from the figures that first appeared in Rejuvenation Research [142], and reprinted with permission from Mary Ann Liebert, Inc.

3.4.3. Changes in the markers of global proliferation, neurogenesis, and activated astrocytes

Upon assessing the short-term effects of IF and RAPA on markers of postsynaptic and presynaptic sites, and autophagic flux, we aimed to understand whether and how these interventions change cell proliferation. We quantified both global and lineage-specific markers to assess overall proliferation rates as well as neurogenic and

gliogenic potentials in the brains of young and old animals subjected to IF or RAPA. The global proliferation marker that we quantified was the proliferating cell nuclear antigen (PCNA), a component of the DNA replication machinery [174], [175]. Since its discovery in late 1970s, it has been used as a marker of proliferation due to its presence in the nucleus of dividing cells [175]. Lineage-specific markers, doublecortin-like kinase 1 (DCAMKL1) and glial fibrillary acidic protein (GFAP) were used as markers of neural progenitor cells (NPCs) and radial glia, respectively [176], [177]. Since GFAP is also used widely as a marker of activated astrocytes, which are known to play a role in neuroinflammation, its quantification allowed us to investigate both the immature precursors and inflammatory status in the brain [177].

Treatment and age significantly affected PCNA expression levels (Figure 3.16.A; $\chi^2_{(2)} = 6.665$, p=0.036 and $\chi^2_{(1)} = 3.930$, p=0.047, respectively). Interestingly, RAPA downregulated PCNA expression in young animals, and the difference between Y-RAPA and Y-AL was significant (*U*= 30.000, p=0.002). The RAPA-induced downregulation of PCNA expression was not observed in old animals, suggesting that RAPA suppressed overall proliferation in an age-dependent manner in the brain. This age effect was also supported by the observation that O-RAPA animals had significantly higher levels of PCNA than Y-RAPA (*U*= 29.000, p=0.026).

The marker of neuronally committed progenitors, DCAMKL1, was affected significantly by treatment (Figure 3.16.B; $\chi^2_{(2)} =13.106$, p=0.001). The IF regimen upregulated DCAMKL1 in both young (*U*= 46.000, p=0.011) and old animals (*U*= 42.000, p=0.019). There were also numerical increases in RAPA animals,

particularly in O-RAPA group, although these failed to reach a statistical significance. These results suggest that IF, and to some extent, RAPA treatment may improve brain health through either increasing the number of NPCs or protecting their existing pool.

Finally, treatment significantly affected GFAP expression levels (Figure 3.16.C; $\chi^2_{(2)}$ = 9.084, p=0.011). This treatment effect was limited to rapamycin-treated old animals, since GFAP levels were decreased in O-RAPA as compared to O-AL and O-IF (*U*= 51.000, p=0.006). These results indicated that RAPA downregulated the expression levels of GFAP in an age-dependent manner. Since other proliferative markers did not follow the same pattern in O-RAPA, the reduced GFAP expression is more likely to reflect a reduction in the number of activated astrocytes, which might imply an impediment to inflammatory response. All bands were observed at the expected molecular weights (Figure 3.17).

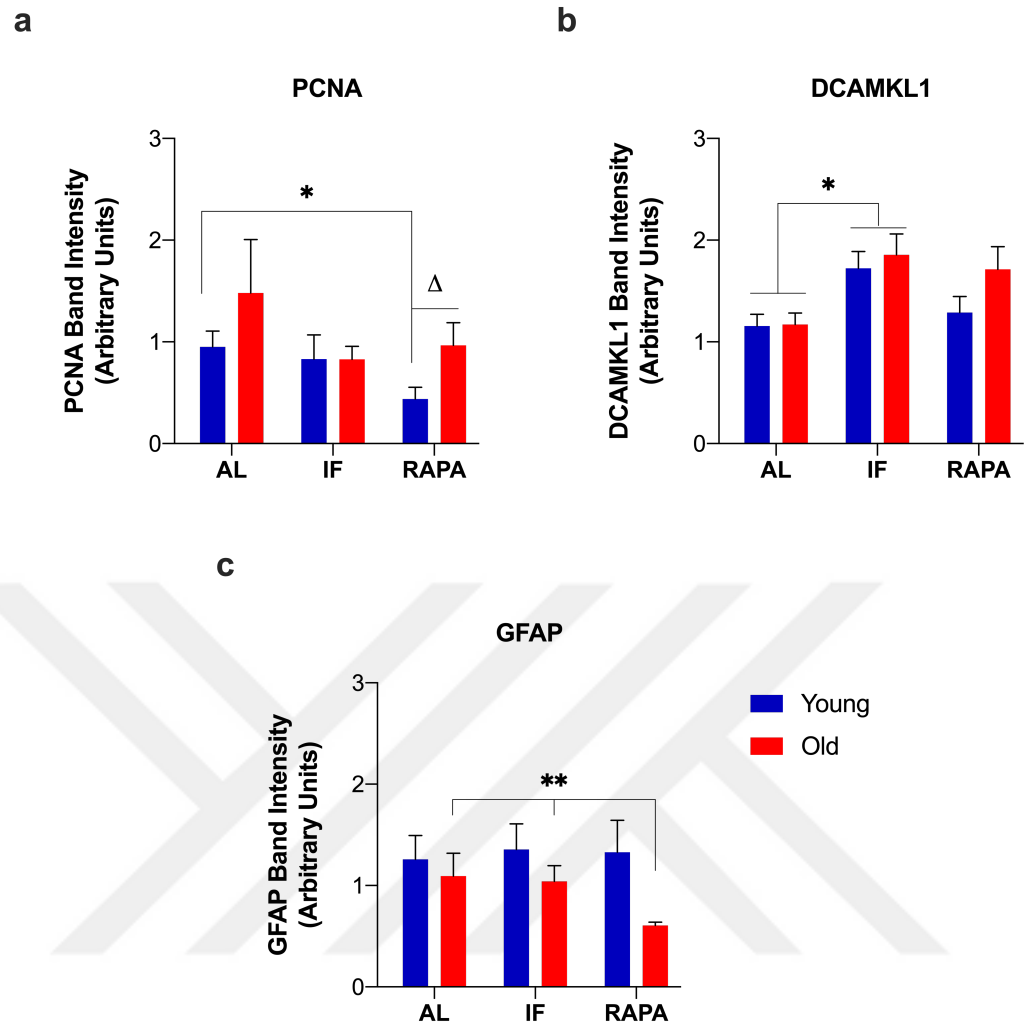

Figure 3.16. Changes in the expression levels of PCNA, DCAMKL1 and GFAP in response to IF and RAPA treatment. The data from different durations are represented as a combined mean for each group. The double-normalized mean band intensity values are given in arbitrary units. Error bars represent one standard error (SE). Empty triangles represent significant age differences (Δ: $p \leq 0.05$). Asterisks represent significant across-group differences (**: $p \leq 0.01$, *: $p \leq 0.05$). N=6-15 for PCNA and 11-16 for DCAMKL1 and GFAP. Reproduced from the figures that first appeared in Rejuvenation Research [142], and reprinted with permission from Mary Ann Liebert, Inc.

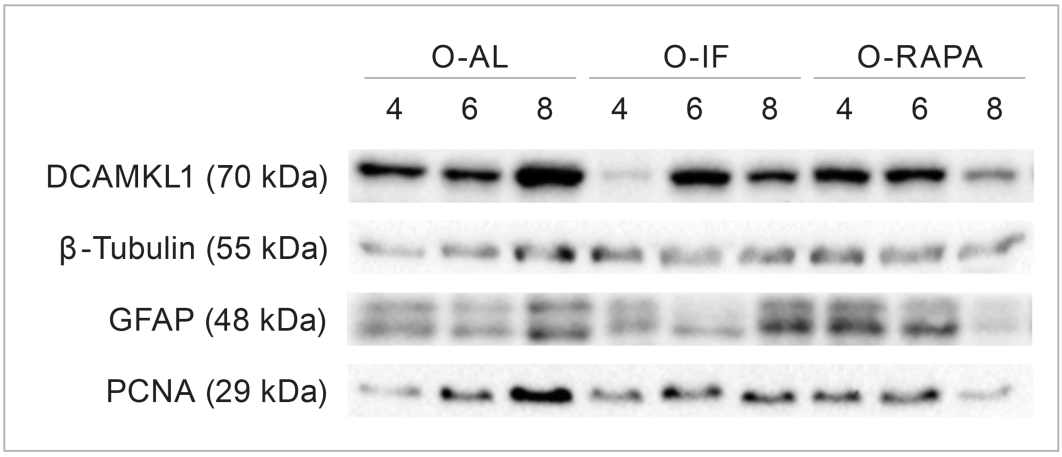

Figure 3.17. Representative western blots for DCAMKL1, GFAP, PCNA and β-tubulin in old experiment groups at 4, 6 and 8 weeks. The bands at approximately 70 kDa correspond to DCAMKL1, at 55 kDa to β-tubulin, at 48 kDa to GFAP and bands at 29 kDa to PCNA. O-AL: old *ad libitum*-fed group, O-IF: old intermittent fasting group, O-RAPA: old rapamycin-treated group. Reprinted with permission from Mary Ann Liebert, Inc.

3.5. The expression levels of genes involved in the mTOR pathway, proliferation and autophagy

The current literature regarding the mechanisms through which IF and RAPA dictate their effects indicates that both interventions modulate the PI3K/AKT/mTOR pathway. However, growing evidence suggest that their mechanisms of action differ in some respects, albeit their consequences are common in being beneficial for the life span and health span. For example, the duration of IF and the dose of RAPA differentially regulate hepatic gene expression [150], [178]. To investigate some of the critical mechanisms that are potentially regulated by these interventions in the

brain, as well as differentiate where they converge or diverge, we quantified the expression levels of genes involved in nutrient signaling, and common to cellular processes in the brain such as dopamine metabolism, proliferation, and autophagy. For the gene expression analysis, we selected the following genes: genes encoding zebrafish mTOR, AKT serine/threonine kinase 1 (AKT1) and insulin-like growth factor (IGF1), *ztor*, *akt1* and *igf1*, respectively, in nutrient signaling; Aromatic-L-amino-acid-decarboxylase (DDC), *ddc,* involved in dopamine metabolism; Forkhead Box M1 (FOXM1), *foxm1,* with roles in proliferation; Autophagy-Related 5 (ATG5) and LC3-Beta, *atg5* and *lc3b*, respectively, both of which are required for autophagic cascades.

3.5.1. Changes in the expression levels of genes in the nutrient signaling pathway

To understand whether the changes in the mTOR activity that we observed at the protein level were reflected in the transcript level, we quantified the expression levels of *ztor*, and the genes encoding two elements upstream to mTOR in the nutrient signaling pathway: *akt1* and *igf1* (Figure 3.18). There were no significant effects of age ($\chi^2_{(1)} = 0.207$, p=0.649) or treatment ($\chi^2_{(2)} = 2.917$, p=0.233) on the $\log_2$ fold change values of *ztor* (Figure 3.18.A). The duration of the treatment, on the other hand, significantly affected *ztor* expression levels (Figure 3.19; $\chi^2_{(2)} = 10.353$, p=0.006). The difference between the *ztor* fold change values at 4 and 6 weeks was significant (U= 189.000, p=0.001). Furthermore, RAPA downregulated *ztor* in old animals from 4 to 6 weeks (Figure 3.19; p=0.008). There were no overall significant

effects of age ($\chi^2_{(1)} = 2.430$, p=0.119), treatment ($\chi^2_{(2)} = 0.702$, p=0.704) or duration ($\chi^2_{(2)} = 2.888$, p=0.236) on *akt1* transcript levels (Figure 3.18.B).

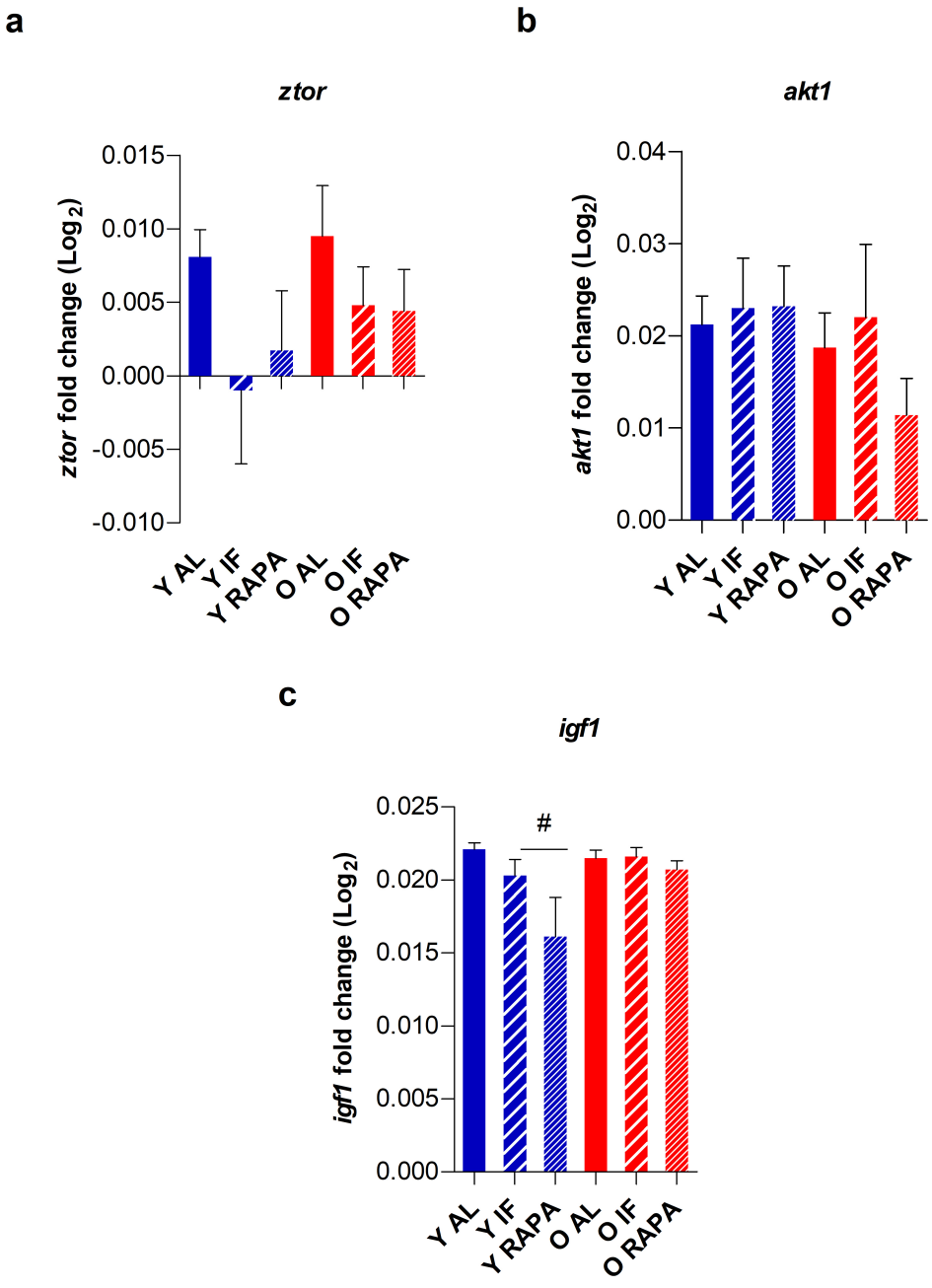

Figure 3.18. Log_2 fold change values in the expression levels of *ztor*, *akt1* and *igf1* transcripts encoding proteins in the nutrient signaling pathway. There were no effects of age and treatment on *ztor* (a) and *akt1* (b). Treatment significantly affected *igf1* (c). AL: *ad libitum*-fed control group, IF: intermittent fasting group,

RAPA: rapamycin-treated group. Hashtag represents significant treatment effect (#: p≤0.05). N=12-15 per group. Reproduced from the figures that first appeared in Rejuvenation Research [142], and reprinted with permission from Mary Ann Liebert, Inc.

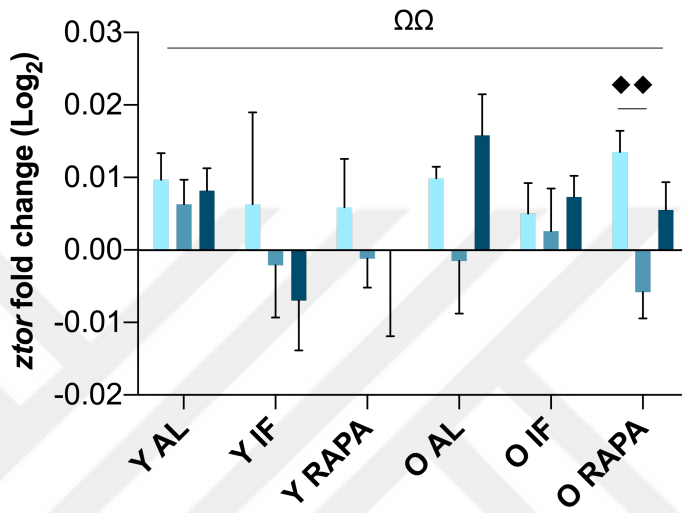

Figure 3.19. Log_2 fold change values in the expression levels of *ztor* in response to different durations of IF and RAPA. Duration significantly affected *ztor* fold change values. Omega represents significant overall duration effect (ΩΩ: p≤0.01), and diamond represents significant within-group differences (◆◆: p≤0.01). AL: *ad libitum*-fed control group, IF: intermittent fasting group, RAPA: rapamycin-treated group. Hashtag represents significant treatment effect (#: p≤0.05). N=3-5 per group at a given duration.

Out of these three genes, the *igf1* gene encodes the most upstream element in the nutrient signaling pathway [179]. Our results showed a significant treatment effect on the fold change levels of *igf1* transcript (Figure 3.18.C; $\chi^2_{(2)} = 7.250$, p=0.027). Rapamycin treatment significantly downregulated the *igf1* expression as compared to

AL (*U*= 245.500, p=0.017) and IF (*U*= 266.500, p=0.026). The effect of RAPA was observed only in young animals since the difference between Y-RAPA and Y-AL was marginally significant where the significance threshold was set to p≤0.025 (*U*= 56.000, p=0.032), and the p value was much larger for O-RAPA (p=0.435). The downregulation of *igf1* in response to mTOR inhibition in young but not in old animals is consistent with the literature [180]. There were no significant effects of age ($\chi^2_{(1)} = 0.005$, p=0.946) or duration ($\chi^2_{(2)} = 1.997$, p=0.368).

3.5.2. Changes in the expression levels of rapamycin-responsive genes

Next, we tested the effects of both IF and RAPA on the brain expression levels of two well-documented rapamycin-sensitive genes in zebrafish. We measured the expression levels of *ddc* and *foxm1*, two genes that have been previously shown to be upregulated and downregulated, respectively, by rapamycin in a zebrafish fibroblast cell line, ZF4 [130]. The DDC protein encoded by *ddc* gene is required for conversion of L-DOPA to dopamine and L-5-hydroxytryptophan to serotonin [181]. FOXM1 is a transcription factor regulating cell cycle progression and adult neurogenesis [176]. Its expression is restricted to neural progenitor cells in adult mice [182], and the gene encoding FOXM1 (i.e. *foxm1)* is markedly downregulated in elderly individuals [183].

Our data demonstrated no overall effects of treatment (Figure 3.20.A; $\chi^2_{(2)} = 1.522$, p=0.467), age ($\chi^2_{(1)} = 0.648$, p=0.421) or duration ($\chi^2_{(2)} = 4.252$, p=0.119) on *ddc*. The expression levels of *foxm1* was affected by both age ($\chi^2_{(2)} = 16.654$, p≤0.001) and treatment (Figure 3.20.B; $\chi^2_{(2)} = 6.339$, p=0.042). The IF regimen significantly upregulated *foxm1* expression (*U*=216.000, p=0.016) compared to AL, while the

upregulation in RAPA-treated animals was marginally significant (U=279.000, p=0.065). The age-specific analysis of treatment effect suggested a significant impact only in old animals ($\chi^2_{(2)}$ = 8.226, p=0.016; O-AL-OIF, p=0.030), but not in young, suggesting an age-dependent upregulation of *foxm1*.

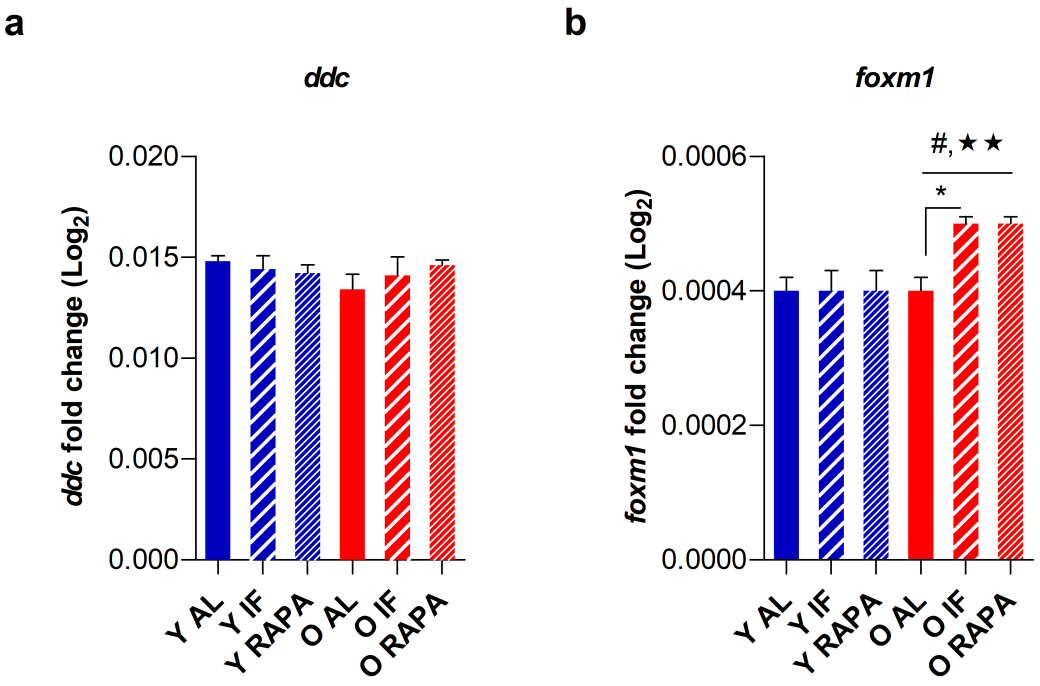

Figure 3.20. Log$_2$ fold change values of rapamycin-responsive genes *ddc* and *foxm1*. There were no effects of age and treatment on *ddc* (a). Treatment and age significantly affected *foxm1* (b). AL: *ad libitum*-fed control group, IF: intermittent fasting group, RAPA: rapamycin-treated group. Hashtag represents significant treatment effect (#: p≤0.05). N=11-15 per group. Reproduced from the figures that first appeared in Rejuvenation Research [142], and reprinted with permission from Mary Ann Liebert, Inc.

3.5.3. Changes in the expression levels of autophagy-related genes

In addition to the quantification of LC3-I and LC3-II protein expression, we wanted to further explore whether IF and RAPA altered the expression levels of autophagy-related genes. The genes encoding the ATG5 (*atg5*) and beta isoform of LC3 (*lc3b*) were evaluated for their fold change responses. There were no overall significant effects of age ($\chi^2_{(1)}$ =0.629, p=0.428), treatment ($\chi^2_{(2)}$ =0.289, p=0.866) or duration on *atg5* levels (Figure 3.21.A; $\chi^2_{(2)}$ =1.769, p=0.413) or *lc3b* (Figure 3.21.B; $\chi^2_{(1)}$ =1.419, p=0.234 for age; $\chi^2_{(2)}$ =2.116, p=0.347 for treatment; and $\chi^2_{(2)}$ =3.158, p=0.206 for duration).

While there no overall effects, the duration significantly affected the *lc3b* expression levels in old animals (Figure 3.22; $\chi^2_{(2)}$ =10.067, p=0.007). The *lc3b* expression levels at 6 weeks were significantly higher than at 4 (*U*= 34.000, p= 0.002) and 8 weeks (*U*= 39.000, p= 0.02) in old animals (Figure 3.22). Nevertheless, the *lc3b* fold change values were comparable across old groups throughout the 8-week experiment, suggesting that treatment did not alter the autophagic markers at the transcript level.

These results were surprising, since both the IF and RAPA have been shown to upregulate *lc3b* expression [184], [185]. However, reports with contradicting results exist, indicating that experimental setup might alter the outcome. Indeed, we observed numerical downregulation of *lc3b* in Y-IF and Y-RAPA, and although this was not significant, the pattern of reduced expression is consistent with previous findings in young mice [171].

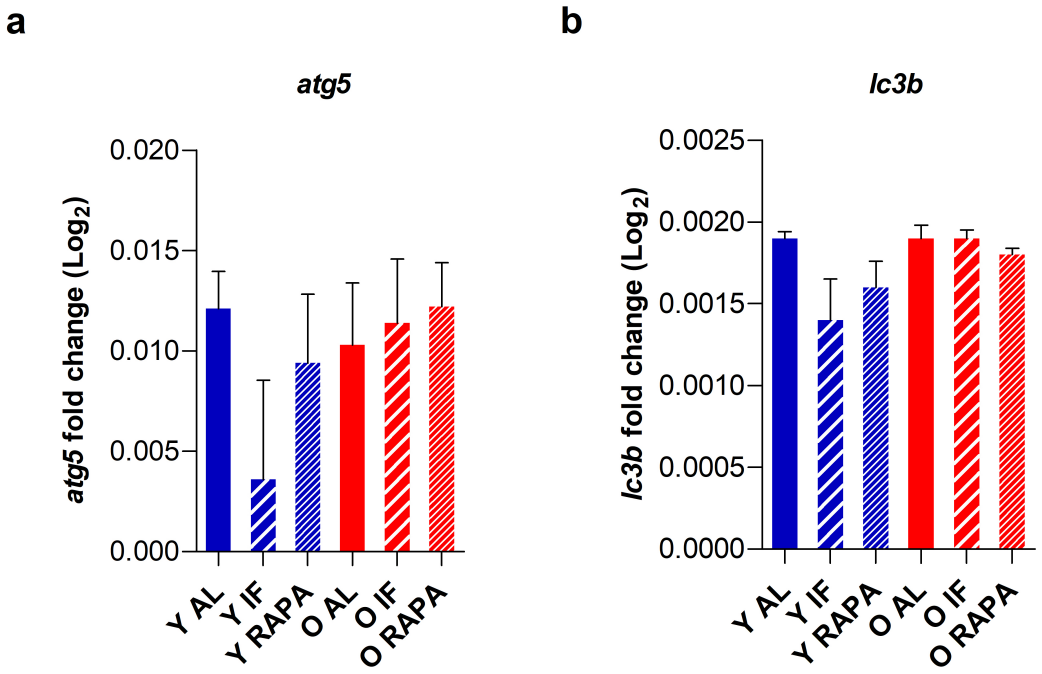

Figure 3.21. Log_2 fold change values of autophagy-related genes *atg5* and *lc3b*. There were no effects of age and treatment on *atg5* (a) and *lc3b* (b). AL: *ad libitum*-fed control group, IF: intermittent fasting group, RAPA: rapamycin-treated group. N=12-15 per group. Reproduced from the figures that first appeared in Rejuvenation Research [142], and reprinted with permission from Mary Ann Liebert, Inc.

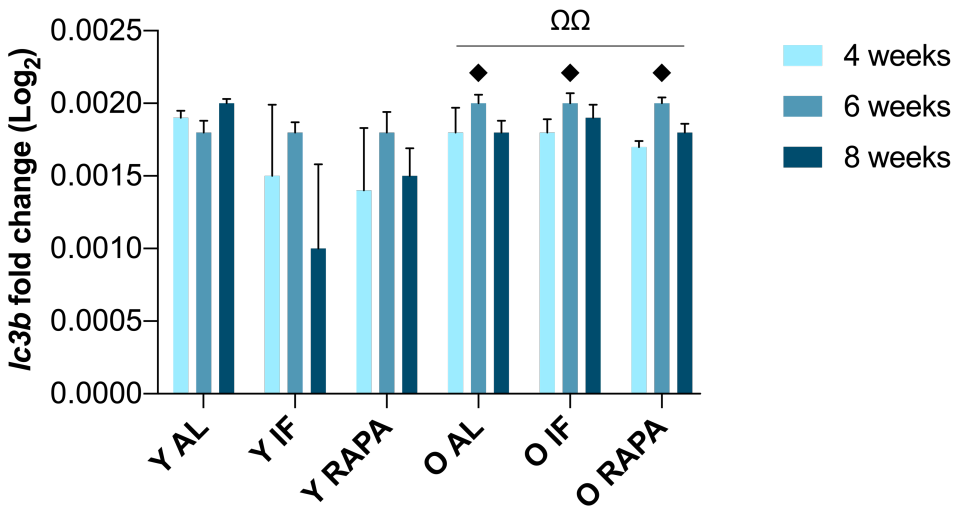

Figure 3.22. Log_2 fold change values of *lc3b* in response to different durations of IF and RAPA. A significant duration effect was observed in old animals. Diamonds represent significant within group differences (◆: $p \leq 0.05$). Omega represents significant duration effect (ΩΩ: $p \leq 0.01$). AL: *ad libitum*-fed control group, IF: intermittent fasting group, RAPA: rapamycin-treated group. N=3-5 per group at a given duration. Reproduced from the figures that first appeared in Rejuvenation Research [142], and reprinted with permission from Mary Ann Liebert, Inc.

3.6. Principal component analysis for the proteins and genes of interest

A principal component analysis (PCA) was performed on the proteins and genes of interest to further evaluate the expression patterns observed in young and old animals following IF and RAPA treatments. PCA permits investigation of how each factor correlates with one another across different age and treatment groups. We ran two separate sets of PCA for gene and protein expression data since data were obtained from separate cohorts.

3.6.1. PCA for the protein expression data

A PCA was applied on the proteins of interest that were significantly affected by age, treatment or duration. Three components were extracted based on eigenvalues (>0.5), which were then validated to be appropriate to use on this dataset with Bartlett's and Kaiser-Meyer-Olkin (KMO) tests. The Bartlett's test was significant, suggesting that the correlations in the correlation matrix were significant ($\chi^2_{(78)}=155.516$, $p<0.001$), and a strong relationship between variables were

observed (KMO=0.434). A Varimax rotation with Kaiser normalization was performed on the components to transform the data. Eigenvalues and the percentage of variance explained by each principal component, as well as component loading scores above 0.4 are given in Table 3.1. The factors with the highest component loading scores are highlighted in green.

Table 3.1. Eigenvalues, explained variance and component loading scores for each principal component of protein expression data. Reproduced from the tables that first appeared in Rejuvenation Research [142], and reprinted with permission from Mary Ann Liebert, Inc.

Principal Component	Eigenvalue	Explained Variance (%)	Component Loading Scores (>0.4)						
1	3.148	24.217	GFAP (0.821)	p-mTOR (0.763)	PCNA (0.710)	p-S6 (0.620)	PSD-95 (0.556)	S6 (0.500)	LC3-II/LC3-I (0.447)
2	2.452	18.860	p-4E-BP1/4E-BP1 (0.860)			p-4E-BP1 (0.829)			DCAMKL1 (-0.764)
3	1.615	12.425	PSD-95/GEP (0.898)			GEP (-0.728)			PSD-95 (0.499)

Table 3.2. Correlation coefficients and significance levels of the correlations for the protein expression data. Reproduced from the tables that first appeared in Rejuvenation Research [142], and reprinted with permission from Mary Ann Liebert, Inc.

		A	B	C	D	E	F	G	H	I	J	K	L	M
Corr. Coef.	A	1	0.22	0.115	0.612	-0.072	0.378	0.138	-0.098	0.399	-0.069	0.127	0.443	0.221
	B	0.22	1	-0.007	0.029	-0.151	-0.221	-0.022	-0.034	0.079	-0.002	0.28	0.039	0.104
	C	0.115	-0.007	1	-0.562	-0.188	-0.137	0.108	0.084	0.185	0.043	-0.027	0.317	-0.111
	D	0.612	0.029	-0.562	1	0.095	0.317	0.073	-0.176	0.13	-0.126	-0.004	0.146	0.149
	E	-0.072	-0.151	-0.188	0.095	1	0.071	0.441	-0.419	0.176	-0.39	0.016	-0.135	0.17
	F	0.378	-0.221	-0.137	0.317	0.071	1	0.142	0.148	0.438	-0.088	0.443	0.364	0.228
	G	0.138	-0.022	0.108	0.073	0.441	0.142	1	0.069	0.227	-0.156	0.14	0.375	0.194
	H	-0.098	-0.034	0.084	-0.176	-0.419	0.148	0.069	1	0.112	0.822	0.193	0.35	-0.085
	I	0.399	0.079	0.185	0.13	0.176	0.438	0.227	0.112	1	0.009	0.72	0.454	0.215
	J	-0.069	-0.002	0.043	-0.126	-0.39	-0.088	-0.156	0.822	0.009	1	0.03	0.263	-0.107
	K	0.127	0.28	-0.027	-0.004	0.016	0.443	0.14	0.193	0.72	0.03	1	0.369	0.243
	L	0.443	0.039	0.317	0.146	-0.135	0.364	0.375	0.35	0.454	0.263	0.369	1	0.29
	M	0.221	0.104	-0.111	0.149	0.17	0.228	0.194	-0.085	0.215	-0.107	0.243	0.29	1

		A	B	C	D	E	F	G	H	I	J	K	L	M
Sig.	A		0.135	0.284	0	0.36	0.026	0.246	0.314	0.02	0.366	0.265	0.01	0.134
	B	0.135		0.487	0.443	0.225	0.134	0.456	0.433	0.348	0.497	0.079	0.423	0.302
	C	0.284	0.487		0.001	0.174	0.249	0.296	0.338	0.178	0.415	0.446	0.054	0.291
	D	0	0.443	0.001		0.318	0.053	0.358	0.19	0.259	0.266	0.492	0.234	0.23
	E	0.36	0.225	0.174	0.318		0.362	0.011	0.015	0.19	0.022	0.469	0.251	0.198
	F	0.026	0.134	0.249	0.053	0.362		0.24	0.23	0.011	0.332	0.01	0.031	0.126
	G	0.246	0.456	0.296	0.358	0.011	0.24		0.365	0.128	0.219	0.242	0.027	0.166
	H	0.314	0.433	0.338	0.19	0.015	0.23	0.365		0.289	0	0.168	0.037	0.337
	I	0.02	0.348	0.178	0.259	0.19	0.011	0.128	0.289		0.482	0	0.009	0.14
	J	0.366	0.497	0.415	0.266	0.022	0.332	0.219	0	0.482		0.441	0.092	0.298
	K	0.265	0.079	0.446	0.492	0.469	0.01	0.242	0.168	0	0.441		0.029	0.111
	L	0.01	0.423	0.054	0.234	0.251	0.031	0.027	0.037	0.009	0.092	0.029		0.071
	M	0.134	0.302	0.291	0.23	0.198	0.126	0.166	0.337	0.14	0.298	0.111	0.071	

The correlation coefficients and significance levels are reported in Table 3.2, and color coded as shades of blue and red. In the upper panel of the Table 3.2, the strongest positive correlations are shown in dark blue, and negative correlations in dark red. In the lower panel, where significance levels are reported, the most

significant correlations are shown in dark blue and the least significant ones in dark red. The letter codes for the significantly affected proteins in Table 3.2 are given in Table 3.3.

Table 3.3. Letter coding for the proteins in Table 3.2.

Letter code	Factor
A	PSD-95
B	SYP
C	GEP
D	PSD-95 / GEP
E	DCAMKL1
F	p-S6
G	S6
H	p-4E-BP1
I	GFAP
J	p-4E-BP1 / 4E-BP1
K	PCNA
L	p-mTOR
M	LC3B-II / LC3B-I

The PCA revealed many significant correlations between the proteins of interest. Some of these correlations were obvious and expected. For instance, PSD-95/GEP was positively correlated with PSD-95 ($p \leq 0.001$) and negatively correlated with GEP ($p = 0.001$). Similarly, the ratio of p-4E-BP1/4E-BP1 was positively correlated with p-4E-BP1 ($p \leq 0.001$).

The factor with the most significant correlations was p-mTOR, being correlated with six factors and marginally correlated with another three factors. Positively correlated factors were p-S6 ($p = 0.031$), S6 ($p = 0.027$), p-4E-BP1 ($p = 0.037$), PSD-95 ($p = 0.01$), GFAP ($p = 0.009$), and PCNA ($p = 0.029$). Since S6 and 4E-BP1 are downstream targets of mTOR, it was expected that p-mTOR was correlated with

their phosphorylated versions. The ratio of p-4E-BP1/4E-BP1 was marginally correlated with p-mTOR (p= 0.092). One interesting observation was that p-mTOR was also correlated with S6, suggesting that mTOR might have a role in regulating total S6 protein expression. Furthermore, the correlations between p-mTOR and proliferation markers GFAP and PCNA indicate the involvement of mTOR in both global and lineage-specific cell proliferation. Activated mTOR has been shown to have consequences in cell growth [186], and our results are in line with the literature. In addition, mTOR has been reported to regulate PSD-95 expression [187], and our observations are consistent with this report since there were significant positive correlations. Finally, since we also observed marginal correlations between p-mTOR and GEP (p= 0.054) and LC3-II/LC3-I (p= 0.071), we concluded that mTOR might be the master regulator of these factors involved in a wide range of critical processes such as synaptic transmission, proliferation, and autophagy.

The next factor in the analysis with the most significant correlations was p-S6. Positively correlated factors were PCNA (p= 0.01), GFAP (p= 0.011) and PSD-95 (p= 0.026), while PSD-95/GEP was marginally correlated with p-S6 (p=0.053). As a downstream effector of mTOR, the correlations of p-S6 with both postsynaptic and proliferative markers confirmed the p-mTOR data.

Another result that is worth emphasizing, and to our knowledge, novel, was the negative correlations between the NPC marker DCAMKL1 and p-4E-BP1 (p=0.015), and p-4E-BP1/4E-BP1 (p= 0.022). While other markers of proliferation were positively correlated with p-mTOR, DCAMKL1 was negatively correlated with its direct downstream target. These results indicated that mTOR has lineage-specific

roles in proliferation, and that markers that are more global in nature were dependent on the p-mTOR expression, while the marker of neuronally committed progenitors were likely to be regulated by p-4E-BP1. Supporting this conclusion, GFAP and PCNA were positively correlated ($p \leq 0.001$), and DCAMKL1 was not correlated with either of these markers.

To visualize these interactions, the components were saved as variables in SPSS and samples were displayed in scatterplot matrices (Figure 3.23). The factors with the highest component loading scores for each principal component (PC) were as follows: GFAP in PC1, p-4E-BP1/4E-BP1 in PC2 and PSD-95/GEP in PC3 (Table 3.2). In IF, both the samples and centers of the clusters formed by young and old groups were closely located on each axis, suggesting a more uniform response to IF across lifespan (Figure 3.23, left panel). In RAPA, although the cluster centers were closely located, samples from young and old animals were distributed distinctly, indicating an age-dependent response (Figure 3.23, right panel).

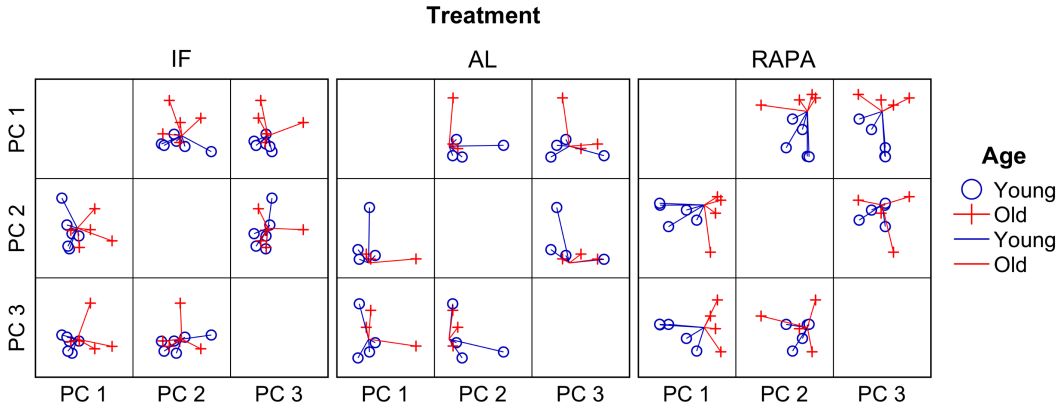

Figure 3.23. Visualization of the samples on scatterplot matrices for the principal components of the significantly affected proteins obtained from PCA. Differential clustering patterns were observed in young and old treatment groups.

AL: *ad libitum*-fed control group, IF: intermittent fasting group, RAPA: rapamycin-treated group. Reproduced from the figures that first appeared in Rejuvenation Research [142], and reprinted with permission from Mary Ann Liebert, Inc.

3.6.2. PCA for the gene expression data

We applied the same criteria in section 3.6.1. for PCA of gene expression data. For the two components that were extracted, the Bartlett's test was significant ($\chi^2(6)=85.774$, $p<0.001$), and KMO was 0.710. Eigenvalues, explained variances and factors with component loading scores >0.4 are given in Table 3.4. The factors with the highest scores are highlighted in green.

In PC 1, the factor with the highest loading score was *lc3b* (0.864). The *igf1* and *foxm1* transcripts followed *lc3b* in this component. In the PC 2, *ztor* had the highest score (0.977), and was the sole factor with a score of >0.4 in this component.

Table 3.4. Eigenvalues, explained variance and component loading scores for each principal component of gene expression data

Principal Component	Eigenvalue	Explained Variance (%)	Component Loading Scores (>0.4)		
1	2.336	58.405	*lc3b* (0.864)	*igf1* (0.826)	*foxm1* (0.733)
2	0.729	18.215	*ztor* (0.977)		

The correlation matrix in Table 3.5 provides information about the correlation coefficients and their significance levels. These were color coded as shades of blue and red as explained in section 3.6.1. for Table 3.3. Interestingly, all the genes in the analysis were positively and significantly correlated with each other. The strongest

contributor of PC 1, *lc3b*, had the most significant correlations, being correlated with all other three genes ($p<0.001$). Although this analysis is only correlative, the causal relationships of autophagy with nutrient signaling and proliferation have been reported, and are consistent with our results [93], [188], [189].

Table 3.5. Correlation coefficients and significance levels of the correlations for the gene expression data

		ztor	*igf1*	*foxm1*	*lc3b*
Correlation	*ztor*	1	0.333	0.310	0.398
	igf1	0.333	1	0.386	0.665
	foxm1	0.310	0.386	1	0.531
	lc3b	0.398	0.665	0.531	1
Sig.	*ztor*		0.001	0.003	0
	igf1	0.001		0	0
	foxm1	0.003	0		0
	lc3b	0	0	0	

The interactions were visualized as was done for the protein expression data and explained in section 3.6.1. The components saved as variables were displayed in a series of scatterplots, not as matrices, since there were only two extracted components (Figure 3.24). Divergent from the patterns of protein expression, IF and RAPA resulted in a very similar clustering motifs in young and old animals. However, the clustering of AL animals was evidently disparate from diet and drug treatment groups. These results indicated that RAPA mimicked IF to a larger extent at the transcript level compared to the patterns at the protein level.

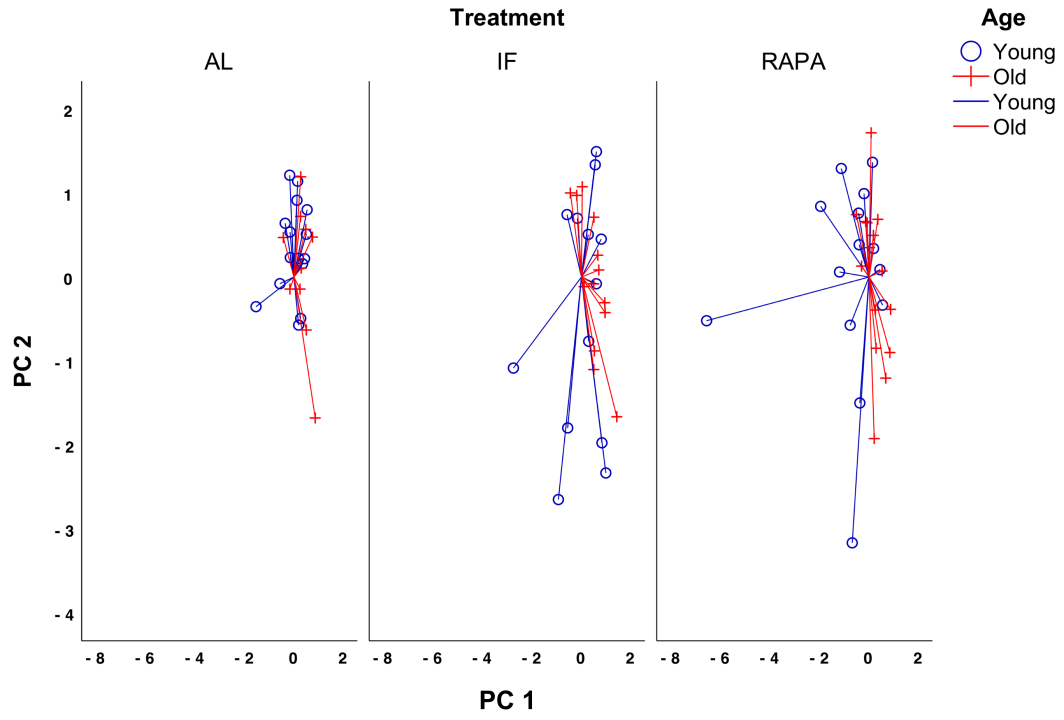

Figure 3.24. Visualization of the samples on scatterplots for the principal components of the significantly affected genes obtained from PCA. The gene expression patterns were very similar in young and old AL animals across lifespan (left panel). IF (middle panel) and RAPA (right panel) extended the clusters in both age groups , however the resulting age clusters had very closely located centers. AL: *ad libitum*-fed control group, IF: intermittent fasting group, RAPA: rapamycin-treated group.

Finally, we visualized $\log_2$ fold change values for all the genes of interest on two heatmaps using the Heatmapper tool (Figure 3.25). Clustering method was average linkage with Pearson as distance measurement method. Clusters were applied to rows, and heatmaps were displayed as shades of red and green, with bright red representing the lowest fold change and bright green representing the highest fold change values.

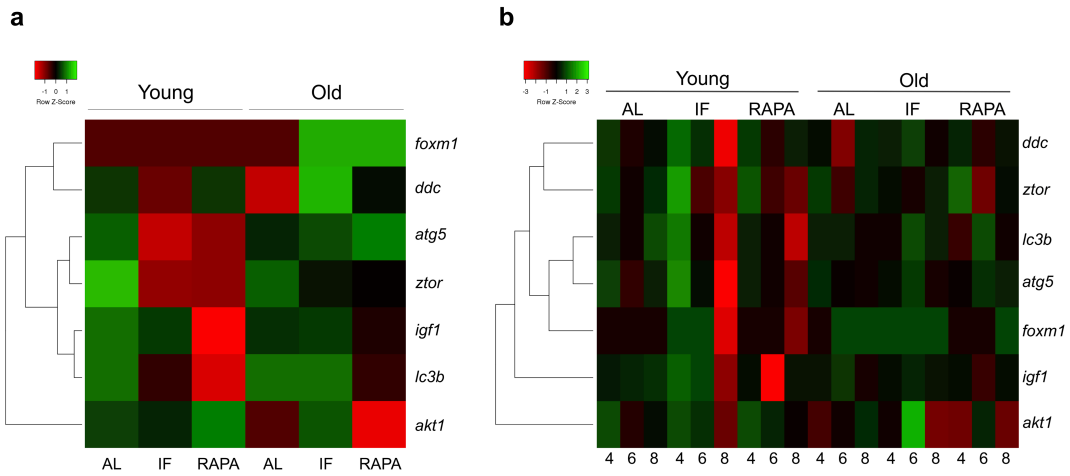

Figure 3.25. Heatmaps for the gene expression data. Log_2 fold change values were visualized on heatmaps for experiment groups without (a) and with duration (b). Heatmaps were created with Heatmapper tool [190].

Chapter 4

Discussion

The current study examined how short-term applications of two anti-aging interventions, IF and RAPA treatment, affected selected physiological, cellular and molecular markers in young and old, male and female zebrafish. We included animals from both genders since majority of the studies are done on either male or female animals, and that there is scarce evidence concerning global changes that are irrespective of the gender of the subjects. To achieve this wider perspective in the context of brain aging, we primarily focused on the alterations in the brain with regards to changes in several health parameters observed in whole-body. With this top-down approach, we aimed to investigate if and how physiological parameters such as body weight, BMI, whole-body glucose and cortisol levels were related to the responses in the brain. Moreover, by studying short-term durations of these interventions, we attempted to provide a ground for translational studies in which long-term applications are largely unsuitable. Finally, we assessed the potential of RAPA as an IF mimetic through the comparison of their individual effects on the cellular and molecular processes in the brain.

The results indicated that the consequences of IF and RAPA depend on the age of the subjects at the onset of the intervention. Age-specific responses were present at

different levels, from whole-body to brain and cellular to molecular. Observation of significant changes as early as 6 weeks in both physiological (i.e. body weight, BMI and glucose) and molecular (i.e. GEP and *ztor*) parameters suggested that short-term applications of both interventions were effective. Nevertheless, overall duration effect was restricted to only a few of the markers that were investigated.

Differential patterns of body weight and BMI were observed throughout 8 weeks in young and old treatment groups. For instance, IF caused significant weight loss in old animals, while only stabilizing the weight in young. Conversely, young AL animals gained weight, but the mean weight of old AL animals remained unchanged. These distinct phenotypes in young and old groups could be explained by the growth rate of zebrafish.

Under normal laboratory conditions, zebrafish reach sexual maturity after 3 months post fertilization, and are considered adults. Although the growth rate varies depending on intrinsic (i.e. genetic background) and extrinsic factors (i.e. water temperature and quality, stocking density), the continuum of growth is evident on several traits such as pigmentation, fin length and size [191]. In fact, size measures have been proposed as better indicators of the postembryonic developmental progress than age itself [192]. Since the growth phase extends beyond ~6 months, which was the time that we initiated the experiments for the young groups, the weight gain in Y-AL was expected. The lack of diet-induced changes in weight in Y-IF as opposed to reductions in O-IF suggest that there are lower limits for the body weight and BMI measures to nurture a healthy state. Indeed, both Y-IF and O-IF had similar BMI levels at the end of 8 weeks.

We also analyzed the body weight and BMI measurements for RAPA-treated animals, since RAPA has been shown to cause loss of appetite in humans and mice [120], [193] and reduce food consumption in rats which resulted in weight loss [194]. In our experimental setup, there were no changes in either of these parameters within Y-RAPA and O-RAPA groups during the 8-week experiment and compared to young and old AL counterparts. Interestingly, Y-RAPA animals did not gain weight although they received the same amount of food as Y-AL. These results suggested that RAPA did not have severe adverse effects, yet might have caused a moderate appetite loss in young animals.

One physiological parameter that emerges as a possible link between metabolism and molecular mechanisms that may underlie age-related changes as well as the response to anti-aging interventions in the brain is glucose. The brain heavily relies on glucose as the main energy source, and accounts for approximately 25% of the total body glucose consumption [147]. Glucose is not only a compulsory energy substrate for brain functioning, but also an essential component of glycolipids and glycoproteins that are required by the brain [195]. Moreover, glucose has been shown to regulate protein synthesis, and be indirectly involved in neurotransmitter synthesis by being incorporated into complex carbohydrates required for their precursors [147].

Blood glucose levels have been reported to decline in response to IF [148]. In our study, we utilized a novel method to measure glucose levels in frozen fish trunks. Although the starting materials were different, we observed significantly lower glucose levels in IF animals of both ages and were able to confirm the results of

previous studies. Interestingly, animals showed a different response to RAPA in terms of glucose levels. To interpret the patterns observed in RAPA animals, there is a need to consider both sides of the comparison. Since both RAPA and AL animals received the same amount of food, the patterns observed in Y-RAPA and O-RAPA were similar to those observed in Y-AL and O-AL, respectively. However, while glucose levels significantly increased in both Y-AL and O-AL from 4 to 6 weeks, this was not observed in RAPA animals. Therefore, RAPA did not lead to a spike in whole-body glucose levels as observed in AL groups and appeared to normalize glucose levels, which is consistent with the literature [156], [196]. On the other hand, a multitude of studies documented rapamycin-induced glucose intolerance and increases in glucose levels [197], [198]. Hence, the glucose levels in RAPA might reflect a mild glucose intolerance when compared to IF animals.

Another observation that was consistent with the literature was higher whole-body glucose levels in old subjects. Progressive increases in blood and plasma glucose levels with age have been reported in humans [149], [199]. Age-related development of hyperglycemia is considered among the pathogenic mechanisms that lead to Diabetes mellitus, and advanced age is one of the major risk factors for this epidemic [199]. Our results were in conjunction with earlier observations, since higher glucose levels were observed in all old animals and age effect was significant in IF and RAPA groups. Plasma levels of glucose correlate with the levels in the CNS [200]. Due to the central role of glucose in brain energy metabolism and its involvement in the synthesis of macromolecules that are critical for normal brain functioning, the diet-induced reductions and age-related increases in glucose levels are likely reflected in our observations.

The other metabolic factor that we investigated was cortisol: a prominent hormone involved in the stress response as an end product of the hypothalamic-pituitary-adrenal axis [201]. In addition to maintenance of homeostasis, there is an established relationship between cortisol and energy availability. For instance, cortisol regulates availability of fuel sources by increasing plasma glucose levels and rate of glucose turnover [202], and gluconeogenesis [153]. These changes have been proposed to cause insulin resistance and metabolic syndrome [202], [203].

In line with these previous observations, our results demonstrated that cortisol levels followed a similar pattern with glucose levels. Interestingly, the IF regimen decreased whole-body cortisol levels in both young and old animals, confirming the regulatory effect of cortisol on glucose levels but being contradictory to earlier studies reporting increase in cortisol levels in response to fasting [204]. However, it is important to note that experimental setup in these studies varied greatly from ours. For example, in two studies by Bergendahl et al. and Vance and Thorner, human subjects were fasted for 5 days, which is different from intermittent fasting [204], [205]. Another study suggested that glucose availability determined the free salivary cortisol levels but only in the presence of a psychological stressor, and after a 8-11 hours of fasting [206]. Therefore, the duration of the fasting and existence of stressors might have an impact on the stress response, and the bilateral relationship between glucose and cortisol could have caused the patterns that we observed.

The modulation of stress response has also emerged as a critical mechanism for the longevity-promoting interventions. The conventional view states that aging occurs as a result of the accumulation of molecular cellular damage over time. However, this

view has been challenged by the observations that life span extending approaches also induce a state of weak stress, termed hormesis. From the mTOR-centric perspective on aging, both IF and rapamycin inhibit damage accumulation by inhibiting the TOR signaling; thereby limiting the detrimental byproducts of growth and metabolism [207]. Our results indicating lower levels of cortisol in animals subjected to IF and higher levels in rapamycin-treated groups may suggest that rapamycin acts faster than IF in activation of hormetic pathways.

The common metabolic traits in young and old IF animals were also translated into responses in the brain. The marker of neuronally committed precursors, DCAMKL1, was upregulated in both Y-IF and O-IF, although the mechanisms that are potentially responsible for this outcome were age-dependent. For example, the increase in neurogenic potential seems to originate from the suppression of mTOR autophosphorylation in young animals, as evidenced by the decrease in p-mTOR^{Ser2481} levels. In old animals, however, p-mTOR^{Ser2481} levels remained unchanged while the autophagic flux marker (i.e. LC3-II/LC3-I) decreased in response to IF. This decrease in LC3-II/LC3-I was accompanied by the upregulation of *foxm1* in O-IF, which was not observed in Y-IF. The expression of FOXM1, a marker of proliferation, has been shown to be restricted to actively-dividing cells and to NPCs in the adult brain [176], [182]. As a transcription factor regulating neurogenesis in the adult brain, FOXM1 is expressed in both GFAP-expressing (GFAP$^+$) immature precursors and DCAMKL1-expressing (DCAMKL1$^+$) NPCs and immature neurons [176]. Therefore, IF not only alters the expression levels of a more specialized DCAMKL1 but also a more general proliferation marker *foxm1* in old animals (Figure 4.1).

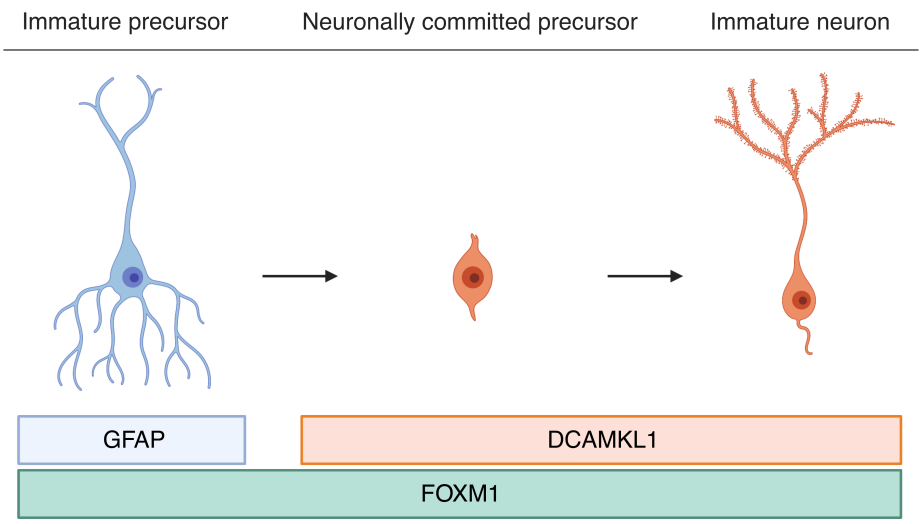

Figure 4.1. Schematic representation of progenitor types identified by the proliferative marker expression in the adult brain. The illustration is adapted from a review by Genin et al., 2014 [176] and the figure is created with BioRender.

Advancing age is associated with lower rates of proliferation and neurogenesis [208], [209], which correlate with *foxm1* downregulation in the aging brain [183]. Furthermore, both glucose and cortisol have been shown to affect adult neurogenesis. For instance, high glucose and cortisol concentrations has been linked to decreases in NPC proliferation and differentiation into neurons [210], [211]. In agreement with these reports, our results indicate that IF has direct implications on the neurogenic potential in young and old animals, which could be related to reduced glucose and cortisol levels.

While short-term applications of IF led to similar metabolic profiles and upregulated proliferation markers across lifespan, its mimetic rapamycin did not induce changes in these markers. In fact, responses to RAPA were utterly divergent in young and old animals. In Y-RAPA group, the mTOR activity was suppressed as indicated by

decreases in p-mTOR^{Ser2481}, p-4E-BP1 and the ratio of p-4E-BP1/4E-BP1. Furthermore, *igf1* transcript was also downregulated in these animals, suggesting that RAPA affected both upstream and downstream elements of mTOR in the nutrient signaling pathway.

Consequences of mTOR inhibition were observed in markers of two closely related cellular processes: autophagy and cell proliferation. Interestingly, both the indicator of global cell proliferation at the protein level (i.e. PCNA) and LC3-II/LC3-I were decreased in Y-RAPA. Autophagy is a double-edged sword: either activating prosurvival cascades in response to metabolic stress such as scarcity of nutrient sources, or cell death [212], [213]. Although how exactly the cell fate is determined by autophagic mechanisms is still a subject to debate, autophagy has been shown to be essential for RAPA-driven neuroprotection [214]. However, studies with contradicting results exist, since CR and/or RAPA have been reported to both upregulate *atg5* and *lc3b*, or downregulate *lc3b* and LC3-II/LC3-I [171], [184], [215]. Since the latter observation was made on young animals, our results regarding reduced LC3-II/LC3-I ratio as well as numerical downregulation of *lc3b* transcript appear to be consistent with the literature [171]. Finally, the reduced PCNA expression in Y-RAPA might suggest a possible age-dependent link between autophagic flux and overall proliferation. Since other markers of proliferation were not altered in these animals, RAPA could be protecting the existing pool of NPCs by preventing their depletion.

The response of old animals to RAPA treatment was considerably different from Y-RAPA, although the metabolic parameters followed similar patterns in RAPA-

treated young and old animals. There were no changes in markers of global proliferation, autophagic flux and mTOR activity. Instead, we observed downregulation of GFAP and GEP in these animals, the latter being with respect to O-IF. GFAP is expressed in various cell types such as immature precursors that differentiate into neuronally-committed DCAMKL^{+} cells, and activated astrocytes [216]. Astrocytes have critical roles in maintaining homeostasis in the CNS, including secretion of inflammatory factors and cytokines involved in immune response, and GFAP has been proposed as a biomarker of inflammation [217]. Therefore, decrease in GFAP expression levels in O-RAPA suggests lower neuroinflammation. Indeed, RAPA has been shown to ameliorate inflammation after spinal cord injury and facilitate recovery by increasing neuronal survival, supporting our conclusion [177].

The reduced GEP expression with no changes in PSD-95 levels, on the other hand, indicated that RAPA might shift the old brains to a more excitable state by altering the E/I ratio. Interestingly, IF increased GEP in old animals, which did not translate into a shift towards an inhibitory state. In fact, E/I ratio as measured by PSD-95/GEP was only altered in O-RAPA groups, suggesting an age- and treatment-specific modulation of E/I. This RAPA-induced alteration of GEP and consequently, E/I balance, is novel.

One possible explanation for this observation is that GEP, as a direct binding partner of mTOR, forms clusters by interacting with mTOR on the postsynaptic site [108], [218]. Reduced mTOR activity might increase the availability of GEP outside the clusters, which is then targeted for degradation [219]. Since PSD-95 was not affected

by the RAPA treatment, this downregulation of GEP might lead to excitotoxicity [220]. Further studies should focus on the effects of RAPA on E/I balance, and assess whether this increase in E/I ratio actually cause excitotoxicity or act in a way that is beneficial for the brain in terms of enhancing excitability.

The lack of treatment effect on presynaptic protein SYP as opposed to treatment-induced changes in GEP suggest that short-term applications of IF and RAPA were more effective on postsynaptic components. The only significant effect on SYP was that of age, with old animals containing higher basal levels of SYP compared to young animals which was consistent with literature [166]. The common effector of IF and RAPA, mTOR, has been shown to carry out distinct functions on presynaptic and postsynaptic compartments [221], [222]. Therefore, whether longer durations of these treatments would be able to alter SYP expression patterns should be investigated.

The patterns of mTOR inhibition in IF and RAPA groups indicated that RAPA was more effective in inhibiting mTOR than IF, but this was age-dependent. The quantification p-mTOR^{Ser2481}, p-4E-BP1 and p-4E-BP1 confirmed that RAPA suppressed mTOR activity in young, and IF in old animals, although the latter was to a much lesser extent. Moreover, the lack of treatment effect on S6 phosphorylation indicates that these interventions selectively modulate 4E-BP1 in brain. This observation supports previous reports RAPA might have tissue-specific effects [128]. While these results suggested that RAPA crossed the blood-brain barrier and was effective at the concentration and duration that were used in this study, why this was limited to young animals should be addressed more in detail.

One possible reason could be changes in pharmacokinetics and pharmacodynamics with age [223]. In addition to age itself, body composition of old animals might affect the outcome of drug treatment since old animals are larger and the RAPA might thus be less effective in these animals. Another explanation could be age-related changes in the activities of mTORC1 and mTORC2. Both complexes have been shown to contain p-mTOR^{Ser2481}, however RAPA-induced reductions in p-mTOR^{Ser2481} is stronger in mTORC1 [158]. In addition, mTORC2 activity increases with advancing age [224], and the increase in mTORC2 activity might compensate for mTORC1. Therefore, future studies using different drug concentrations in young and old animals, and examining additional markers of mTOR are required.

Finally, the evaluation of rapamycin as an IF mimetic by both molecular techniques and PCA indicated that they have differential effects on the total and post-transcriptionally modified levels of proteins, whereas there were similar gene expression patterns in the IF and rapamycin-treated groups. Furthermore, we observed larger changes in the protein expression levels when compared to gene expression. This observation could be due to different contributions of intrinsic and environmental mechanisms to transcriptomic and proteomic profiles. For example, one study showed that intrinsic mechanisms such as growth and maturation had a larger impact on the proteome and transcriptome. On the other hand, a more environmentally-driven mechanism such as circalunar clock had a minor impact on the transcriptome while having a strong regulatory effect on the proteome [225]. Indeed, both IF and rapamycin are considered as environmental interventions and the absence of significant treatment effect may be due this phenomenon.

Moreover, discordance between transcription and translation has been observed across species, which probably arises from different rates of translation and mRNA degradation depending on the needs of tissues or cell types [226], [227]. The dissonant transcriptome-proteome profiles are also evident in the brain [228], which could be due to the larger number of noncoding RNAs in the brain when compared to other tissues [229]. Additionally, the axons can extend to make long-range connections. Given the calculated rates of transport for the macromolecules and the maximum distance between the soma and distal axon, there should be alternative mechanisms that allow faster response to external stimuli. Indeed, there is emerging evidence that neurons depend highly on localized protein synthesis, and that the mRNA content of distal axons may differ from that in soma with functional consequences [230]. Therefore, further studies analyzing changes at both mRNA and protein level as well as quantifying axonal mRNA content are needed.

Chapter 5

Conclusion and Future Directions

With this study, we provided evidence for age-dependent responses in the brain to two interventions that have been shown to extend health and life span. We investigated the whole-body levels of metabolic parameters and markers of several biological processes that might have a role in cognitive enhancement that has been reported in response to IF and rapamycin treatments. The metabolic profiles induced by these interventions were distinct, but each intervention led to similar patterns in the glucose and cortisol levels in young and old animals. While the cellular and molecular responses to IF were fairly comparable at young and old ages, they were different in rapamycin-treated groups.

This study revealed a need for further studies focusing on the age-specific responses to short-term applications of IF and rapamycin. For example, it is crucial to assess why mTOR inhibition was more prominent in young animals than in old animals. Moreover, the inhibitory potentials of IF and rapamycin varied, with rapamycin having a stronger inhibition on the phosphorylation levels of both mTOR and its downstream effector, 4E-BP1. Despite the stronger inhibition of mTOR activity with rapamycin treatment when compared to IF, the drug treatment caused significant reductions in the phosphoprotein levels only in the young animals. Nevertheless, we

observed alterations in the PSD-95/GEP and GFAP expression levels in the old rapamycin-treated group. These results indicated that both IF and RAPA may exert their effects through both mTOR-dependent and mTOR-independent mechanisms. Studies testing the effects of IF and rapamycin on mTOR mutants that have reduced mTOR activity or overactive mTOR could provide possible additional mechanisms through which IF exerts its effects.

Another interesting observation that requires further attention is the differential responses to rapamycin in young and old animals. In addition to lack of significant changes in the mTOR activity in old animals, markers of proliferation, inflammation and autophagy were altered in an age-specific manner. Whether this is due to changes in drug metabolism during aging which necessitates the use of a higher dose in old animals should be addressed. Finding optimum drug concentrations for use in zebrafish across lifespan would allow better understanding of the rapamycin's potential as an IF mimetic.

Further studies combining IF and rapamycin treatment across lifespan could provide better insight into molecular mechanisms through which they exert their effects as well as the age-dependent responses to these interventions. Whether they have synergistic effects and the potentially beneficial outcomes could be enhanced by their simultaneous application should be investigated to increase our understanding of their consequences. Moreover, this approach could also allow studying the efficacy of rapamycin and other pharmacological agents as CR mimetics, which would provide a ground for translational studies.

Additionally, more markers of autophagic flux, inflammation and proliferation should be investigated to dissect out possible links between these mechanisms. Since autophagy occurs through different cascades, studying how changes in a cascade effects the fate of a certain lineage (i.e. neuron, glia), as well as the changes in anti- and pro-inflammatory molecules in response to IF and rapamycin could reveal new therapeutic targets. This could be done by using immunohistochemical methods such as bromodeoxyuridine (BrdU) assay to count actively proliferating cells in specific brain areas that are linked to critical cognitive processes, and double- or triple-labeling with antibodies against markers of autophagy, inflammation and cell lineage. As an alternative, transgenic fish expressing fluorescent proteins in their neurons or glia could be subjected to IF or rapamycin and injected with BrdU before euthanasia. Both approaches would allow the quantification of changes in the proliferation rates both at the global levels and lineage-specific manner.

Supplementing the proteomics and transcriptomics data with evidence regarding the changes in neuronal activity networks could implement links between physiological and cognitive processes. Recent advances in the imaging techniques led to development of methods such as Light Sheet Fluorescent Microscopy, which allows the imaging of functional and architectural changes in the living organisms, including zebrafish [231], [232]. Use of such techniques to investigate structural reorganization (i.e. neuron number, the patterns and density of dendrites and synapses) in the adult whole-brain in response to IF and/or rapamycin treatment could help us determine whether changes at the molecular level are translated into functional networks.

Behavioral experiments should also be carried out in both wild type and mutant animals to investigate whether changes at the cellular and molecular levels are reflected in the cognitive performance. Identifying the behavioral correlates of the biological alterations in the brain could provide a better understanding of the mechanisms through which IF and rapamycin extend health span and improve cognitive skills. The results from such studies could be the foundations for the development and assessment of novel therapeutic approaches that hold a high potential to be utilized in translational research.

As a final remark, potential sexually dimorphic responses should be investigated. In this study, we mainly focused on the global changes regardless of the gender in the young and old brains subjected to IF or rapamycin treatments. This line of research including representatives from both genders is often neglected due to both technical difficulties and hormonal cycles affecting the biological processes in question as well as the aging itself. There is growing knowledge on gender-specific alterations during normal and pathological aging that may justify favoring one gender in studies, which is often males, since gender is still being considered a confounding factor [233].

While using only one gender may yield more clear patterns during data interpretation, inevitably leaves a large gap between the evolutionarily conserved mechanisms of aging in phylogenetically higher and lower organisms. Accordingly, our approach of including both genders provided a vital link between life and health span extending interventions and gender-independent mechanisms. Nevertheless, preliminary results from our study which we did not present here, as well as

published data identified sexual dimorphism in different processes associated with aging. These include differences in immune system [234], adaptive homeostasis [235] and cognitive impairment [236], and across species including zebrafish [75], [237], [238]. Therefore, further research regarding gender-specific changes in the aging brain and in response to anti-aging interventions are required to dissociate global mechanisms of aging from those that are affected by gender.

Bibliography

[1] "WHO | Healthy Ageing and the Sustainable Development Goals." [Online]. Available: https://www.who.int/ageing/sdgs/en/. [Accessed: 10-Jan-2020].

[2] WHO, *World report on Ageing And Health*. 2015.

[3] R. Levy, "Report Aging-Associated Cognitive Decline," *Int. Psychogeriatrics*, vol. 6, no. 1, pp. 63–68, Mar. 1994.

[4] W. J. Evans and W. W. Campbell, "Sarcopenia and age-related changes in body composition and functional capacity.," *J. Nutr.*, vol. 123, no. 2 Suppl, pp. 465–8, 1993.

[5] X. Wang, X. Shen, X. Li, and C. Mauli Agrawal, "Age-related changes in the collagen network and toughness of bone," *Bone*, vol. 31, no. 1, pp. 1–7, 2002.

[6] H. Oxenham and N. Sharpe, "Cardiovascular aging and heart failure," *Eur. J. Heart Fail.*, vol. 5, no. 4, pp. 427–434, Aug. 2003.

[7] P. J. Busse and S. K. Mathur, "Age-related changes in immune function: Effect on airway inflammation," *Journal of Allergy and Clinical Immunology*, vol. 126, no. 4. pp. 690–699, Oct-2010.

[8] R. Soleimani, S. Shokrgozar, M. Fallahi, H. Kafi, and M. Kiani, "An investigation into the prevalence of cognitive impairment and the performance of older adults in Guilan province," *J. Med. Life*, vol. 11, no. 3, pp. 247–253, Jul. 2018.

[9] E. Rodríguez-Sánchez, S. Mora- Simón, M. C. Patino-Alonso, R. García-García, A. Escribano-Hernández, L. García-Ortiz, M. V. Perea- Bartolomé, and M. A. Gómez-Marcos, "Prevalence of cognitive impairment in individuals aged over 65 in an urban area: DERIVA study," *BMC Neurol.*, vol. 11, Nov. 2011.

[10] M. Giri, T. Chen, W. Yu, and Y. Lü, "Prevalence and correlates of cognitive impairment and depression among elderly people in the world's fastest growing city, Chongqing, People's Republic of China," *Clin. Interv. Aging*, vol. 11, pp. 1091–1098, Aug. 2016.

[11] R. Patel and U. Singh, "Prevalence study of cognitive impairment and its associated sociodemographic variables using mini-mental status examination among elderly population residing in field practice areas of a medical college," *Indian J. Community Med.*, vol. 43, no. 2, pp. 113–116, Apr. 2018.

[12] E. Jaul and J. Barron, "Age-Related Diseases and Clinical and Public Health Implications for the 85 Years Old and Over Population," *Front. Public Heal.*, vol. 5, Dec. 2017.

[13] M. L. Ancelin, S. Artero, F. Portet, A. M. Dupuy, J. Touchon, and K. Ritchie, "Non-degenerative mild cognitive impairment in elderly people and use of anticholinergic drugs: Longitudinal cohort study," *Br. Med. J.*, vol. 332, no. 7539, pp. 455–458, Feb. 2006.

[14] R. C. Petersen, G. E. Smith, S. C. Waring, R. J. Ivnik, E. G. Tangalos, and E. Kokmen, "Mild cognitive impairment: Clinical characterization and outcome," *Arch. Neurol.*, vol. 56, no. 3, pp. 303–308, 1999.

[15] D. L. Murman, "The Impact of Age on Cognition," *Semin. Hear.*, vol. 36, no. 3, pp. 111–121, Aug. 2015.

[16] R. Fernández-Ballesteros, J. Botella, M.D. Zamarrón, M.A. Molina, E. Cabras, R. Schettini, and L. Tárraga, "Cognitive plasticity in normal and pathological aging," *Clin. Interv. Aging*, pp. 7–15, 2012.

[17] D. J. Selkoe, "Aging Brain, Aging Mind," vol. 267, no. 3, pp. 134–143, 1992.

[18] H. Brody, "Organization of the cerebral cortex. III. A study of aging in the

human cerebral cortex," *J. Comp. Neurol.*, vol. 102, no. 2, pp. 511–556, Apr. 1955.

[19] P. D. Coleman and D. G. Flood, "Neuron numbers and dendritic extent in normal aging and Alzheimer's disease," *Neurobiology of Aging*, vol. 8, no. 6. pp. 521–545, 1987.

[20] H. Haug, "The evaluation of cell-densities and of nerve-cell-size distribution by stereological procedures in a layered tissue (cortex cerebri).," *Microsc. Acta*, vol. 82, no. 2, pp. 147–61, Sep. 1979.

[21] H. Haug, S. Kuhl, and E. Mecke, "The significance of morphometric procedures in the investigation of age changes in cytoarchitectonic structures of human brain," *J. Hirnforsch.*, vol. 25, no. 4, pp. 353–374, 1984.

[22] M. J. West and H. J. G. Gundersen, "Unbiased stereological estimation of the number of neurons in the human hippocampus," *J. Comp. Neurol.*, vol. 296, no. 1, pp. 1–22, 1990.

[23] M. J. West, "Regionally specific loss of neurons in the aging human hippocampus," *Neurobiol. Aging*, vol. 14, no. 4, pp. 287–293, 1993.

[24] M. J. West, P. D. Coleman, D. G. Flood, and J. C. Troncoso, "Differences in the pattern of hippocampal neuronal loss in normal ageing and Alzheimer's disease," *Lancet*, vol. 344, no. 8925, pp. 769–772, Sep. 1994.

[25] H. Haug, "Are Neurons of the Human Cerebral Cortex Really Lost During Aging? A Morphometric Examination," in *Senile Dementia of the Alzheimer Type*, 1985, pp. 150–163.

[26] T. Gómez-Isla, J. L. Price, D. W. McKeel, J. C. Morris, J. H. Growdon, and B. T. Hyman, "Profound loss of layer II entorhinal cortex neurons occurs in very mild Alzheimer's disease," *J. Neurosci.*, vol. 16, no. 14, pp. 4491–4500, Jul. 1996.

[27] T. Rasmussen, T. Schliemann, J. C. Sørensen, J. Zimmer, and M. J. West, "Memory impaired aged rats: No loss of principal hippocampal and subicular neurons," *Neurobiol. Aging*, vol. 17, no. 1, pp. 143–147, 1996.

[28] J. H. Morrison and P. R. Hof, “Life and death of neurons in the aging brain,” *Science (80-.).*, vol. 278, no. 5337, pp. 412–419, Oct. 1997.

[29] G. Tavosanis, “Dendritic structural plasticity,” *Dev. Neurobiol.*, vol. 72, no. 1, pp. 73–86, Jan. 2012.

[30] S. Buell and P. Coleman, “Dendritic growth in the aged human brain and failure of growth in senile dementia,” *Science (80-.).*, vol. 206, no. 4420, pp. 854–856, Nov. 1979.

[31] C. J. Cupp and E. Uemura, “Age-related changes in prefrontal cortex of Macaca mulatta: Quantitative analysis of dendritic branching patterns,” *Exp. Neurol.*, 1980.

[32] S. Nakamura, I. Akiguchi, M. Kameyama, and N. Mizuno, “Age-related changes of pyramidal cell basal dendrites in layers III and V of human motor cortex: a quantitative Golgi study.,” *Acta Neuropathol.*, vol. 65, no. 3–4, pp. 281–4, 1985.

[33] D. W. Vaughan, “Age-related deterioration of pyramidal cell basal dendrites in rat auditory cortex,” *J. Comp. Neurol.*, vol. 171, no. 4, pp. 501–515, Feb. 1977.

[34] H. Haug and R. Eggers, “Morphometry of the human cortex cerebri and corpus striatum during aging,” *Neurobiol. Aging*, vol. 12, no. 4, pp. 336–338, Jul. 1991.

[35] S. M. Resnick, D. L. Pham, M. A. Kraut, A. B. Zonderman, and C. Davatzikos, “Longitudinal magnetic resonance imaging studies of older adults: A shrinking brain,” *J. Neurosci.*, vol. 23, no. 8, pp. 3295–3301, Apr. 2003.

[36] G. Bartzokis, J. L. Cummings, D. Sultzer, V. W. Henderson, K. H. Nuechterlein, and J. Mintz, “White matter structural integrity in healthy aging adults and patients with Alzheimer disease: A magnetic resonance imaging study,” *Arch. Neurol.*, vol. 60, no. 3, pp. 393–398, Mar. 2003.

[37] R. D. Terry, E. Masliah, D. P. Salmon, N. Butters, R. DeTeresa, R. Hill, L. A. Hansen, and R. Katzman, “Physical basis of cognitive alterations in

alzheimer's disease: Synapse loss is the major correlate of cognitive impairment," *Ann. Neurol.*, vol. 30, no. 4, pp. 572–580, Oct. 1991.

[38] E. Masliah, M. Mallory, L. Hansen, R. DeTeresa, and R. D. Terry, "Quantitative synaptic alterations in the human neocortex during normal aging," *Neurology*, vol. 43, no. 1, pp. 192–197, 1993.

[39] Y. Geinisman, L. Detoledo-Morrell, F. Morrell, and R. E. Heller, "Hippocampal markers of age-related memory dysfunction: Behavioral, electrophysiological and morphological perspectives," *Progress in Neurobiology*. 1995.

[40] I. G. Newton, M. E. Forbes, M. C. Linville, H. Pang, E. M. Tucker, D. R. Riddle, and J. K. Brunso-Bechtold, "Effects of aging and caloric restriction on dentate gyrus synapses and glutamate receptor subunits," *Neurobiol. Aging*, vol. 29, no. 9, pp. 1308–1318, 2008.

[41] C. López-Otín, M. A. Blasco, L. Partridge, M. Serrano, and G. Kroemer, "The hallmarks of aging," *Cell*, vol. 153, no. 6, p. 1194, 2013.

[42] M. P. Mattson and T. V. Arumugam, "Hallmarks of Brain Aging: Adaptive and Pathological Modification by Metabolic States," *Cell Metabolism*, vol. 27, no. 6. Cell Press, pp. 1176–1199, 05-Jun-2018.

[43] P. Greengard, F. Valtorta, A. J. Czernik, and F. Benfenati, "Synaptic Vesicle Phosphoproteins and Regulation of Synaptic Function."

[44] T. C. Südhof, "The Synaptic Vesicle Cycle," *Annu. Rev. Neurosci.*, vol. 27, no. 1, pp. 509–547, Jul. 2004.

[45] A. Becher, A. Drenckhahn, I. Pahner, M. Margittai, R. Jahn, and G. Ahnert-Hilger, "The Synaptophysin-Synaptobrevin Complex: a Hallmark of Synaptic Vesicle Maturation," 1998.

[46] Y. Geinisman, L. de Toledo-Morrell, and F. Morrell, "Loss of perforated synapses in the dentate gyrus: morphological substrate of memory deficit in aged rats.," *Proc. Natl. Acad. Sci. U. S. A.*, vol. 83, no. 9, pp. 3027–3031, 1986.

[47] T. D. Smith, M. M. Adams, M. Gallagher, J. H. Morrison, and P. R. Rapp, “Circuit-specific alterations in hippocampal synaptophysin immunoreactivity predict spatial learning impairment in aged rats,” *J. Neurosci.*, vol. 20, no. 17, pp. 6587–6593, Sep. 2000.

[48] E. Head, M. M. Corrada, K. Kahle-Wrobleski, R. C. Kim, F. Sarsoza, M. Goodus, and C. H. Kawas, “Synaptic proteins, neuropathology and cognitive status in the oldest-old,” *Neurobiol. Aging*, vol. 30, no. 7, pp. 1125–1134, Jul. 2009.

[49] C.-I. Sze, J. C. Troncoso, C. Kawas, P. Moution, D. L. Price, And L. J. Martin, “Loss of the Presynaptic Vesicle Protein Synaptophysin in Hippocampus Correlates with Cognitive Decline in Alzheimer Disease,” *J. Neuropathol. Exp. Neurol.*, vol. 56, no. 8, pp. 933–944, Aug. 1997.

[50] B. P. F. Rutten, N. M. Van der Kolk, S. Schafer, M. A. M. J. van Zandvoort, T. A. Bayer, H. W. M. Steinbusch, and C. Schmitz, “Age-related loss of synaptophysin immunoreactive presynaptic boutons within the hippocampus of APP751SL, PS1M146L, and APP751 SL/PS1M146L transgenic mice,” *Am. J. Pathol.*, vol. 167, no. 1, pp. 161–173, 2005.

[51] B. Ojo, P. Rezaie, P. L. Gabbott, H. Davies, F. Colyer, T. R. Cowley, M. Lynch, M. G. Stewart, “Age-related changes in the hippocampus (loss of synaptophysin and glial-synaptic interaction) are modified by systemic treatment with an NCAM-derived peptide, FGL,” *Brain. Behav. Immun.*, vol. 26, no. 5, pp. 778–788, Jul. 2012.

[52] E. A. Nimchinsky, B. L. Sabatini, and K. Svoboda, “Structure and Function of Dendritic Spines,” *Annu. Rev. Physiol.*, vol. 64, no. 1, pp. 313–353, Mar. 2002.

[53] M. Kneussel and H. Betz, “Clustering of inhibitory neurotransmitter receptors at developing postsynaptic sites: The membrane activation model,” *Trends in Neurosciences*, vol. 23, no. 9. Elsevier Ltd, pp. 429–435, 01-Sep-2000.

[54] H. Husi, M. A. Ward, J. S. Choudhary, W. P. Blackstock, and S. G. N. Grant, “Proteomic analysis of NMDA receptor-adhesion protein signaling complexes,” *Nat. Neurosci.*, vol. 3, no. 7, pp. 661–669, Jul. 2000.

[55] M. Sheng, “Molecular organization of the postsynaptic specialization,” *Proc.*

Natl. Acad. Sci. U. S. A., vol. 98, no. 13, pp. 7058–7061, Jun. 2001.

[56] S. Cull-Candy, S. Brickley, and M. Farrant, "NMDA receptor subunits: Diversity, development and disease," *Current Opinion in Neurobiology*, vol. 11, no. 3. Elsevier Ltd, pp. 327–335, 01-Jun-2001.

[57] R. J. Wenthold, R. S. Petralia, J. Blahos, and A. S. Niedzielski, "Evidence for multiple AMPA receptor complexes in hippocampal CA1/CA2 neurons," *J. Neurosci.*, vol. 16, no. 6, pp. 1982–1989, Mar. 1996.

[58] M. M. Adams, L. Shi, M. C. Linville, M. E. Forbes, A. B. Long, C. Bennett, I. G. Newton, C. S. Carter, W. E. Sonntag, D. R. Riddle, and J. K. Brunso-Bechtold, "Caloric restriction and age affect synaptic proteins in hippocampal CA3 and spatial learning ability," *Exp. Neurol.*, vol. 211, no. 1, pp. 141–149, 2008.

[59] P. R. Hof, H. Duan, T. L. Page, M. Einstein, B. Wicinski, Y. He, J. M. Erwin, and J. Morrison, "Age-related changes in GluR2 and NMDAR1 glutamate receptor subunit protein immunoreactivity in corticocortically projecting neurons in macaque and patas monkeys," *Brain Res.*, vol. 928, no. 1–2, pp. 175–186, Feb. 2002.

[60] R. A. Rissman, A. L. De Blas, and D. M. Armstrong, "GABA $_{A}$ receptors in aging and Alzheimer's disease," *J. Neurochem.*, vol. 103, no. 4, pp. 1285–1292, Nov. 2007.

[61] D. M. Kullmann, A. Ruiz, D. M. Rusakov, R. Scott, A. Semyanov, and M. C. Walker, "Presynaptic, extrasynaptic and axonal GABAA receptors in the CNS: Where and why?," *Progress in Biophysics and Molecular Biology*, vol. 87, no. 1 SPEC. ISS. Elsevier Ltd, pp. 33–46, 2005.

[62] G. L. Wenk, L. C. Walker, D. L. Price, and L. C. Cork, "Loss of NMDA, but not GABA-A, binding in the brains of aged rats and monkeys," *Neurobiol. Aging*, 1991.

[63] S. Govoni, M. Memo, L. Saiani, P. F. Spano, and M. Trabucchi, "Impairment of brain neurotransmitter receptors in aged rats," *Mech. Ageing Dev.*, vol. 12, no. 1, pp. 39–46, 1980.

[64] A. Maggi, M. J. Schmidt, B. Ghetti, and S. J. Enna, “Effect of aging on neurotransmitter receptor binding in rat and human brain,” *Life Sci.*, vol. 24, no. 4, pp. 367–373, Jan. 1979.

[65] S. J. Allen, J. S. Benton, M. J. Goodhardt, E. A. Haan, N. R. Sims, C. C. Smith, J. A. Spillane, D. M. Bowen, and A. N. Davison, “Biochemical Evidence of Selective Nerve Cell Changes in the Normal Ageing Human and Rat Brain,” *J. Neurochem.*, vol. 41, no. 1, pp. 256–265, 1983.

[66] M. Wyszynski, J. G. Valtschanoff, S. Naisbitt, A. W. Dunah, E. Kim, D. G. Standaert, R. Weinberg, and M. Sheng, “Association of AMPA receptors with a subset of glutamate receptor- interacting protein in vivo,” *J. Neurosci.*, vol. 19, no. 15, pp. 6528–6537, Aug. 1999.

[67] K. W. Roche, S. Standley, J. McCallum, C. Dune Ly, M. D. Ehlers, and R. J. Wenthold, “Molecular determinants of NMDA receptor internalization,” *Nat. Neurosci.*, vol. 4, no. 8, pp. 794–802, 2001.

[68] M. Sassoè-Pognetto and J.-M. Fritschy, “Gephyrin, a major postsynaptic protein of GABAergic synapses,” *Eur. J. Neurosci.*, vol. 12, no. 7, pp. 2205–2210, Jul. 2000.

[69] H. C. Kornau, L. T. Schenker, M. B. Kennedy, and P. H. Seeburg, “Domain interaction between NMDA receptor subunits and the postsynaptic density protein PSD-95,” *Science (80-.).*, vol. 269, no. 5231, pp. 1737–1740, 1995.

[70] C. Essrich, M. Lorez, J. A. Benson, J. M. Fritschy, and B. Lüscher, “Postsynaptic clustering of major GABAA receptor subtypes requires the γ2 subunit and gephyrin,” *Nat. Neurosci.*, vol. 1, no. 7, pp. 563–571, 1998.

[71] M. Majdi, A. Ribeiro-da-Silva, and A. C. Cuello, “Variations in excitatory and inhibitory postsynaptic protein content in rat cerebral cortex with respect to aging and cognitive status,” *Neuroscience*, vol. 159, no. 2, pp. 896–907, 2009.

[72] E. M. Snyder, Y. Nong, C. G. Almeida, S. Paul, T. Moran, E. Y. Choi, A. C. Nairn, M. W. Salter, P. J. Lombroso, G. K. Gouras, and P. Greengard, “Regulation of NMDA receptor trafficking by amyloid-β,” *Nat. Neurosci.*, vol. 8, no. 8, pp. 1051–1058, Aug. 2005.

[73] D. Preissmann, G. Leuba, C. Savary, A. Vernay, R. Kraftsik, I. M. Riederer, F. Schenk, B. M. Riederer, and A. Savioz, "Increased postsynaptic density protein-95 expression in the frontal cortex of aged cognitively impaired rats," *Exp. Biol. Med.*, vol. 237, no. 11, pp. 1331–1340, Nov. 2012.

[74] A. Savioz, G. Leuba, and P. G. Vallet, "A framework to understand the variations of PSD-95 expression in brain aging and in Alzheimer's disease," *Ageing Research Reviews*, vol. 18. Elsevier Ireland Ltd, pp. 86–94, 01-Jan-2014.

[75] E. T. Karoglu, D. O. Halim, B. Erkaya, F. Altaytas, A. Arslan-Ergul, O. Konu, and M. M. Adams, "Aging alters the molecular dynamics of synapses in a sexually dimorphic pattern in zebrafish (Danio rerio)," *Neurobiol. Aging*, vol. 54, pp. 10–21, 2017.

[76] L. Viltono, A. Patrizi, J.-M. Fritschy, and M. Sassoè-Pognetto, "Synaptogenesis in the cerebellar cortex: Differential regulation of gephyrin and GABAA receptors at somatic and dendritic synapses of Purkinje cells," *J. Comp. Neurol.*, vol. 508, no. 4, pp. 579–591, Jun. 2008.

[77] H. Wang, J. G. Turner, L. Ling, J. L. Parrish, L. F. Hughes, and D. M. Caspary, "Age-related changes in glycine receptor subunit composition and binding in dorsal cochlear nucleus," *Neuroscience*, vol. 160, no. 1, pp. 227–239, Apr. 2009.

[78] C. M. Hales, H. Rees, N. T. Seyfried, E. B. Dammer, D. M. Duong, M. Gearing, T. J. Montine, J. C. Troncoso, M. Thambisetty, A. I. Levey, J. J. Lah, and T. S. Wingo, "Abnormal Gephyrin immunoreactivity associated with Alzheimer disease pathologic changes," *J. Neuropathol. Exp. Neurol.*, vol. 72, no. 11, pp. 1009–1015, Nov. 2013.

[79] S. Agarwal, R. K. Tannenberg, and P. R. Dodd, "Reduced expression of the inhibitory synapse scaffolding protein gephyrin in Alzheimer's disease," *J. Alzheimer's Dis.*, vol. 14, no. 3, pp. 313–321, 2008.

[80] W. Legon, S. Punzell, E. Dowlati, S. E. Adams, A. B. Stiles, and R. J. Moran, "Altered Prefrontal Excitation/Inhibition Balance and Prefrontal Output: Markers of Aging in Human Memory Networks," *Cereb. Cortex*, vol. 26, no. 11, pp. 4315–4326, 2016.

[81] T. P. Wong, G. Marchese, M. A. Casu, A. Ribeiro-Da-Silva, A. C. Cuello, and Y. De Koninck, “Imbalance towards inhibition as a substrate of aging-associated cognitive impairment,” *Neurosci. Lett.*, vol. 397, no. 1–2, pp. 64–68, Apr. 2006.

[82] C. Bories, Z. Husson, M. J. Guitton, and Y. De Koninck, “Differential Balance of Prefrontal Synaptic Activity in Successful versus Unsuccessful Cognitive Aging,” *J. Neurosci.*, vol. 33, no. 4, pp. 1344–1356, 2013.

[83] M. Majdi, A. Ribeiro-da-Silva, and A. C. Cuello, “Cognitive impairment and transmitter-specific pre- and postsynaptic changes in the rat cerebral cortex during ageing,” *Eur. J. Neurosci.*, vol. 26, no. 12, pp. 3583–3596, Dec. 2007.

[84] S. Schmidt, C. Bruehl, C. Frahm, C. Redecker, and O. W. Witte, “Age dependence of excitatory-inhibitory balance following stroke,” *Neurobiol. Aging*, vol. 33, no. 7, pp. 1356–1363, Jul. 2012.

[85] A. Rozycka and M. Liguz-Lecznar, “The space where aging acts: focus on the GABAergic synapse,” *Aging Cell*, vol. 16, no. 4, pp. 634–643, 2017.

[86] D. Gems and L. Partridge, “Genetics of Longevity in Model Organisms: Debates and Paradigm Shifts,” *Annu. Rev. Physiol.*, vol. 75, no. 1, pp. 621–644, Feb. 2013.

[87] F. U. Hartl, A. Bracher, and M. Hayer-Hartl, “Molecular chaperones in protein folding and proteostasis,” *Nature*, vol. 475, no. 7356. pp. 324–332, 21-Jul-2011.

[88] D. C. Rubinsztein, G. Mariño, and G. Kroemer, “Autophagy and aging,” *Cell*, vol. 146, no. 5. pp. 682–695, 02-Sep-2011.

[89] U. Tomaru, S. Takahashi, A. Ishizu, Y. Miyatake, A. Gohda, S. Suzuki, A. Ono, J. Ohara, T. Baba, S. Murata, K. Tanaka, and M. Kasahara, “Decreased proteasomal activity causes age-related phenotypes and promotes the development of metabolic abnormalities,” *Am. J. Pathol.*, vol. 180, no. 3, pp. 963–972, Mar. 2012.

[90] I. Bjedov, J. M. Toivonen, F. Kerr, C. Slack, J. Jacobson, A. Foley, and L. Partridge, “Mechanisms of Life Span Extension by Rapamycin in the Fruit

Fly Drosophila melanogaster," *Cell Metab.*, vol. 11, no. 1, pp. 35–46, Jan. 2010.

[91] F. Madeo, N. Tavernarakis, and G. Kroemer, "Can autophagy promote longevity?," *Nature Cell Biology*, vol. 12, no. 9. Nature Publishing Group, pp. 842–846, 2010.

[92] S. Zhang, E. Eitan, and M. P. Mattson, "Early involvement of lysosome dysfunction in the degeneration of cerebral cortical neurons caused by the lipid peroxidation product 4-hydroxynonenal," *J. Neurochem.*, vol. 140, no. 6, pp. 941–954, Mar. 2017.

[93] A. Efeyan, W. C. Comb, and D. M. Sabatini, "Nutrient-sensing mechanisms and pathways," *Nature*, vol. 517, no. 7534. Nature Publishing Group, pp. 302–310, 15-Jan-2015.

[94] E. Sibille, "Molecular aging of the brain, neuroplasticity, and vulnerability to depression and other brain-related disorders," 2013.

[95] C. Vézina, A. Kudelski, and S. N. Sehgal, "Rapamycin (AY-22,989), a new antifungal antibiotic. I. Taxonomy of the producing streptomycete and isolation of the active principle.," *J. Antibiot. (Tokyo).*, vol. 28, no. 10, pp. 721–6, Oct. 1975.

[96] J. Heitman, N. R. Movva, and M. N. Hall, "Targets for cell cycle arrest by the immunosuppressant rapamycin in yeast," *Science (80-.).*, vol. 253, no. 5022, pp. 905–909, 1991.

[97] D. M. Sabatini, H. Erdjument-Bromage, M. Lui, P. Tempst, and S. H. Snyder, "RAFTI: A Mammalian Protein That Binds to FKBP12 in a Rapamycin-Dependent Fashion and Is Homologous to Yeast TORs," 1994.

[98] C. T. Keith and S. L. Schreiber, "PIK-related kinases: DNA repair, recombination, and cell cycle checkpoints.," *Science*, vol. 270, no. 5233, pp. 50–1, Oct. 1995.

[99] X. Long, C. Spycher, Z. S. Han, A. M. Rose, F. Müller, and J. Avruch, "TOR Deficiency in C. elegans Causes Developmental Arrest and Intestinal Atrophy by Inhibition of mRNA Translation," *Curr. Biol.*, vol. 12, no. 17, pp. 1448–

1461, Sep. 2002.

[100] S. Oldham, “Genetic and biochemical characterization of dTOR, the Drosophila homolog of the target of rapamycin,” *Genes Dev.*, vol. 14, no. 21, pp. 2689–2694, Nov. 2000.

[101] K. Makky, J. Tekiela, and A. N. Mayer, “Target of rapamycin (TOR) signaling controls epithelial morphogenesis in the vertebrate intestine,” *Dev. Biol.*, vol. 303, no. 2, pp. 501–513, 2007.

[102] M. Laplante and D. M. Sabatini, “Regulation of mTORC1 and its impact on gene expression at a glance.,” *J. Cell Sci.*, vol. 126, no. Pt 8, pp. 1713–9, Apr. 2013.

[103] R. Zoncu, A. Efeyan, and D. M. Sabatini, “mTOR: from growth signal integration to cancer, diabetes and ageing.,” *Nat. Rev. Mol. Cell Biol.*, vol. 12, no. 1, pp. 21–35, Jan. 2011.

[104] M. Laplante and D. M. Sabatini, “mTOR signaling in growth control and disease.,” *Cell*, vol. 149, no. 2, pp. 274–93, Apr. 2012.

[105] D. D. Sarbassov, S. M. Ali, S. Sengupta, J.-H. Sheen, P. P. Hsu, A. F. Bagley, A. L. Markhard, and D. M. Sabatini, “Prolonged rapamycin treatment inhibits mTORC2 assembly and Akt/PKB.,” *Mol. Cell*, vol. 22, no. 2, pp. 159–68, Apr. 2006.

[106] C. S. Jernigan, D. B. Goswami, M. C. Austin, A. H. Iyo, A. Chandran, C. A. Stockmeier, and B. Karolewicz, “The mTOR signaling pathway in the prefrontal cortex is compromised in major depressive disorder,” *Prog. Neuro-Psychopharmacology Biol. Psychiatry*, vol. 35, no. 7, pp. 1774–1779, 2011.

[107] J. M. Dwyer, A. E. Lepack, and R. S. Duman, “MTOR activation is required for the antidepressant effects of mGluR 2/3 blockade,” *Int. J. Neuropsychopharmacol.*, vol. 15, no. 4, pp. 429–434, 2012.

[108] D. M. Sabatini, R. K. Barrow, S. Blackshaw, P. E. Burnett, M. M. Lai, M. E. Field, B. A. Bahr, J. Kirsch, H. Betz, and S. H. Snyder, “Interaction of RAFT1 with gephyrin required for rapamycin-sensitive signaling,” *Science (80-.).*, vol. 284, no. 5417, pp. 1161–1164, 1999.

[109] M. Perluigi, F. Di Domenico, and D. A. Butterfield, “mTOR signaling in aging and neurodegeneration: At the crossroad between metabolism dysfunction and impairment of autophagy,” *Neurobiol. Dis.*, vol. 84, pp. 39–49, 2015.

[110] O. Lazarov, M. P. Mattson, D. A. Peterson, S. W. Pimplikar, and H. van Praag, “When neurogenesis encounters aging and disease.,” *Trends Neurosci.*, vol. 33, no. 12, pp. 569–79, Dec. 2010.

[111] G. M. Bernal and D. A. Peterson, “Neural stem cells as therapeutic agents for age-related brain repair,” *Aging Cell*, vol. 3, no. 6, pp. 345–351, Oct. 2004.

[112] J. L. Bizon, H. J. Lee, and M. Gallagher, “Neurogenesis in a rat model of age-related cognitive decline,” *Aging Cell*, vol. 3, no. 4, pp. 227–234, Jul. 2004.

[113] L. S. Wright, K. R. Prowse, K. Wallace, M. H. K. Linskens, and C. N. Svendsen, “Human progenitor cells isolated from the developing cortex undergo decreased neurogenesis and eventual senescence following expansion in vitro,” *Exp. Cell Res.*, vol. 312, no. 11, pp. 2107–2120, Jul. 2006.

[114] C. M. McCay, M. F. Crowell, and L. A. Maynard, “The Effect of Retarded Growth Upon the Length of Life Span and Upon the Ultimate Body Size,” *J. Nutr.*, vol. 10, no. 1, pp. 63–79, Jul. 1935.

[115] M. D. W. Piper, L. Partridge, D. Raubenheimer, and S. J. Simpson, “Dietary restriction and aging: A unifying perspective,” *Cell Metabolism*, vol. 14, no. 2. pp. 154–160, 03-Aug-2011.

[116] R. de Cabo and M. P. Mattson, “Effects of Intermittent Fasting on Health, Aging, and Disease,” *N. Engl. J. Med.*, vol. 381, no. 26, pp. 2541–2551, Dec. 2019.

[117] R. Weindruch and R. S. Sohal, “Caloric Intake and Aging,” *N. Engl. J. Med.*, vol. 337, no. 14, pp. 986–994, Oct. 1997.

[118] C. L. Goodrick, D. K. Ingram, M. A. Reynolds, J. R. Freeman, and N. L. Cider, “Effects of Intermittent Feeding Upon Growth and Life Span in Rats,” *Gerontology*, vol. 28, no. 4, pp. 233–241, 1982.

[119] D. Wahl, S. C. Coogan, S. M. Solon-Biet, R. de Cabo, J. B. Haran, D. Raubenheimer, V. C. Cogger, M. P. Mattson, S. J. Simpson, and D. G. Le Couteur, "Cognitive and behavioral evaluation of nutritional interventions in rodent models of brain aging and dementia," *Clinical Interventions in Aging*, vol. 12. Dove Medical Press Ltd., pp. 1419–1428, 08-Sep-2017.

[120] FDA, "RAPAMUNE (sirolimus) ORAL SOLUTION AND TABLETS," pp. 1–46, 1999.

[121] G. S. Gerhard and K. C. Cheng, "A call to fins! Zebrafish as a gerontological model," *Aging Cell*, vol. 1, no. 2, pp. 104–111, 2002.

[122] I. V. Zhdanova, L. Yu, M. Lopez-Patino, E. Shang, S. Kishi, and E. Guelin, "Aging of the circadian system in zebrafish and the effects of melatonin on sleep and cognitive performance," *Brain Research Bulletin*, vol. 75, no. 2–4. pp. 433–441, 18-Mar-2008.

[123] S. Kishi, J. Uchiyama, A. M. Baughman, T. Goto, M. C. Lin, and S. B. Tsai, "The zebrafish as a vertebrate model of functional aging and very gradual senescence," in *Experimental Gerontology*, 2003, vol. 38, no. 7, pp. 777–786.

[124] M. L. Cayuela, K. B. M. Claes, M. G. Ferreira, C. M. Henriques, F. van Eeden, M. Varga, J. Vierstraete, and M. C. Mione, "The Zebrafish as an Emerging Model to Study DNA Damage in Aging, Cancer and Other Diseases," *Front. Cell Dev. Biol.*, vol. 6, no. January, pp. 1–9, 2019.

[125] A. V. Kalueff, A. M. Stewart, and R. Gerlai, "Zebrafish as an emerging model for studying complex brain disorders," *Trends in Pharmacological Sciences*, vol. 35, no. 2. pp. 63–75, Feb-2014.

[126] J. M. Keller and E. T. Keller, "The Use of Mature Zebrafish (Danio rerio) as a Model for Human Aging and Disease," in *Conn's Handbook of Models for Human Aging*, Elsevier, 2018, pp. 351–359.

[127] R. E. Patterson and D. D. Sears, "Metabolic Effects of Intermittent Fasting," *Annu. Rev. Nutr.*, vol. 37, no. 1, pp. 371–393, Aug. 2017.

[128] K. a. Rodriguez, S. G. Dodds, R. Strong, V. Galvan, Z. D. Sharp, and R. Buffenstein, "Divergent tissue and sex effects of rapamycin on the

proteasome-chaperone network of old mice," *Front. Mol. Neurosci.*, vol. 7, no. November, pp. 1–17, 2014.

[129] T. Sasore and B. Kennedy, "Deciphering combinations of PI3K/AKT/mTOR pathway drugs augmenting anti-angiogenic efficacy in vivo," *PLoS One*, vol. 9, no. 8, pp. 1–13, 2014.

[130] C. Sucularli, H. Shehwana, C. Kuscu, D. C. Dungul, H. Ozdag, and O. Konu, "Functionally conserved effects of rapamycin exposure on zebrafish," *Mol. Med. Rep.*, vol. 13, no. 5, pp. 4421–4430, 2016.

[131] X. H. Meng, B. Chen, and J. P. Zhang, "Intracellular insulin and impaired autophagy in a zebrafish model and a cell model of type 2 diabetes," *Int. J. Biol. Sci.*, vol. 13, no. 8, pp. 985–995, 2017.

[132] A. Arslan-Ergul and M. M. Adams, "Gene expression changes in aging Zebrafish (Danio rerio) brains are sexually dimorphic," *BMC Neurosci.*, vol. 15, no. 1, p. 29, 2014.

[133] M. Matthews, B. Trevarrow, and J. Matthews, "A virtual tour of the Guide for zebrafish users," *Lab Animal*, vol. 31, no. 3. pp. 34–40, 01-Mar-2002.

[134] K. Lidster, G. D. Readman, M. J. Prescott, and S. F. Owen, "International survey on the use and welfare of zebrafish *Danio rerio* in research," *J. Fish Biol.*, vol. 90, no. 5, pp. 1891–1905, May 2017.

[135] N. Goodwin, L. Westall, N. A. Karp, D. Hazlehurst, C. Kovacs, R. Keeble, P. Thompson, R. Collins, and J. Bussell, "Evaluating and Optimizing Fish Health and Welfare during Experimental Procedures," *Zebrafish*, vol. 13, no. Suppl 1, pp. S127–S131, Jul. 2016.

[136] M. Pavlidis, N. Digka, A. Theodoridi, A. Campo, K. Barsakis, G. Skouradakis, A. Samaras, and A. Tsalafouta, "Husbandry of Zebrafish, Danio Rerio , and the Cortisol Stress Response ," *Zebrafish*, vol. 10, no. 4, pp. 524–531, 2013.

[137] A. Arslan-Ergul, B. Erbaba, E. T. Karoglu, D. O. Halim, and M. M. Adams, "Short-term dietary restriction in old zebrafish changes cell senescence mechanisms," *Neuroscience*, vol. 334, pp. 64–75, 2016.

[138] D. Celebi-Birand, B. Erbaba, A. T. Ozdemir, H. Kafaligonul, and M. Adams, "Zebrafish Aging Models and Possible Interventions," *Recent Adv. Zebrafish Res.*, pp. 3–26, 2018.

[139] M. I. Goldsmith, M. K. Iovine, T. O'Reilly-Pol, and S. L. Johnson, "A developmental transition in growth control during zebrafish caudal fin development," *Dev. Biol.*, vol. 296, no. 2, pp. 450–457, 2006.

[140] A. Avdesh, M. Chen, M. T. Martin-Iverson, A. Mondal, D. Ong, S. Rainey-Smith, K. Taddei, M. Lardelli, D. M. Groth, G. Verdile, and R. N. Martins, "Regular care and maintenance of a Zebrafish (Danio rerio) laboratory: An introduction," *J. Vis. Exp.*, no. 69, 2012.

[141] A. Pereira, A. P. Carvalho, C. Cruz, and A. Saraiva, "Histopathological changes and zootechnical performance in juvenile zebrafish (Danio rerio) under chronic exposure to nitrate," *Aquaculture*, vol. 473, pp. 197–205, 2017.

[142] D. Celebi-Birand, N. I. Ardic, E. T. Karoglu Eravsar, G. F. Sengul, H. Kafaligonul, and M. Adams, "Dietary and Pharmacological Interventions that Inhibit Mammalian Target of Rapamycin (mTOR) Activity Alter the Brain Expression Levels of Neurogenic and Glial Markers in An Age- and Treatment-Dependent Manner," *Rejuvenation Res.*, p. rej.2019.2297, Apr. 2020.

[143] H. N. Munro, "General Aspects of the Regulation of Protein Metabolism by Diet and by Hormones," in *Mammalian Protein Metabolism*, Elsevier, 1964, pp. 381–481.

[144] J. L. Sonnenburg and F. Bäckhed, "Diet-microbiota interactions as moderators of human metabolism," *Nature*, vol. 535, no. 7610. Nature Publishing Group, pp. 56–64, 06-Jul-2016.

[145] H. J. Flint, S. H. Duncan, K. P. Scott, and P. Louis, "Links between diet, gut microbiota composition and gut metabolism," in *Proceedings of the Nutrition Society*, 2014, vol. 760, no. 1, pp. 13–22.

[146] M. Bélanger, I. Allaman, and P. J. Magistretti, "Brain energy metabolism: Focus on Astrocyte-neuron metabolic cooperation," *Cell Metabolism*, vol. 14, no. 6. Cell Press, pp. 724–738, 07-Dec-2011.

[147] P. Mergenthaler, U. Lindauer, G. A. Dienel, and A. Meisel, “Sugar for the brain: The role of glucose in physiological and pathological brain function,” *Trends in Neurosciences*, vol. 36, no. 10. NIH Public Access, pp. 587–597, Oct-2013.

[148] Y. Cho, N. Hong, K-W. Kim, S. J. Cho, M. Lee, Y.-H. Lee, Y.-H. Lee, E. S. Kang, B.-S. Cha, and B.-W. Lee, “The Effectiveness of Intermittent Fasting to Reduce Body Mass Index and Glucose Metabolism: A Systematic Review and Meta-Analysis,” *J. Clin. Med.*, vol. 8, no. 10, p. 1645, Oct. 2019.

[149] J. B. O’Sullivan, “Age gradient in blood glucose levels: Magnitude and clinical implications,” *Diabetes*, vol. 23, no. 8, pp. 713–715, Aug. 1974.

[150] Z. Yu, R. Wang, W. C. Fok, A. Coles, A. B. Salmon, and V. I. Pérez, “Rapamycin and dietary restriction induce metabolically distinctive changes in mouse liver,” *Journals Gerontol. - Ser. A Biol. Sci. Med. Sci.*, vol. 70, no. 4, pp. 410–420, 2015.

[151] D. H. Hellhammer, S. Wüst, and B. M. Kudielka, “Salivary cortisol as a biomarker in stress research,” *Psychoneuroendocrinology*, vol. 34, no. 2, pp. 163–171, Feb. 2009.

[152] J. J. Christiansen, C. B. Djurhuus, C. H. Gravholt, P. Iversen, J. S. Christiansen, O. Schmitz, J. Weeke, J. Otto L. Jørgensen, and N. Møller, “Effects of Cortisol on Carbohydrate, Lipid, and Protein Metabolism: Studies of Acute Cortisol Withdrawal in Adrenocortical Failure,” *J. Clin. Endocrinol. Metab.*, vol. 92, no. 9, pp. 3553–3559, Sep. 2007.

[153] S. Khani and J. A. Tayek, “Cortisol increases gluconeogenesis in humans: Its role in the metabolic syndrome,” *Clin. Sci.*, vol. 101, no. 6, pp. 739–747, 2001.

[154] A. J. Tomiyama, T. Mann, D. Vinas, J. M. Hunger, J. Dejager, and S. E. Taylor, “Low calorie dieting increases cortisol.,” *Psychosom. Med.*, vol. 72, no. 4, pp. 357–64, 2010.

[155] A. E. Kofman, M. R. McGraw, and C. J. Payne, “Rapamycin increases oxidative stress response gene expression in adult stem cells,” *Aging (Albany. NY).*, vol. 4, no. 4, pp. 279–289, 2012.

[156] M. V. Blagosklonny, “Fasting and rapamycin: diabetes versus benevolent glucose intolerance,” *Cell Death and Disease*, vol. 10, no. 8. Nature Publishing Group, pp. 1–10, 01-Aug-2019.

[157] A. Sekulić, C. C. Hudson, J. L. Homme, P. Yin, D. M. Otterness, L. M. Karnitz, and R. T. Abraham, “A Direct Linkage between the Phosphoinositide 3-Kinase-AKT Signaling Pathway and the Mammalian Target of Rapamycin in Mitogen-stimulated and Transformed Cells,” *Cancer Res.*, vol. 60, no. 13, 2000.

[158] G. A. Soliman, H. A. Acosta-Jaquez, E. A. Dunlop, B. Ekim, N. E. Maj, A. R. Tee, and D. C. Fingar, “mTOR Ser-2481 autophosphorylation monitors mTORC-specific catalytic activity and clarifies rapamycin mechanism of action,” *J. Biol. Chem.*, vol. 285, no. 11, pp. 7866–7879, Mar. 2010.

[159] D. C. Fingar, S. Salama, C. Tsou, E. Harlow, and J. Blenis, “Mammalian cell size is controlled by mTOR and its downstream targets S6K1 and 4EBP1/eIF4E.,” *Genes Dev.*, vol. 16, no. 12, pp. 1472–87, Jun. 2002.

[160] B. Martin, M. P. Mattson, and S. Maudsley, “Caloric restriction and intermittent fasting: Two potential diets for successful brain aging,” *Ageing Res. Rev.*, vol. 5, no. 3, pp. 332–353, 2006.

[161] V. Vijayan and P. Verstreken, “Autophagy in the presynaptic compartment in health and disease,” *Journal of Cell Biology*, vol. 216, no. 7. Rockefeller University Press, pp. 1895–1906, 01-Jul-2017.

[162] A. Peinemann, C. Lehner, B. Conrad, and H. R. Siebner, “Age-related decrease in paired-pulse intracortical inhibition in the human primary motor cortex,” *Neurosci. Lett.*, vol. 313, no. 1–2, pp. 33–36, 2001.

[163] A. E. Greene, M. T. Todorova, and T. N. Seyfried, “Perspectives on the metabolic management of epilepsy through dietary reduction of glucose and elevation of ketone bodies,” *J. Neurochem.*, vol. 86, no. 3, pp. 529–537, 2003.

[164] F. Valtorta, M. Pennuto, D. Bonanomi, and F. Benfenati, “Synaptophysin: Leading actor or walk-on role in synaptic vesicle exocytosis?,” *BioEssays*, vol. 26, no. 4, pp. 445–453, 2004.

[165] Z. Xiao, J. Peng, L. Wu, A. Arafat, and F. Yin, “The effect of IL-1β on synaptophysin expression and electrophysiology of hippocampal neurons through the PI3K/Akt/mTOR signaling pathway in a rat model of mesial temporal lobe epilepsy,” *Neurol. Res.*, vol. 39, no. 7, pp. 640–648, 2017.

[166] S. Ando, Y. Tanaka, Y. Toyoda, K. Kon, and S. I. Kawashima, “Turnover of synaptic membranes: Age-related changes and modulation by dietary restriction,” *J. Neurosci. Res.*, vol. 70, no. 3, pp. 290–297, 2002.

[167] S. W. Park, J. G. Lee, M. K. Seo, C. H. Lee, H. Y. Cho, B. J. Lee, W. Seol, and Y. H. Kim, “Differential effects of antidepressant drugs on mTOR signalling in rat hippocampal neurons,” *Int. J. Neuropsychopharmacol.*, vol. 17, no. 11, pp. 1831–1846, 2014.

[168] S. L. Eastwood, C. S. Weickert, M. J. Webster, M. M. Herman, J. E. Kleinman, and P. J. Harrison, “Synaptophysin protein and mRNA expression in the human hippocampal formation from birth to old age,” *Hippocampus*, vol. 16, no. 8, pp. 645–654, Aug. 2006.

[169] F. Nazio, F. Strappazzon, M. Antonioli, P. Bielli, V. Cianfanelli, M. Bordi, C. Gretzmeier, J. Dengjel, M. Piacentini, G. M. Fimia, and F. Cecconi “MTOR inhibits autophagy by controlling ULK1 ubiquitylation, self-association and function through AMBRA1 and TRAF6,” *Nat. Cell Biol.*, vol. 15, no. 4, pp. 406–416, 2013.

[170] T. Finkel, “The metabolic regulation of aging,” *Nature Medicine*, vol. 21, no. 12. Nature Publishing Group, pp. 1416–1423, 08-Dec-2015.

[171] Y. Sheng, S. Lv, M. Huang, Y. Lv, J. Yu , J. Liu, T. Tang, H. Qi, W. Di, and G. Ding, “Opposing effects on cardiac function by calorie restriction in different-aged mice,” *Aging Cell*, vol. 16, no. 5, pp. 1155–1167, 2017.

[172] D. J. Klionsky *et al.*, “Guidelines for the use and interpretation of assays for monitoring autophagy,” *Autophagy*, vol. 8, no. 4. Taylor & Francis, pp. 445–544, Apr-2012.

[173] I. Tanida, T. Ueno, and E. Kominami, “LC3 and autophagy,” *Methods Mol. Biol.*, vol. 445, pp. 77–88, 2008.

[174] G. L. Moldovan, B. Pfander, and S. Jentsch, “PCNA, the Maestro of the Replication Fork,” *Cell*, vol. 129, no. 4. Cell Press, pp. 665–679, 18-May-2007.

[175] Z. Kelman, “PCNA: Structure, functions and interactions,” *Oncogene*, vol. 14, no. 6. Nature Publishing Group, pp. 629–640, 13-Feb-1997.

[176] E. C. Genin, N. Caron, R. Vandenbosch, L. Nguyen, and B. Malgrange, “Concise review: Forkhead pathway in the control of adult neurogenesis,” *Stem Cells*, vol. 32, no. 6. pp. 1398–1407, 2014.

[177] Y. Goldshmit, S. Kanner, M. Zacs, F. Frisca, A. R. Pinto, P. D. Currie, and R.Pinkas-Kramarski, “Rapamycin increases neuronal survival, reduces inflammation and astrocyte proliferation after spinal cord injury,” *Mol. Cell. Neurosci.*, vol. 68, pp. 82–91, 2015.

[178] R. A. Miller, D. E. Harrison, C. M. Astle, E. Fernandez, K. Flurkey, M. Han, M. A. Javors, X. Li, N. L. Nadon, J. F. Nelson, S. Pletcher, A. B. Salmon, Z. D. Sharp, S. Van Roekel, L. Winkleman, and R. Strong, “Rapamycin-mediated lifespan increase in mice is dose and sex dependent and metabolically distinct from dietary restriction,” *Aging Cell*, vol. 13, no. 3, pp. 468–477, 2014.

[179] D. W. Lamming, “Diminished mTOR signaling : a common mode of action for endocrine longevity factors,” *Springerplus*, vol. 3, no. 735, pp. 1–11, 2014.

[180] W. E. Sonntag, J. E. Lenham, and R. L. Ingram, “Effects of Aging and Dietary Restriction on Tissue Protein Synthesis: Relationship to Plasma Insulin-like Growth Factor-1,” *J. Gerontol.*, vol. 47, no. 5, pp. B159–B163, Sep. 1992.

[181] M. De Luca, N. V. Roshina, G. L. Geiger-Thornsberry, R. F. Lyman, E. G. Pasyukova, and T. F. C. Mackay, “Dopa decarboxylase (Ddc) affects variation in Drosophila longevity,” *Nat. Genet.*, vol. 34, no. 4, pp. 429–433, 2003.

[182] K. Joshi, Y. Banasavadi-Siddegowda, X. Mo, S-H. Kim, P. Mao, C. Kig, D. Nardini, R. W. Sobol, L. M. L. Chow, H. I. Kornblum, R. Waclaw, M. Beullens, and I. Nakano, “MELK-Dependent FOXM1 Phosphorylation is Essential for Proliferation of Glioma Stem Cells,” pp. 1051–1063, 2013.

[183] S. Vaughan and P. S. Jat, “Deciphering the role of nuclear factor-κB in cellular senescence,” *Aging (Albany. NY).*, vol. 3, no. 10, pp. 913–919, 2011.

[184] E. M. Mercken, S. D. Crosby, D. W. Lamming, L. JeBailey, S. Krzysik-Walker, D. T. Villareal, M. Capri, C. Franceschi, Y. Zhang, K. Becker, D. M. Sabatini, R. de Cabo, and L. Fontana,“Calorie restriction in humans inhibits the PI3K/AKT pathway and induces a younger transcription profile,” *Aging Cell*, vol. 12, no. 4, pp. 645–651, 2013.

[185] W.-J. Zhou, K.-K. Chang, K. Wu, H.-L. Yang, J. Mei, F. Xie, D.-J. Li, and M.-Q. Li, “Rapamycin Synergizes with Cisplatin in Antiendometrial Cancer Activation by Improving IL-27–Stimulated Cytotoxicity of NK Cells,” *Neoplasia (United States)*, vol. 20, no. 1, pp. 69–79, 2018.

[186] R. Loewith, E. Jacinto, S. Wullschleger, A. Lorberg, J. L. Crespo, D. Bonenfant, W. Oppliger P. Jenoe, and M. N. Hall, “Two TOR Complexes, Only One of which Is Rapamycin Sensitive, Have Distinct Roles in Cell Growth Control” *Mol. Cell*, vol. 10, pp. 457–468, 2002.

[187] W. Zhang, X.-F. Sun, J.-H. Bo, J. Zhang, X.-J. Liu, L.-P. Wu, Z.-L. Ma, and X.-P. Gu, “Activation of mTOR in the spinal cord is required for pain hypersensitivity induced by chronic constriction injury in mice,” *Pharmacol. Biochem. Behav.*, vol. 111, pp. 64–70, Oct. 2013.

[188] S. L. Hands, C. G. Proud, and A. Wyttenbach, “mTOR’s role in ageing: protein synthesis or autophagy?,” *Aging (Albany. NY).*, vol. 1, no. 7, pp. 586–597, 2009.

[189] M. Yazdankhah, S. Farioli-Vecchioli, A. B. Tonchev, A. Stoykova, and F. Cecconi, “The autophagy regulators Ambra1 and Beclin 1 are required for adult neurogenesis in the brain subventricular zone,” *Cell Death Dis.*, vol. 5, no. 9, pp. 1–8, 2014.

[190] S. Babicki, D. Arndt, A. Marcu, Y. Liang, J. R. Grant, A. Maciejewski, and D. S. Wishart, “Heatmapper: web-enabled heat mapping for all,” *Nucleic Acids Res.*, vol. 44, no. W1, pp. W147–W153, 2016.

[191] C. Singleman and N. G. Holtzman, “ Growth and Maturation in the Zebrafish, Danio Rerio : A Staging Tool for Teaching and Research ,” *Zebrafish*, vol. 11, no. 4, pp. 396–406, 2014.

[192] D. M. Parichy, M. R. Elizondo, M. G. Mills, T. N. Gordon, and R. E. Engeszer, “Normal table of postembryonic zebrafish development: Staging by externally visible anatomy of the living fish,” *Dev. Dyn.*, vol. 238, no. 12, pp. 2975–3015, Dec. 2009.

[193] S.-B. Yang, A.-C. Tien, G. Boddupalli, A. W. Xu, Y. N. Jan, and L. Y. Jan, “Rapamycin ameliorates age-dependent obesity associated with increased mTOR signaling in hypothalamic POMC neurons.,” *Neuron*, vol. 75, no. 3, pp. 425–36, Aug. 2012.

[194] P. J. Scarpace, M. Matheny, K. Y. E. Strehler, H. Z. Toklu, N. Kirichenko, C. S. Carter, D. Morgan, and N. Tümer, “Rapamycin Normalizes Serum Leptin by Alleviating Obesity and Reducing Leptin Synthesis in Aged Rats,” *J Gerontol A Biol Sci Med Sci*, vol. 71, no. 7, pp. 891–899, 2016.

[195] P. J. Magistretti and I. Allaman, “Brain energy metabolism,” in *Neuroscience in the 21st Century: From Basic to Clinical*, Springer New York, 2013, pp. 1591–1620.

[196] P. C. Reifsnyder, K. Flurkey, A. Te, and D. E. Harrison, “Rapamycin treatment benefits glucose metabolism in mouse models of type 2 diabetes,” *Aging (Albany. NY).*, vol. 8, no. 11, pp. 3120–3130, 2016.

[197] P. C. Reifsnyder, A. Te, and D. E. Harrison, “Differential Effects of Rapamycin on Glucose Metabolism in Nine Inbred Strains,” *J Gerontol A Biol Sci Med Sci*, vol. 75, no. 1, pp. 50–57, 2020.

[198] G. R. Chang, Y. S. Chiu, Y. Y. Wu, Y. C. Lin, P. H. Hou, and F. C. Mao, “Rapamycin impairs HPD-induced beneficial effects on glucose homeostasis,” *Br. J. Pharmacol.*, vol. 172, no. 15, pp. 3793–3804, Aug. 2015.

[199] G. T. C. Ko, H. P. S. Wai, and J. S. F. Tang, “Effects of age on plasma glucose levels in non-diabetic Hong Kong Chinese,” *Croat. Med. J.*, vol. 47, no. 5, pp. 709–713, Oct. 2006.

[200] R. Gruetter, K. Ugurbil, and E. R. Seaquist, “Steady-State Cerebral Glucose Concentrations and Transport in the Human Brain,” *J. Neurochem.*, vol. 70, no. 1, pp. 397–408, Nov. 2002.

[201] G. Russell and S. Lightman, “The human stress response,” *Nature Reviews Endocrinology*, vol. 15, no. 9. Nature Publishing Group, pp. 525–534, 01-Sep-2019.

[202] R. A. Rizza, L. J. Mandarino, and J. E. Gerich, “Cortisol-Induced Insulin Resistance in Man: Impaired Suppression of Glucose Production and Stimulation of Glucose Utilization due to a Postreceptor Defect of Insulin Action,” *J. Clin. Endocrinol. Metab.*, vol. 54, no. 1, pp. 173–176, 1982.

[203] P. Darmon, F. Dadoun, S. Boullu-Ciocca, M. Grino, M.-C. Alessi, and A. Dutour, “Insulin resistance induced by hydrocortisone is increased in patients with abdominal obesity,” *Am. J. Physiol. Metab.*, vol. 291, no. 5, pp. E995–E1002, Nov. 2006.

[204] M. Bergendahl, M. L. Vance, M. 0 Thorner, and J. D. Veldhuis, “Fasting as a Metabolic Stress Paradigm Selectively Amplifies Cortisol Secretory Burst Mass and Delays the Time of Maximal Nyctohemeral Cortisol Concentrations in Healthy Men*,” 1996.

[205] M. L. Vance and M. O. Thorner, “Fasting alters pulsatile and rhythmic cortisol release in normal man,” *J. Clin. Endocrinol. Metab.*, vol. 68, no. 6, pp. 1013–1018, Jun. 1989.

[206] C. Kirschbaum, E. Gonzalez Bono, N. Rohleder, C. Gessner, K. M. Pirke, A. Salvador, and D. H. Hellhammer, “Effects of Fasting and Glucose Load on Free Cortisol Responses to Stress and Nicotine*,” 1997.

[207] M. V. Blagosklonny, “Hormesis does not make sense except in the light of TOR-driven aging,” *Aging (Albany. NY).*, vol. 3, no. 11, pp. 1051–1062, 2011.

[208] V. M. Heine, S. Maslam, M. Joëls, and P. J. Lucassen, “Prominent decline of newborn cell proliferation, differentiation, and apoptosis in the aging dentate gyrus, in absence of an age-related hypothalamus-pituitary-adrenal axis activation,” *Neurobiol. Aging*, vol. 25, no. 3, pp. 361–375, 2004.

[209] H. G. Kuhn, H. Dickinson-Anson, and F. H. Gage, “Neurogenesis in the dentate gyrus of the adult rat: age-related decrease of neuronal progenitor proliferation.,” *J. Neurosci.*, vol. 16, no. 6, pp. 2027–33, 1996.

[210] S. Fusco, L. Leone, S. A. Barbati, D. Samengo, R. Piacentini, G. Maulucci, G. Toietta, M. Spinelli, M. McBurney, G. Pani, and C. Grassi, "A CREB-Sirt1-Hes1 Circuitry Mediates Neural Stem Cell Response to Glucose Availability," *Cell Rep.*, vol. 14, no. 5, pp. 1195–1205, Feb. 2016.

[211] H. Odaka, N. Adachi, and T. Numakawa, "Impact of glucocorticoid on neurogenesis," *Neural Regeneration Research*, vol. 12, no. 7. Medknow Publications, pp. 1028–1035, 01-Jul-2017.

[212] E. White and R. S. DiPaola, "The double-edged sword of autophagy modulation in cancer," *Clinical Cancer Research*, vol. 15, no. 17. pp. 5308–5316, 01-Sep-2009.

[213] G. Kroemer and B. Levine, "Autophagic cell death: The story of a misnomer," *Nature Reviews Molecular Cell Biology*, vol. 9, no. 12. Nature Publishing Group, pp. 1004–1010, 30-Dec-2008.

[214] T. Pan, P. Rawal, Y. Wu, W. Xie, J. Jankovic, and W. Le, "Rapamycin protects against rotenone-induced apoptosis through autophagy induction," *Neuroscience*, vol. 164, no. 2, pp. 541–551, 2009.

[215] S. E. Lee, E. Y. Kim, H. Y. Choi, J. J. Moon, M. J. Park, J. B. Lee, C. J. Jeong, and S. P. Park, "Rapamycin rescues the poor developmental capacity of aged porcine oocytes," *Asian-Australasian J. Anim. Sci.*, vol. 27, no. 5, pp. 635–647, 2014.

[216] M. Pekny and M. Pekna, "Astrocyte intermediate filaments in CNS pathologies and regeneration," *Journal of Pathology*, vol. 204, no. 4. pp. 428–437, Nov-2004.

[217] R. Kassubek, R. Kassubek, M. Gorges, M. Schocke, V. A. M. Hagenston, A. Huss, A. C. Ludolph, J. Kassubek, and H. Tumani, "GFAP in early multiple sclerosis: A biomarker for inflammation," *Neurosci. Lett.*, vol. 657, pp. 166–170, Sep. 2017.

[218] J. Wuchter, S. Beuter, F. Treindl, T. Herrmann, G. Zeck, M. F. Templin, and H. Volkmer, "A Comprehensive Small Interfering RNA Screen Identifies Signaling Pathways Required for Gephyrin Clustering," *J. Neurosci.*, vol. 32, no. 42, pp. 14821–14834, 2012.

[219] S. K. Tyagarajan, H. Ghosh, G. E. Yévenes, I. Nikonenko, C. Ebeling, C. Schwerdel, C. Sidler, H. U. Zeilhofer, B. Gerrits, D. Muller, and J.-M. Fritschy, "Regulation of GABAergic synapse formation and plasticity by GSK3β-dependent phosphorylation of gephyrin," *Proc. Natl. Acad. Sci. U. S. A.*, vol. 108, no. 1, pp. 379–384, Jan. 2011.

[220] S. Agarwal, R. K. Tannenberg, and P. R. Dodd, "Reduced expression of the inhibitory synapse scaffolding protein gephyrin in Alzheimer's disease.," *J. Alzheimers. Dis.*, vol. 14, no. 3, pp. 313–21, Jul. 2008.

[221] F. Niere and K. F. Raab-Graham, "mTORC1 is a local, postsynaptic voltage sensor regulated by positive and negative feedback pathways," *Front. Cell. Neurosci.*, vol. 11, May 2017.

[222] M. P. McCabe, E. R. Cullen, C. M. Barrows, A. N. Shore, K. I. Tooke, K. A. Laprade, J. M. Stafford, and M. C. Weston, "Genetic inactivation of mTORC1 or mTORC2 in neurons reveals distinct functions in glutamatergic synaptic transmission," *Elife*, vol. 9, Mar. 2020.

[223] A. A. Mangoni and S. H. D. Jackson, "Age-related changes in pharmacokinetics and pharmacodynamics: basic principles and practical applications," *Br. J. Clin. Pharmacol.*, vol. 57, no. 1, pp. 6–14, Nov. 2003.

[224] K. Chellappa, J. A. Brinkman, S. Mukherjee, M. Morrison, M. I. Alotaibi, K. A. Carbajal, A. L. Alhadeff, I. J. Perron, R. Yao, C. S. Purdy, D. M. DeFelice, M. H. Wakai, J. Tomasiewicz, A. Lin, E. Meyer, Y. Peng, S. I. A. Apelo, L. Puglielli, J. N. Betley, G. K. Paschos, J. A. Baur, and D. W. Lamming, "Hypothalamic mTORC2 is essential for metabolic health and longevity," *Aging Cell*, vol. 18, no. 5, Oct. 2019.

[225] S. Schenk, S. C. Bannister, F. J. Sedlazeck, D. Anrather, B. Q. Minh, A. Bileck, M. Hartl, A. von Haeseler, C. Gerner, F. Raible, and K. Tessmar-Raible, "Combined transcriptome and proteome profiling reveals specific molecular brain signatures for sex, maturation and circalunar clock phase," *Elife*, vol. 8, Feb. 2019.

[226] R. De Sousa Abreu, L. O. Penalva, E. M. Marcotte, and C. Vogel, "Global signatures of protein and mRNA expression levels," *Molecular BioSystems*, vol. 5, no. 12. NIH Public Access, pp. 1512–1526, 2009.

[227] J. M. Lemée, A. Clavreul, M. Aubry, E. Com, M. de Tayrac, J. Mosser, and P. Menei, "Integration of transcriptome and proteome profiles in glioblastoma: Looking for the missing link," *BMC Mol. Biol.*, vol. 19, no. 1, p. 13, Nov. 2018.

[228] C. G. Mangleburg, T. Wu, H. K. Yalamanchili, C. Guo, Y.-C. Hsieh, D. M. Duong, E. B. Dammer, P. L. De Jager, N. T. Seyfried, Z. Liu, and J. M. Shulman, "Integrated analysis of the aging brain transcriptome and proteome in tauopathy," *bioRxiv*, p. 2020.02.19.954578, Feb. 2020.

[229] M. Francescatto, M. Vitezic, P. Heutink, and A. Saxena, "Brain-specific noncoding RNAs are likely to originate in repeats and may play a role in up-regulating genes in cis," *Int. J. Biochem. Cell Biol.*, vol. 54, pp. 331–337, 2014.

[230] P. K. Sahoo, D. S. Smith, N. Perrone-Bizzozero, and J. L. Twiss, "Axonal mRNA transport and translation at a glance," *J. Cell Sci.*, vol. 131, no. 8, Apr. 2018.

[231] Z.-F. Jiao, C.-F. Shang, Y.-F. Wang, Z. Yang, C. Yang, F.-N. Li, J-Z. Xie, J.-W. Pan, L. Fu, and J.-L. Du, "All-optical imaging and manipulation of whole-brain neuronal activities in behaving larval zebrafish," *Biomed. Opt. Express*, vol. 9, no. 12, p. 6154, Dec. 2018.

[232] P. Fei, J. Lee, R. R. S. Packard, K.-I. Sereti, H. Xu, J. Ma, Y. Ding, H. Kang, H. Chen, K. Sung, R. Kulkarni, R. Ardehali, C-C J. Kuo, X. Xu, C.-M. Ho, and T. K. Hsiai, "Cardiac Light-Sheet Fluorescent Microscopy for Multi-Scale and Rapid Imaging of Architecture and Function," *Sci. Rep.*, vol. 6, Mar. 2016.

[233] N. K. Sampathkumar, J. I. Bravo, Y. Chen, P. S. Danthi, E. K. Donahue, R. W. Lai, R. Lu, L. T. Randall, N. Vinson, and B. A. Benayoun, "Widespread sex dimorphism in aging and age-related diseases," *Human Genetics*, vol. 139, no. 3. Springer, pp. 333–356, 01-Mar-2020.

[234] E. J. Márquez, C.-h. Chung, R. Marches, R. J. Rossi, D. Nehar-Belaid, A. Eroglu, D. J. Mellert, G. A. Kuchel, J. Banchereau, and D. Ucar, "Sexual-dimorphism in human immune system aging," *Nat. Commun.*, vol. 11, no. 1, pp. 1–17, Dec. 2020.

[235] L. C. D. Pomatto, J. Tower, and K. J. A. Davies, “Sexual dimorphism and aging differentially regulate adaptive homeostasis,” *Journals Gerontol. - Ser. A Biol. Sci. Med. Sci.*, vol. 73, no. 2, pp. 141–149, 2018.

[236] L. O’Dwyer, F. Lamberton, A. L. W. Bokde, M. Ewers, Y. O. Faluyi, C. Tanner, B. Mazoyer, D. O’Neill, M. Bartley, R. Collins, T. Coughlan, D. Prvulovic, and H. Hampel, “Sexual Dimorphism in Healthy Aging and Mild Cognitive Impairment: A DTI Study,” *PLoS One*, vol. 7, no. 7, p. e37021, Jul. 2012.

[237] E. M. Santos, P. Kille, V. L. Workman, G. C. Paull, and C. R. Tyler, “Sexually dimorphic gene expression in the brains of mature zebrafish,” *Comp. Biochem. Physiol. - A Mol. Integr. Physiol.*, vol. 149, no. 3, pp. 314–324, Mar. 2008.

[238] A. Arslan-Ergul and M. M. Adams, “Gene expression changes in aging zebrafish (Danio rerio) brains are sexually dimorphic.,” *BMC Neurosci.*, vol. 15, no. 1, p. 29, Jan. 2014.

Curriculum Vitae and Publications

PERSONAL INFORMATION

Name Surname	Ergül Dilan Çelebi Birand
Date of Birth	October 26, 1989
Nationality	Turkish
Languages spoken	Turkish (Native)
	English (Fluent)
	French (Elementary)
Address	UNAM, 505B, Ihsan Dogramaci Bilkent University,
	06800, Ankara, Turkey
Phone	Work phone: +90 312 290 8968
E-mail	dilan.celebi@bilkent.edu.tr, edilancelebi@gmail.com

EDUCATION

2014 – Present: PhD student at Ihsan Dogramaci Bilkent University, Neuroscience Graduate Program

2012 – 2013: Special student at Ihsan Dogramaci Bilkent University, Department of Molecular Biology and Genetics

2006 – 2010: BSc in Molecular Biology and Genetics, Ihsan Dogramaci Bilkent University, Ankara, Turkey (Graduation Date: May 29, 2010)

2003 - 2006: Gazi Anatolian High School, Ankara, Turkey (Major courses: Science, Mathematics)

PUBLICATIONS

D. Celebi-Birand*, M. U. Tuz Sasik*, N. I. Ardic, H. O. Aydogan, B. Erbaba, E. T. Karoglu Eravsar, H. Kafaligonul, M. M. Adams, "The Zebrafish (*Danio rerio*) and its uses for understanding the neuroscience of aging: applications and observation," *Neuroscience of Aging*, 2020, in press.

*These authors contributed equally to this work.

D. Celebi-Birand, N. I. Ardic, E. T. Karoglu Eravsar, G. F. Sengul, H. Kafaligonul, and M. Adams, "Dietary and Pharmacological Interventions that Inhibit Mammalian Target of Rapamycin (mTOR) Activity Alter the Brain Expression Levels of Neurogenic and Glial Markers in An Age- and Treatment-Dependent Manner," *Rejuvenation Res.*, p. rej.2019.2297, Apr. 2020.

D. Celebi-Birand, B. Erbaba, A. T. Ozdemir, H. Kafaligonul, and M. Adams, "Zebrafish Aging Models and Possible Interventions," *Recent Adv. Zebrafish Res.*, pp. 3–26, 2018.

E. D. Celebi-Birand, E. T. Karoglu, F. Doldur-Balli, and M. M. Adams, "Mammalian Target of Rapamycin (mTOR), Aging, Neuroscience, and Their Association with Aging-Related Diseases". *Molecules to Medicine with mTOR*, 12/2016: p.p. 185-203; ISBN: 9780128027332, DOI:10.1016/B978-0-12-802733-2.00007-4, 2016.

ABSTRACT PUBLICATIONS

Celebi-Birand, D., Sengul, G. F., Ardic, N. I., Kafaligonul, H., Adams, M. Effects of short-term of caloric restriction and rapamycin treatments on cellular and synaptic components in young and old zebrafish (Danio rerio). Program No. 663.15. 2017 Neuroscience Meeting Planner. Washington, DC: Society for Neuroscience, 2017. Online.

Celebi-Birand, E. D., Sengul, G. F., Ardic, N. I., Kafaligonul, H., and Adams, M. M. 2018. Effects of short-term caloric restriction and rapamycin on brain aging in zebrafish (Danio rerio). Anatomy 12 (Suppl.1), 85. doi: 10.2399/ana.18.001s

SCHOLARSHIPS

1- Project bursary, The Scientific and Technological Research Council of Turkey (TUBITAK 1001 grant, 214S236), "The Interaction between Caloric Restriction and Age in mTOR Mutants", 15 April 2015-15 October 2018 (Duration: 40 months)

2- Full scholarship**,** Graduate education, Bilkent University, Graduate Program of Neuroscience (2014 – 2019)

3- Full scholarship**,** Special student, Bilkent University, Molecular Biology and Genetics Department (2012 – 2013).

CONGRESS & SYMPOSIUM & WORKSHOP PARTICIPATIONS

1. ZEISS Advanced Microscopy Techniques Workshop, Ankara, Turkey, 28 January, 2020.
2. 16th National Neuroscience Congress, Istanbul, Turkey, 20-23 May, 2018.
3. Society for Neuroscience, Neuroscience 2017 Meeting, Washington DC, USA, 11-15 November, 2017.
4. EMBO Young Investigator PhD Course, Heidelberg, Germany, 30 November – 5 December, 2015.

CERTIFICATES

1. ZEISS Advanced Microscopy Techniques Workshop: January 28, 2020
2. Use of Laboratory Animals handed out by Ihsan Dogramaci Bilkent University Animal Experiments Local Ethics Committee (BILHADYEK):

SOCIETY MEMBERSHIPS

Society for Neuroscience

Appendix

Copyright Permissions

GRANTED: 337220 Permission request for WHO copyrighted material

From permissions <permissions@who.int> on 2020-05-05 05:33

Details Plain text

Dear Mrs Celebi Birand,

We thank you for your request for permission to reprint and reproduce certain WHO copyrighted material .

On behalf of the World Health Organization, we are pleased to authorize your request to reproduce the WHO materials as detailed in the form below, subject to the terms and conditions of the non-exclusive licence below.

REFERENCE OF REQUESTED MATERIAL

World Health Organization. World Health Report
https://www.who.int/life-course/publications/2015-ageing-report/en/

https://apps.who.int/iris/bitstream/handle/10665/186463/9789240694811_eng.pdf
"Figure 3.2 Proportion of population aged 60 years or older, by country, 2050 projections" on page 44 of the report.

If you have any further queries regarding this authorization, please contact me at permissions@who.int.

We thank you for your interest in WHO published materials.

With our best regards,

Ms Dolores Campanario
WORLD HEALTH ORGANIZATION PRESS *(Permission Management, Reprint Rights and Licensing)*
20 Avenue Appiah, Office E169, 1211 Geneva 27, Switzerland - E-mail:
campanariod@who.int or **permissions@who.int**

- To request for permission to reproduce or translate any WHO copyrighted material, please complete this **WHO PERMISSION FORM:** https://www.who.int/about/who-we-are/publishing-policies/permissions

Web: www.who.int
Follow WHO on Facebook; Twitter; YouTube; Instagram

World Health Organization

Figure A.1. Copyright permission for Figure 1.1. The permission is granted by WHO.

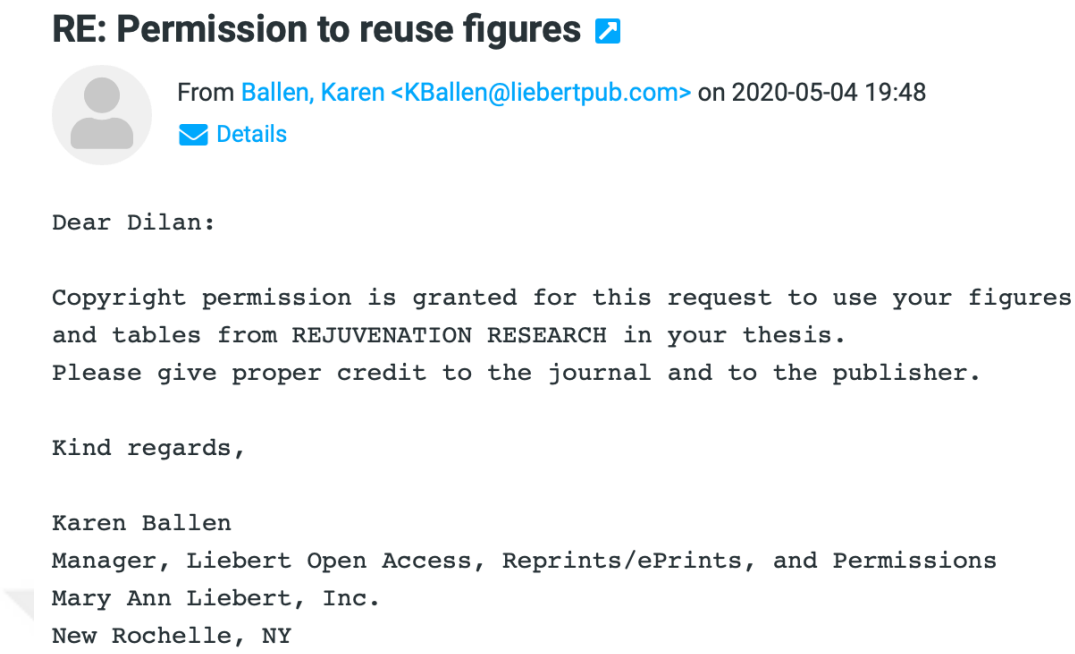

RE: Permission to reuse figures

From Ballen, Karen <KBallen@liebertpub.com> on 2020-05-04 19:48

Details

Dear Dilan:

Copyright permission is granted for this request to use your figures and tables from REJUVENATION RESEARCH in your thesis.
Please give proper credit to the journal and to the publisher.

Kind regards,

Karen Ballen
Manager, Liebert Open Access, Reprints/ePrints, and Permissions
Mary Ann Liebert, Inc.
New Rochelle, NY

Figure A.2. Copyright permission for reuse of figures published in Rejuvenation Research. The permission is granted by Mary Ann Liebert, Inc.